

Majorization Minimization Methods for Distributed Pose Graph Optimization

Taosha Fan and Todd Murphey

Abstract—We consider the problem of distributed pose graph optimization (PGO) that has important applications in multi-robot simultaneous localization and mapping (SLAM). We propose the majorization minimization (MM) method for distributed PGO (MM-PGO) that applies to a broad class of robust loss kernels. The MM-PGO method is guaranteed to converge to first-order critical points under mild conditions. Furthermore, noting that the MM-PGO method is reminiscent of proximal methods, we leverage Nesterov’s method and adopt adaptive restarts to accelerate convergence. The resulting accelerated MM methods for distributed PGO—both with a master node in the network (AMM-PGO^{*}) and without (AMM-PGO[#])—have faster convergence in contrast to the MM-PGO method without sacrificing theoretical guarantees. In particular, the AMM-PGO[#] method, which needs no master node and is fully decentralized, features a novel adaptive restart scheme and has a rate of convergence comparable to that of the AMM-PGO^{*} method using a master node to aggregate information from all the nodes. The efficacy of this work is validated through extensive applications to 2D and 3D SLAM benchmark datasets and comprehensive comparisons against existing state-of-the-art methods, indicating that our MM methods converge faster and result in better solutions to distributed PGO.

I. INTRODUCTION

Pose graph optimization (PGO) is a nonlinear and non-convex optimization problem estimating unknown poses from noisy relative pose measurements. PGO associates each pose with a vertex and each relative pose measurement with an edge, from which the optimization problem is well represented through a graph. PGO has important applications in a number of areas, including but not limited to robotics [1]–[3], autonomous driving [4], and computational biology [5], [6]. Recent advances [7]–[16] suggest that PGO can be well solved using iterative optimization. Nevertheless, the aforementioned techniques [7]–[16] are difficult to distribute across a network due to communication and computational limitations, and are only applicable to small- and medium-sized problems with at most tens of thousands poses. In addition, their centralized pipelines are equivalent to using a master node to aggregate information from the entire network, making it impossible to meet potential privacy requirements one may wish to impose [17], [18].

In multi-robot simultaneous localization and mapping (SLAM) [19]–[28], each robot estimates not only its own poses but those of the others as well to build an environment map. Even though such a problem can be solved by PGO, communication between robots is restricted and multi-robot SLAM has more unknown poses than single-robot SLAM.

Thus, instead of using centralized PGO [7]–[16], it is more reasonable to formulate this large-sized estimation problem involving multiple robots as distributed PGO—each robot in multi-robot SLAM is represented as a node and two nodes (robots) are said to be neighbors if there exists a noisy relative pose measurement between them (a more detailed description of distributed PGO can be found in Section IV). In most cases, it is assumed that inter-node communication only occurs between neighboring nodes and most of these iterative optimization methods are infeasible due to the expensive communication cost of solving linear system and performing line search [7]–[16], which renders distributed PGO more challenging than centralized PGO.

In this paper, we propose majorization minimization (MM) methods [29], [30] for distributed PGO. As the name would suggest, MM methods have two steps. First, in the majorization step, we construct a surrogate function that majorizes the objective function, i.e., the surrogate function is an upper bound of the objective function except for the current iterate at which both functions attain the same value. Then, in the minimization step, we minimize the surrogate function instead of the original objective function to improve the current iterate. Even though straightforward, MM methods remain difficult for practical use, e.g., the surrogate function, whose construction and minimization can not be more difficult than solving the optimization problem itself, is not generally evident, and MM methods might fail to converge and suffer from slow convergence for nonconvex optimization. Therefore, the implementation of MM methods on large-scale, complicated and nonconvex optimization problems like distributed PGO is nontrivial, and inter-node communication requirements impose extra restrictions making it more so. All of these issues are addressed in our MM methods for distributed PGO both theoretically and empirically.

This paper extends the preliminary results in our previous works [31], [32], where we developed MM methods for centralized and distributed PGO that are guaranteed to converge to first-order critical points. In [31], [32], we also introduced and elaborated on the use of Nesterov’s method [33], [34] and adaptive restart [35] for the first time to accelerate the convergence of PGO. Beyond the initial results in [31], [32], this paper presents completely redesigned MM methods for distributed PGO and provides more comprehensive theoretical and empirical results. In particular, our MM methods in this paper are capable of handling a broad class of robust loss kernels, no longer require each iteration to attain a local optimal solution to the surrogate function for the convergence guarantees, and adopt a novel adaptive restart scheme for distributed PGO without a master node to make full use of Nesterov’s acceleration.

Taosha Fan and Todd Murphey are with the Department of Mechanical Engineering, Northwestern University, Evanston, IL 60201, USA. E-mail: taosha.fan@u.northwestern.edu, t-murphey@northwestern.edu

In summary, the contributions of this paper are the following:

- 1) We derive a class of surrogate functions that suit well with MM methods for distributed PGO. These surrogate functions apply to a broad class of robust loss kernels in robotics and computer vision.
- 2) We develop MM methods for distributed PGO that are guaranteed to converge to first-order critical points under mild conditions. Our MM methods for distributed PGO implement a novel update rule such that each iteration does not have to minimize the surrogate function to a local optimal solution.
- 3) We leverage Nesterov’s methods and adaptive restart to accelerate MM methods for distributed PGO and achieve significant improvement in convergence without any compromise of theoretical guarantees.
- 4) We present a decentralized adaptive restart scheme to make full use of Nesterov’s acceleration such that accelerated MM methods for distributed PGO without a master node are almost as fast as those requiring a master node.

The rest of this paper is organized as follows. Section II reviews the state-of-the-art methods for distributed PGO. Section III introduces mathematical notation and preliminaries that are used in this paper. Section IV formulates the problem of distributed PGO. Sections V and VI present surrogate functions for individual loss terms and the overall distributed PGO, respectively, which are fundamental to our MM methods. Sections VII to IX present unaccelerated and accelerated MM methods for distributed PGO that are guaranteed to converge to first-order critical points, which are the major contributions of this paper. Section X implements our MM methods for distributed PGO on a number of simulated and real-world SLAM datasets and make extensive comparisons against existing state-of-the-art methods [36], [37]. Section XI concludes this paper and discusses future work.

II. RELATED WORK

In the last decade, multi-robot SLAM has been becoming increasingly popular, which promotes the research of distributed PGO [36]–[39].

Choudhary et al. [36] present a two-stage algorithm that implements either Jacobi Over-Relaxation or Successive Over-Relaxation as distributed linear system solvers. Similar to centralized methods, [36] first evaluates the chordal initialization [40] and then improves the initial guess with a single Gauss-Newton step. However, one step of Gauss-Newton method in most cases can not lead to sufficient convergence for distributed PGO. In addition, no line search is performed in [36] due to the communication limitation, and thus, the behaviors of the single Gauss-Newton step is totally unpredictable and might result in bad solutions.

Tian et al. [37] present the distributed certifiably correct PGO using Riemannian block coordinate descent method, which is later generalized to asynchronous and parallel distributed PGO [41]. Specially, their method makes use of Riemannian staircase optimization to solve the semidefinite relaxation of distributed PGO and is guaranteed to converge to

global optimal solutions under moderate measurement noise. Following our previous works [31], [32], they implement Nesterov’s method for acceleration as well. Contrary to our MM methods, a major drawback of [37] is that their method has to precompute red-black coloring assignment for block aggregation and keep part of the blocks in idle for estimate updates. In addition, although several strategies for block selection (e.g., greedy/importance sampling) and Nesterov’s acceleration (e.g., adaptive/fixed restarts) are adopted in [37] to improve the convergence, most of them are either inapplicable without a master node or at the sacrifice of computational efficiency and theoretical guarantees. In contrast, our MM methods are much faster (see Section X) but have no such restrictions for acceleration. More recently, Tian et al. further apply Riemannian block coordinate descent method to distributed PGO with robust loss kernels [28]. However, they solve robust distributed PGO by trivially updating the weights using graduated nonconvexity [42] and no formal proofs of convergence are provided. Again, this is contrast to the work presented here that has provable convergence to first-order critical points for a broad class of robust loss kernels.

Tron and Vidal [38] present a consensus-based method for distributed PGO using Riemannian gradient. The authors derive a condition for convergence guarantees related with the stepsize of the method and the degree of the pose graph. Nonetheless, their method estimates rotation and translation separately, fails to handle robust loss kernels, and needs extra computation to find the convergence-guaranteed stepsize.

Cristofalo et al. [39] present a novel distributed PGO method using Lyapunov theory and multi-agent consensus. Their method is guaranteed to converge if the pose graph has certain topological structures. However, [39] updates rotations without exploiting the translational measurements and only applies to pairwise consistent PGO with nonrobust loss kernels.

In comparison to these aforementioned techniques, our MM methods have the mildest conditions (not requiring any specific pose graph structures, any extra computation for preprocessing, any master nodes for information aggregation, etc.) to converge to first-order critical points, apply to a broad class of robust loss kernels in robotics and computer vision, and manage to implement decentralized acceleration with convergence guarantees. Most importantly, as is shown in Section X, our MM methods outperform existing state-of-the-art methods in terms of both efficiency and accuracy on a variety of SLAM benchmark datasets.

III. NOTATION¹

Miscellaneous Sets. \mathbb{R} denotes the sets of real numbers; \mathbb{R}^+ denotes the sets of nonnegative real numbers; $\mathbb{R}^{m \times n}$ and \mathbb{R}^n denote the sets of $m \times n$ matrices and $n \times 1$ vectors, respectively. $SO(d)$ denotes the set of special orthogonal groups and $SE(d)$ denotes the set of special Euclidean groups. The notation $|\cdot|$ denotes the cardinality of a set.

Matrices. For a matrix $X \in \mathbb{R}^{m \times n}$, the notation $[X]_{ij}$ denotes the (i, j) -th entry or (i, j) -th block of X , and the

¹A more complete summary of the notation used in this paper is given in Appendix A.

notation $[X]_i$ denotes the i -th entry or i -th block of X . For symmetric matrices $X, Y \in \mathbb{R}^{n \times n}$, $X \succeq Y$ (or $Y \preceq X$) and $X \succ Y$ (or $Y \prec X$) mean that $X - Y$ is positive (or negative) semidefinite and definite, respectively.

Inner Products. For a matrix $M \in \mathbb{R}^{n \times n}$, $\langle \cdot, \cdot \rangle_M : \mathbb{R}^{m \times n} \times \mathbb{R}^{m \times n} \rightarrow \mathbb{R}$ denotes the function

$$\langle X, Y \rangle_M \triangleq \text{trace}(XMY^\top) \quad (1)$$

where $X, Y \in \mathbb{R}^{m \times n}$, and if M is the identity matrix, $\langle \cdot, \cdot \rangle_M$ might also be denoted as $\langle \cdot, \cdot \rangle : \mathbb{R}^{m \times n} \times \mathbb{R}^{m \times n} \rightarrow \mathbb{R}$ such that

$$\langle X, Y \rangle \triangleq \text{trace}(XY^\top). \quad (2)$$

Norms. The notation $\| \cdot \|$ denotes the Frobenius norm of matrices and vectors. The notation $\| \cdot \|_2$ denotes the induced 2-norms of matrices and linear operators. For a positive semidefinite matrix $M \in \mathbb{R}^{n \times n}$, $\| \cdot \|_M : \mathbb{R}^{m \times n} \rightarrow \mathbb{R}^+$ denotes the function

$$\|X\|_M \triangleq \sqrt{\text{trace}(XMX^\top)} \quad (3)$$

where $X \in \mathbb{R}^{m \times n}$.

Riemannian Geometry. If $F(\cdot) : \mathbb{R}^{m \times n} \rightarrow \mathbb{R}$ is a function, $\mathcal{M} \subset \mathbb{R}^{m \times n}$ is a Riemannian manifold and $X \in \mathcal{M}$, the notation $\nabla F(X)$ and $\text{grad } F(X)$ denote the Euclidean and Riemannian gradients, respectively.

Graph Theory. Let $\vec{\mathcal{G}} = (\mathcal{V}, \vec{\mathcal{E}})$ be a directed graph whose vertices are ordered pairs. For any vertices (α, i) and $(\beta, j) \in \mathcal{V}$, the notation $\vec{\mathcal{E}}^{\alpha\beta}$ denotes the set

$$\vec{\mathcal{E}}^{\alpha\beta} \triangleq \{(i, j) | ((\alpha, i), (\beta, j)) \in \vec{\mathcal{E}}\}, \quad (4)$$

and the notation \mathcal{N}_-^α denotes the set

$$\mathcal{N}_-^\alpha \triangleq \{\beta | \vec{\mathcal{E}}^{\alpha\beta} \neq \emptyset \text{ and } \alpha \neq \beta\}, \quad (5)$$

and the notation \mathcal{N}_+^α denotes the set

$$\mathcal{N}_+^\alpha \triangleq \{\beta | \vec{\mathcal{E}}^{\beta\alpha} \neq \emptyset \text{ and } \alpha \neq \beta\}, \quad (6)$$

and the notation \mathcal{N}^α denotes the set

$$\mathcal{N}^\alpha \triangleq \mathcal{N}_-^\alpha \cup \mathcal{N}_+^\alpha. \quad (7)$$

Optimization. For optimization variables $X, X^\alpha, R^\alpha, t^\alpha$, etc., the notation $X^{(k)}, X^{\alpha(k)}, R^{\alpha(k)}, t^{\alpha(k)}$, etc. denotes the k -th iterate of corresponding optimization variables.

IV. PROBLEM FORMULATION

A. Distributed Pose Graph Optimization

In distributed PGO [32], [36]–[38], we are given $|\mathcal{A}|$ nodes $\mathcal{A} \triangleq \{1, 2, \dots, |\mathcal{A}|\}$ and each node $\alpha \in \mathcal{A}$ has n_α poses $g_1^\alpha, g_2^\alpha, \dots, g_{n_\alpha}^\alpha \in SE(d)$. Let $g_{(\cdot)}^\alpha \triangleq (t_{(\cdot)}^\alpha, R_{(\cdot)}^\alpha)$ where $t_{(\cdot)}^\alpha \in \mathbb{R}^d$ is the translation and $R_{(\cdot)}^\alpha \in SO(d)$ the rotation. We consider the problem of estimating unknown poses $g_1^\alpha, g_2^\alpha, \dots, g_{n_\alpha}^\alpha \in SE(d)$ for all the nodes $\alpha \in \mathcal{A}$ given intra-node noisy measurements $\tilde{g}_{ij}^{\alpha\alpha} \triangleq (\tilde{t}_{ij}^{\alpha\alpha}, \tilde{R}_{ij}^{\alpha\alpha}) \in SE(d)$ of the relative pose

$$g_{ij}^{\alpha\alpha} \triangleq (g_i^\alpha)^{-1} g_j^\alpha \in SE(d) \quad (8)$$

within a single node α , and inter-node noisy measurements $\tilde{g}_{ij}^{\alpha\beta} \triangleq (\tilde{t}_{ij}^{\alpha\beta}, \tilde{R}_{ij}^{\alpha\beta}) \in SE(d)$ of the relative pose

$$g_{ij}^{\alpha\beta} \triangleq (g_i^\alpha)^{-1} g_j^\beta \in SE(d) \quad (9)$$

between different nodes $\alpha \neq \beta$. In Eqs. (8) and (9), note that $\tilde{t}_{ij}^{\alpha\alpha}$ and $\tilde{t}_{ij}^{\alpha\beta} \in \mathbb{R}^d$ are translational measurements, and $\tilde{R}_{ij}^{\alpha\alpha}$ and $\tilde{R}_{ij}^{\alpha\beta} \in SO(d)$ are rotational measurements.

Following [8], we model distributed PGO as a directed graph $\vec{\mathcal{G}} \triangleq (\mathcal{V}, \vec{\mathcal{E}})$ whose vertices are ordered pairs consisting of node index, e.g., α and β and pose index, e.g., i and j . In the directed graph $\vec{\mathcal{G}}$, the vertex $(\alpha, i) \in \mathcal{V}$ is in one-to-one correspondence with the unknown pose $g_i^\alpha \in SE(d)$ and the directed edge $((\alpha, i), (\beta, j)) \in \vec{\mathcal{E}}$ is in one-to-one correspondence with the noisy measurement $\tilde{g}_{ij}^{\alpha\beta} \in SE(d)$. Note that $\vec{\mathcal{E}}^{\alpha\beta}$, \mathcal{N}_-^α , \mathcal{N}_+^α and \mathcal{N}^α in Eqs. (4) to (7) are well defined for distributed PGO.

From the convention of distributed PGO, nodes α and $\beta \in \mathcal{A}$ are referred as neighbors as long as either $\vec{\mathcal{E}}^{\alpha\beta} \neq \emptyset$ or $\vec{\mathcal{E}}^{\beta\alpha} \neq \emptyset$. We remark that \mathcal{N}^α is the set of neighbors that has a directed edge connected with node α , and \mathcal{N}_-^α and \mathcal{N}_+^α are the sets of neighbors that have a directed edge from and to node α , respectively.

In the rest of this paper, we make the following assumption that each node can communicate with its neighbors and the network topology is unchanged during optimization. These assumptions are common in distributed PGO [36]–[39].

Assumption 1. Each node α can communicate with its neighbors $\beta \in \mathcal{N}^\alpha$ and the network topology is unchanged.

B. Loss Kernels

In practice, it is inevitable that there exist inter-node measurements that are outliers resulting from false loop closures; these adversely affect the overall performance of distributed PGO. To address this issue, it is popular to use non-trivial loss kernels—e.g., Huber and Welsch losses—to enhance the robustness of distributed PGO against outliers [43]–[45].

In this paper, we make the following assumption that applies to a broad class of loss kernels $\rho(\cdot) : \mathbb{R}^+ \rightarrow \mathbb{R}$ in robotics and computer vision.

Assumption 2. The loss kernel $\rho(\cdot) : \mathbb{R}^+ \rightarrow \mathbb{R}$ satisfies the following properties:

- $\rho(s) \geq 0$ for any $s \in \mathbb{R}^+$ and the equality “=” holds if and only if $s = 0$;
- $\rho(\cdot) : \mathbb{R}^+ \rightarrow \mathbb{R}$ is continuously differentiable;
- $\rho(\cdot) : \mathbb{R}^+ \rightarrow \mathbb{R}$ is a concave function;
- $0 \leq \nabla \rho(s) \leq 1$ for any $s \in \mathbb{R}^+$ and $\nabla \rho(0) = 1$;
- $\varphi(\cdot) : \mathbb{R}^{m \times n} \rightarrow \mathbb{R}$ with $\varphi(X) \triangleq \rho(\|X\|^2)$ has Lipschitz continuous gradient, i.e., there exists $\mu > 0$ such that $\|\nabla \varphi(X) - \nabla \varphi(X')\| \leq \mu \cdot \|X - X'\|$ for any $X, X' \in \mathbb{R}^{m \times n}$.

In the following, we present some examples of loss kernels (see Fig. 1) satisfying Assumption 2.

Example 1 (Trivial Loss).

$$\rho(s) = s. \quad (10)$$

Example 2 (Huber Loss).

$$\rho(s) = \begin{cases} s, & |s| \leq a, \\ 2\sqrt{a|s|} - a, & |s| \geq a \end{cases} \quad (11)$$

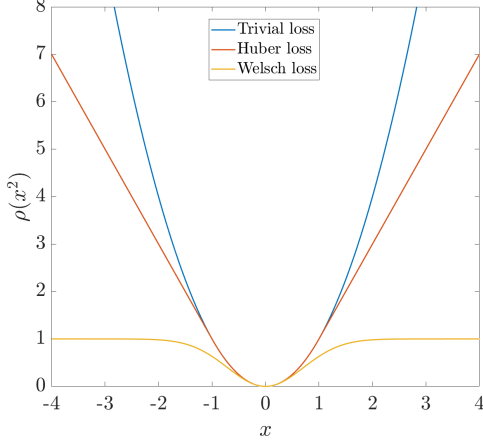


Fig. 1: $\rho(x^2)$ for trivial, Huber, Welsch losses.

where $a > 0$.

Example 3 (Welsch Loss).

$$\rho(s) = a - a \exp\left(-\frac{s}{a}\right) \quad (12)$$

where $a > 0$.

C. Objective Function

Recall that each node $\alpha \in \mathcal{A}$ has n_α unknown poses $g_1^\alpha, g_2^\alpha, \dots, g_{n_\alpha}^\alpha \in SE(d)$. For notational simplicity, we define \mathcal{X}^α and \mathcal{X} as

$$\mathcal{X}^\alpha \triangleq \mathbb{R}^{d \times n_\alpha} \times SO(d)^{n_\alpha}$$

and

$$\mathcal{X} \triangleq \mathcal{X}^1 \times \dots \times \mathcal{X}^{|\mathcal{A}|} \subset \mathbb{R}^{d \times (d+1)n},$$

respectively, where $n \triangleq \sum_{\alpha \in \mathcal{A}} n_\alpha$. Furthermore, we represent $g_i^\alpha \in SE(d)$, i.e., the i -th pose of node $\alpha \in \mathcal{A}$, as a $d \times (d+1)$ matrix

$$X_i^\alpha \triangleq \begin{bmatrix} t_i^\alpha & R_i^\alpha \end{bmatrix} \in SE(d) \subset \mathbb{R}^{d \times (d+1)}, \quad (13)$$

represent $(g_1^\alpha, g_2^\alpha, \dots, g_{n_\alpha}^\alpha) \in SE(d)^{n_\alpha}$, i.e., all the poses of node $\alpha \in \mathcal{A}$, as an element of \mathcal{X}^α as well as a $d \times (d+1)n_\alpha$ matrix

$$X^\alpha \triangleq \begin{bmatrix} t^\alpha & R^\alpha \end{bmatrix} \in \mathcal{X}^\alpha \subset \mathbb{R}^{d \times (d+1)n_\alpha}, \quad (14)$$

where

$$t^\alpha \triangleq [t_1^\alpha \quad \dots \quad t_{n_\alpha}^\alpha] \in \mathbb{R}^{d \times n_\alpha}$$

and

$$R^\alpha \triangleq [R_1^\alpha \quad \dots \quad R_{n_\alpha}^\alpha] \in SO(d)^{n_\alpha} \subset \mathbb{R}^{d \times dn_\alpha},$$

and represent $\{(g_1^\alpha, g_2^\alpha, \dots, g_{n_\alpha}^\alpha)\}_{\alpha \in \mathcal{A}} \in SE(d)^n$, i.e., all the poses of distributed PGO, as an element of \mathcal{X} as well as a $d \times (d+1)n$ matrix

$$X \triangleq [X^1 \quad \dots \quad X^{|\mathcal{A}|}] \in \mathcal{X} \subset \mathbb{R}^{d \times (d+1)n}. \quad (15)$$

Remark 1. \mathcal{X}^α and \mathcal{X} are by definition homeomorphic to $SE(d)^{n_\alpha}$ and $SE(d)^n$, respectively. Thus, $X^\alpha \in \mathcal{X}^\alpha$ and $X \in \mathcal{X}$ are sufficient to represent elements of $SE(d)^{n_\alpha}$ and $SE(d)^n$.

Following [8], [31], [32], distributed PGO can be formulated as an optimization problem on $X = [X^1 \quad \dots \quad X^{|\mathcal{A}|}] \in \mathcal{X}$:

Problem 1 (Distributed Pose Graph Optimization).

$$\min_{X \in \mathcal{X}} F(X). \quad (16)$$

The objective function $F(X)$ in Eq. (16) is defined as

$$\begin{aligned} F(X) \triangleq & \sum_{\alpha \in \mathcal{A}} \sum_{(i,j) \in \vec{\mathcal{E}}^{\alpha\alpha}} \frac{1}{2} \left[\kappa_{ij}^{\alpha\alpha} \|R_i^\alpha \tilde{R}_{ij}^{\alpha\alpha} - R_j^\alpha\|^2 + \right. \\ & \left. \tau_{ij}^{\alpha\alpha} \|R_i^\alpha \tilde{t}_{ij}^{\alpha\alpha} + t_i^\alpha - t_j^\alpha\|^2 \right] + \\ & \sum_{\substack{\alpha, \beta \in \mathcal{A}, \\ \alpha \neq \beta}} \sum_{(i,j) \in \vec{\mathcal{E}}^{\alpha\beta}} \frac{1}{2} \left[\rho \left(\kappa_{ij}^{\alpha\beta} \|R_i^\alpha \tilde{R}_{ij}^{\alpha\beta} - R_j^\beta\|^2 + \right. \right. \\ & \left. \left. \tau_{ij}^{\alpha\beta} \|R_i^\alpha \tilde{t}_{ij}^{\alpha\beta} + t_i^\alpha - t_j^\beta\|^2 \right) \right], \quad (17) \end{aligned}$$

where $\kappa_{ij}^{\alpha\alpha}, \tau_{ij}^{\alpha\alpha}, \kappa_{ij}^{\alpha\beta}, \tau_{ij}^{\alpha\beta}$ are the weights and $\rho(\cdot) : \mathbb{R}^+ \rightarrow \mathbb{R}$ is the loss kernel.

For notational simplicity, $F(X)$ in Eq. (17) can be also rewritten as

$$\begin{aligned} F(X) = & \sum_{\alpha \in \mathcal{A}} \sum_{(i,j) \in \vec{\mathcal{E}}^{\alpha\alpha}} F_{ij}^{\alpha\alpha}(X) + \\ & \sum_{\substack{\alpha, \beta \in \mathcal{A}, \\ \alpha \neq \beta}} \sum_{(i,j) \in \vec{\mathcal{E}}^{\alpha\beta}} F_{ij}^{\alpha\beta}(X), \quad (18) \end{aligned}$$

where

$$\begin{aligned} F_{ij}^{\alpha\alpha}(X) \triangleq & \frac{1}{2} \kappa_{ij}^{\alpha\alpha} \|R_i^\alpha \tilde{R}_{ij}^{\alpha\alpha} - R_j^\alpha\|^2 + \\ & \frac{1}{2} \tau_{ij}^{\alpha\alpha} \|R_i^\alpha \tilde{t}_{ij}^{\alpha\alpha} + t_i^\alpha - t_j^\alpha\|^2, \quad (19) \end{aligned}$$

and

$$\begin{aligned} F_{ij}^{\alpha\beta}(X) \triangleq & \frac{1}{2} \rho \left(\kappa_{ij}^{\alpha\beta} \|R_i^\alpha \tilde{R}_{ij}^{\alpha\beta} - R_j^\beta\|^2 + \right. \\ & \left. \frac{1}{2} \tau_{ij}^{\alpha\beta} \|R_i^\alpha \tilde{t}_{ij}^{\alpha\beta} + t_i^\alpha - t_j^\beta\|^2 \right), \quad (20) \end{aligned}$$

Note that $F_{ij}^{\alpha\alpha}(X)$ and $F_{ij}^{\alpha\beta}$ corresponds to intra- and inter-node measurements, respectively.

In the next sections, we will present MM methods for distributed PGO, which is the major contribution of this paper.

V. THE MAJORIZATION OF LOSS KERNELS

In this section, we will present surrogate functions majorizing the loss kernels $\rho(\cdot)$. The resulting surrogate functions lead to an intermediate upper bound of distributed PGO while attaining the same value as the original objective function at each iterate.

It is straightforward to show that there exists sparse and positive semidefinite matrices $M_{ij}^{\alpha\beta} \in \mathbb{R}^{(d+1)n \times (d+1)n}$ for either $\alpha = \beta$ or $\alpha \neq \beta$ such that

$$\begin{aligned} \frac{1}{2} \|X\|_{M_{ij}^{\alpha\beta}}^2 = & \frac{1}{2} \kappa_{ij}^{\alpha\beta} \|R_i^\alpha \tilde{R}_{ij}^{\alpha\beta} - R_j^\beta\|^2 + \\ & \frac{1}{2} \tau_{ij}^{\alpha\beta} \|R_i^\alpha \tilde{t}_{ij}^{\alpha\beta} + t_i^\alpha - t_j^\beta\|^2. \quad (21) \end{aligned}$$

Then, in terms of intra-node measurements with $\alpha = \beta$ and inter-node measurements with $\alpha \neq \beta$, $F_{ij}^{\alpha\alpha}(X)$ and $F_{ij}^{\alpha\beta}$ take the form of

$$F_{ij}^{\alpha\alpha}(X) \triangleq \frac{1}{2} \|X\|_{M_{ij}^{\alpha\alpha}}^2 \quad (22)$$

and

$$F_{ij}^{\alpha\beta}(X) \triangleq \frac{1}{2} \rho(\|X\|_{M_{ij}^{\alpha\beta}}^2), \quad (23)$$

respectively. From Eqs. (19) and (20), we obtain an upper bound of $F_{ij}^{\alpha\alpha}(X)$ and $F_{ij}^{\alpha\beta}(X)$ as the following proposition states.

Proposition 1. Let $X^{(k)} = [X^{1(k)} \ \dots \ X^{|\mathcal{A}|(k)}] \in \mathcal{X}$ with $X^{\alpha(k)} \in \mathcal{X}^\alpha$ be an iterate of Eq. (16). If $\rho(\cdot) : \mathbb{R}^+ \rightarrow \mathbb{R}$ is a loss kernel that satisfies Assumption 2, then we obtain

$$\frac{1}{2} \omega_{ij}^{\alpha\beta(k)} \|X - X^{(k)}\|_{M_{ij}^{\alpha\beta}}^2 + \langle \nabla F_{ij}^{\alpha\beta}(X^{(k)}), X - X^{(k)} \rangle + F_{ij}^{\alpha\beta}(X^{(k)}) \geq F_{ij}^{\alpha\beta}(X) \quad (24)$$

for any X and $X^{(k)} \in \mathbb{R}^{d \times (d+1)n}$, in which $\omega_{ij}^{\alpha\beta(k)} \in \mathbb{R}$ is defined as

$$\omega_{ij}^{\alpha\beta(k)} \triangleq \begin{cases} 1, & \alpha = \beta, \\ \nabla \rho(\|X^{(k)}\|_{M_{ij}^{\alpha\beta}}^2), & \alpha \neq \beta. \end{cases} \quad (25)$$

In Eq. (24), the equality “=” holds as long as $X = X^{(k)}$.

Proof. See Appendix B. \square

Note that $F(X)$, as is shown in Eq. (18), is equivalent to the sum of all $F_{ij}^{\alpha\alpha}(X)$ and $F_{ij}^{\alpha\beta}(X)$. Then, an immediate upper bound of $F(X)$ resulting from Proposition 1 is

$$\frac{1}{2} \|X - X^{(k)}\|_{M^{(k)}}^2 + \langle \nabla F(X^{(k)}), X - X^{(k)} \rangle + F(X^{(k)}) \geq F(X) \quad (26)$$

in which $M^{(k)} \in \mathbb{R}^{(d+1)n \times (d+1)n}$ is a positive semidefinite matrix that is defined as

$$M^{(k)} \triangleq \sum_{\alpha \in \mathcal{A}} \sum_{(i,j) \in \vec{\mathcal{E}}^{\alpha\alpha}} M_{ij}^{\alpha\alpha} + \sum_{\substack{\alpha, \beta \in \mathcal{A}, \\ \alpha \neq \beta}} \sum_{(i,j) \in \vec{\mathcal{E}}^{\alpha\beta}} \omega_{ij}^{\alpha\beta(k)} \cdot M_{ij}^{\alpha\beta} \in \mathbb{R}^{(d+1)n \times (d+1)n}. \quad (27)$$

In addition, the equality “=” in Eq. (26) holds as long as $X = X^{(k)}$.

Remark 2. If the loss kernel $\rho(\cdot)$ is non-trivial, $\omega_{ij}^{\alpha\beta(k)}$ is a function of $X^{(k)}$ as defined in Eq. (25), and $M^{(k)}$ is a positive semidefinite matrix depending on $X^{(k)}$ as well.

It is obvious that Eq. (26) has $X^\alpha \in \mathcal{X}^\alpha$ of different nodes coupled with each other, and as a result, is difficult to be used for distributed PGO. In spite of that, as is shown in the next sections, Eq. (26) is still useful for the development and analysis of our MM methods for distributed PGO.

VI. THE MAJORIZATION OF DISTRIBUTED POSE GRAPH OPTIMIZATION

In this section, following a similar procedure to our previous works [31], [32], we will present surrogate functions $G(X|X^{(k)})$ and $H(X|X^{(k)})$ that majorize the objective function $F(X)$. The surrogate functions $G(X|X^{(k)})$ and $H(X|X^{(k)})$ decouple unknown poses of different nodes, and thus, are critical to our MM methods for distributed PGO.

A. The Majorization of $F_{ij}^{\alpha\beta}(X)$

For any matrices B, C and $P \in \mathbb{R}^{m \times n}$, it can be shown that

$$\frac{1}{2} \|B - C\|_{M_{ij}^{\alpha\beta}}^2 \leq \|B - P\|_{M_{ij}^{\alpha\beta}}^2 + \|C - P\|_{M_{ij}^{\alpha\beta}}^2 \quad (28)$$

as long as $M_{ij}^{\alpha\beta} \in \mathbb{R}^{n \times n}$ is positive semidefinite, where “=” holds if

$$P = \frac{1}{2}B + \frac{1}{2}C.$$

If we let $P = \mathbf{0}$, Eq. (28) becomes

$$\frac{1}{2} \|B - C\|_{M_{ij}^{\alpha\beta}}^2 \leq \|B\|_{M_{ij}^{\alpha\beta}}^2 + \|C\|_{M_{ij}^{\alpha\beta}}^2. \quad (29)$$

Applying Eq. (29) on the right-hand side of Eq. (21), we obtain

$$\begin{aligned} \frac{1}{2} \|X\|_{M_{ij}^{\alpha\beta}}^2 &\leq \kappa_{ij}^{\alpha\beta} \|R_i^\alpha \tilde{R}_{ij}^{\alpha\beta}\|^2 + \kappa_{ij}^{\alpha\beta} \|R_j^\beta\|^2 + \\ &\quad \tau_{ij}^{\alpha\beta} \|R_i^\alpha \tilde{t}_{ij}^{\alpha\beta} + t_i^\alpha\|^2 + \tau_{ij}^{\alpha\beta} \|t_j^\beta\|^2 \\ &= \kappa_{ij}^{\alpha\beta} \|R_i^\alpha\|^2 + \kappa_{ij}^{\alpha\beta} \|R_j^\beta\|^2 + \\ &\quad \tau_{ij}^{\alpha\beta} \|R_i^\alpha \tilde{t}_{ij}^{\alpha\beta} + t_i^\alpha\|^2 + \tau_{ij}^{\alpha\beta} \|t_j^\beta\|^2, \end{aligned} \quad (30)$$

where the last equality is due to $(\tilde{R}_{ij}^{\alpha\beta})^\top \tilde{R}_{ij}^{\alpha\beta} = \tilde{R}_{ij}^{\alpha\beta} (\tilde{R}_{ij}^{\alpha\beta})^\top = \mathbf{I}$. Furthermore, there exists a positive semidefinite matrix $\Omega_{ij}^{\alpha\beta} \in \mathbb{R}^{(d+1)n \times (d+1)n}$ such that the right-hand side of Eq. (30) can be rewritten as

$$\begin{aligned} \frac{1}{2} \|X\|_{\Omega_{ij}^{\alpha\beta}}^2 &= \kappa_{ij}^{\alpha\beta} \|R_i^\alpha\|^2 + \kappa_{ij}^{\alpha\beta} \|R_j^\beta\|^2 + \\ &\quad \tau_{ij}^{\alpha\beta} \|R_i^\alpha \tilde{t}_{ij}^{\alpha\beta} + t_i^\alpha\|^2 + \tau_{ij}^{\alpha\beta} \|t_j^\beta\|^2, \end{aligned} \quad (31)$$

where $\Omega_{ij}^{\alpha\beta}$ is a block diagonal matrix decoupling unknown poses of different nodes. Replacing the right-hand side of Eq. (30) with Eq. (31) results in

$$\frac{1}{2} \|X\|_{M_{ij}^{\alpha\beta}}^2 \leq \frac{1}{2} \|X\|_{\Omega_{ij}^{\alpha\beta}}^2$$

for any $X \in \mathbb{R}^{d \times (d+1)n}$, which suggests

$$\Omega_{ij}^{\alpha\beta} \succeq M_{ij}^{\alpha\beta}. \quad (32)$$

With $\Omega_{ij}^{\alpha\beta} \in \mathbb{R}^{(d+1)n \times (d+1)n}$ in Eqs. (31) and (32), we define $E_{ij}^{\alpha\beta}(\cdot|X^{(k)}) : \mathbb{R}^{d \times (d+1)n} \rightarrow \mathbb{R}$:

$$\begin{aligned} E_{ij}^{\alpha\beta}(X|X^{(k)}) &\triangleq \frac{1}{2} \omega_{ij}^{\alpha\beta(k)} \|X - X^{(k)}\|_{\Omega_{ij}^{\alpha\beta}}^2 \\ &\quad \langle \nabla F_{ij}^{\alpha\beta}(X^{(k)}), X - X^{(k)} \rangle + F_{ij}^{\alpha\beta}(X^{(k)}), \end{aligned} \quad (33)$$

where $\omega_{ij}^{\alpha\beta(k)}$ is given in Eq. (25). From the equation above, it can be concluded that $E_{ij}^{\alpha\beta}(X|X^{(k)})$ majorizes $F_{ij}^{\alpha\beta}(X)$ as

the following proposition states, which is important for the construction of surrogate functions for distributed PGO.

Proposition 2. Given any nodes $\alpha, \beta \in \mathcal{A}$ with either $\alpha = \beta$ or $\alpha \neq \beta$, if $\rho(\cdot) : \mathbb{R}^+ \rightarrow \mathbb{R}$ is a loss kernel that satisfies Assumption 2, then we obtain

$$E_{ij}^{\alpha\beta}(X|X^{(k)}) \geq F_{ij}^{\alpha\beta}(X). \quad (34)$$

for any $X \in \mathbb{R}^{d \times (d+1)n}$. In the equation above, the equality “=” holds if $X = X^{(k)}$.

Proof. See Appendix C. \square

B. The Majorization of $F(X)$

From Proposition 2, it is straightforward to construct surrogate functions that majorize $F(X)$ in Eqs. (17) and (18) as the following proposition states.

Proposition 3. Let $X^{(k)} = [X^{1(k)} \ \dots \ X^{|\mathcal{A}|(k)}] \in \mathcal{X}$ with $X^{\alpha(k)} \in \mathcal{X}^\alpha$ be an iterate of $X \in \mathcal{X}$ for Eq. (16). Let $G(\cdot|X^{(k)}) : \mathbb{R}^{d \times (d+1)n} \rightarrow \mathbb{R}$ be a function that is defined as

$$G(X|X^{(k)}) \triangleq \sum_{\alpha \in \mathcal{A}} \sum_{(i,j) \in \vec{\mathcal{E}}^{\alpha\alpha}} F_{ij}^{\alpha\alpha}(X) + \sum_{\substack{\alpha, \beta \in \mathcal{A}, \\ \alpha \neq \beta}} \sum_{(i,j) \in \vec{\mathcal{E}}^{\alpha\beta}} E_{ij}^{\alpha\beta}(X|X^{(k)}) + \frac{\xi}{2} \|X - X^{(k)}\|^2 \quad (35)$$

where $\xi \in \mathbb{R}$ and $\xi \geq 0$. Then, we have the following results:

(a) For any node $\alpha \in \mathcal{A}$, there exists positive-semidefinite matrices $\Gamma^{\alpha(k)} \in \mathbb{R}^{(d+1)n_\alpha \times (d+1)n_\alpha}$ such that $G(X|X^{(k)})$ is equivalent to

$$G(X|X^{(k)}) = \sum_{\alpha \in \mathcal{A}} G^\alpha(X^\alpha|X^{(k)}) + F(X^{(k)}), \quad (36)$$

where $G^\alpha(X^\alpha|X^{(k)})$ is defined as

$$G^\alpha(X^\alpha|X^{(k)}) \triangleq \frac{1}{2} \|X^\alpha - X^{\alpha(k)}\|_{\Gamma^{\alpha(k)}}^2 + \langle \nabla_{X^\alpha} F(X^{(k)}), X^\alpha - X^{\alpha(k)} \rangle. \quad (37)$$

In Eq. (37), $\nabla_{X^\alpha} F(X^{(k)})$ is the Euclidean gradient of $F(X)$ with respect to $X^\alpha \in \mathcal{X}^\alpha$ at $X^{(k)} \in \mathcal{X}$.

(b) $G(X|X^{(k)})$ is a proximal operator of $F(X)$ at $X^{(k)} \in \mathcal{X}$ and can be written as

$$G(X|X^{(k)}) = \frac{1}{2} \|X - X^{(k)}\|_{\Gamma^{(k)}}^2 + \langle \nabla F(X^{(k)}), X - X^{(k)} \rangle + F(X^{(k)}), \quad (38)$$

where $\Gamma^{(k)} \in \mathbb{R}^{(d+1)n \times (d+1)n}$ is a block diagonal matrix

$$\Gamma^{(k)} \triangleq \text{diag}\{\Gamma^{1(k)}, \dots, \Gamma^{|\mathcal{A}|(k)}\} \in \mathbb{R}^{(d+1)n \times (d+1)n}, \quad (39)$$

and $\nabla F(X^{(k)}) \in \mathbb{R}^{d \times (d+1)n}$ is the Euclidean gradient of $F(X)$ at $X^{(k)} \in \mathcal{X}$. Furthermore, we have

$$G(X|X^{(k)}) \geq F(X) \quad (40)$$

where the equality “=” holds if $X = X^{(k)}$.

(c) $\Gamma^{(k)} \succeq M^{(k)}$ where $M^{(k)}$ is given in Eq. (27).

(d) $\Gamma^{(k)}$ is bounded, i.e., there exists a constant positive-semidefinite matrix $\Gamma \in \mathbb{R}^{(d+1)n \times (d+1)n}$ such that $\Gamma \succeq \Gamma^{(k)}$ holds for any $k \geq 0$.

Proof. See Appendix D. \square

Remark 3. From Proposition 3, $G(X|X^{(k)})$ in Eq. (35) is a proximal operator and an upper bound of $F(X)$. Furthermore, Eq. (36) indicates that $G(X|X^{(k)})$ can be decomposed as the sum of $G^\alpha(X^\alpha|X^{(k)})$ that is a function of $X^\alpha \in \mathcal{X}^\alpha \subset \mathbb{R}^{d \times (d+1)n_\alpha}$ within a single node $\alpha \in \mathcal{A}$, making $G(X|X^{(k)})$ well-suited for distributed PGO.

If substituting Eqs. (33) and (34) into Eq. (35) and replacing $F_{ij}^{\alpha\alpha}(X|X^{(k)})$ with $E_{ij}^{\alpha\alpha}(X|X^{(k)})$, we have $F(X)$ as well as $G(X|X^{(k)})$ further majorized as the following proposition states.

Proposition 4. Let $X^{(k)} = [X^{1(k)} \ \dots \ X^{|\mathcal{A}|(k)}] \in \mathcal{X}$ with $X^{\alpha(k)} \in \mathcal{X}^\alpha$ be an iterate of $X \in \mathcal{X}$ for Eq. (16), and $X_i^{\alpha(k)} = [t^{\alpha(k)} \ R^{\alpha(k)}] \in SE(d)$ be the corresponding iterate of $X_i^\alpha \in SE(d)$. Let $H(\cdot|X^{(k)}) : \mathbb{R}^{d \times (d+1)n} \rightarrow \mathbb{R}$ be a function that is defined as

$$H(X|X^{(k)}) = \sum_{\alpha \in \mathcal{A}} \sum_{(i,j) \in \vec{\mathcal{E}}^{\alpha\alpha}} E_{ij}^{\alpha\alpha}(X|X^{(k)}) + \sum_{\substack{\alpha, \beta \in \mathcal{A}, \\ \alpha \neq \beta}} \sum_{(i,j) \in \vec{\mathcal{E}}^{\alpha\beta}} E_{ij}^{\alpha\beta}(X|X^{(k)}) + \frac{\zeta}{2} \|X - X^{(k)}\|^2. \quad (41)$$

In Eq. (41), $\zeta \in \mathbb{R}$ and $\zeta \geq \xi \geq 0$ where $\xi \in \mathbb{R}$ is given in $G(X|X^{(k)})$ of Eq. (35). Then, we have the following results:

(a) For any node $\alpha \in \mathcal{A}$ and $i \in \{1, \dots, n_\alpha\}$, there exists positive-semidefinite matrices $\Pi^{\alpha(k)} \in \mathbb{R}^{(d+1)n_\alpha \times (d+1)n_\alpha}$ and $\Pi_i^{\alpha(k)} \in \mathbb{R}^{(d+1) \times (d+1)}$ such that

$$H(X|X^{(k)}) = \sum_{\alpha \in \mathcal{A}} H^\alpha(X^\alpha|X^{(k)}) + F(X^{(k)}) \quad (42)$$

and

$$H^\alpha(X^\alpha|X^{(k)}) = \sum_{i=1}^{n_\alpha} H_i^\alpha(X_i^\alpha|X^{(k)}), \quad (43)$$

where $H^\alpha(X^\alpha|X^{(k)})$ and $H_i^\alpha(X_i^\alpha|X^{(k)})$ are defined as

$$H^\alpha(X^\alpha|X^{(k)}) = \frac{1}{2} \|X^\alpha - X^{\alpha(k)}\|_{\Pi^{\alpha(k)}}^2 + \langle \nabla_{X^\alpha} F(X^{(k)}), X^\alpha - X^{\alpha(k)} \rangle \quad (44)$$

and

$$H_i^\alpha(X_i^\alpha|X^{(k)}) = \frac{1}{2} \|X_i^\alpha - X_i^{\alpha(k)}\|_{\Pi_i^{\alpha(k)}}^2 + \langle \nabla_{X_i^\alpha} F(X^{(k)}), X_i^\alpha - X_i^{\alpha(k)} \rangle, \quad (45)$$

respectively. In Eqs. (44) and (45), $\nabla_{X^\alpha} F(X^{(k)})$ and $\nabla_{X_i^\alpha} F(X^{(k)})$ are the Euclidean gradients of $F(X)$ with respect to $X^\alpha \in \mathcal{X}^\alpha$ and $X_i^\alpha \in SE(d)$ at $X^{(k)} \in \mathcal{X}$, respectively.

- (b) $H(X|X^{(k)})$ is a proximal operator of $F(X)$ at $X^{(k)} \in \mathcal{X}$ and can be written as

$$H(X|X^{(k)}) = \frac{1}{2} \|X - X^{(k)}\|_{\Pi^{(k)}}^2 + \langle \nabla F(X^{(k)}), X - X^{(k)} \rangle + F(X^{(k)}), \quad (46)$$

where $\Pi^{(k)} \in \mathbb{R}^{(d+1)n \times (d+1)n}$ is a block diagonal matrix

$$\Pi^{(k)} \triangleq \text{diag}\{\Pi^1(k), \dots, \Pi^{|\mathcal{A}|}(k)\} \in \mathbb{R}^{(d+1)n \times (d+1)n}, \quad (47)$$

and $\nabla F(X^{(k)}) \in \mathbb{R}^{d \times (d+1)n}$ is the Euclidean gradient of $F(X)$ at $X^{(k)} \in \mathcal{X}$. Furthermore, we have

$$H(X|X^{(k)}) \geq G(X|X^{(k)}) \geq F(X) \quad (48)$$

where the equality “=” holds if $X = X^{(k)}$.

- (c) $\Pi^{(k)} \succeq \Gamma^{(k)} \succeq M^{(k)}$ where $M^{(k)}$ and $\Gamma^{(k)}$ are given in Eqs. (27) and (39), respectively.
- (d) $\Pi^{(k)}$ is bounded, i.e., there exists a constant positive-semidefinite matrix $\Pi \in \mathbb{R}^{(d+1)n \times (d+1)n}$ such that $\Pi \succeq \Pi^{(k)}$ holds for any $k \geq 0$.
- (e) $H^\alpha(X^\alpha|X^{(k)}) \geq G^\alpha(X^\alpha|X^{(k)})$ where $G^\alpha(X^\alpha|X^{(k)})$ is given in Eq. (37) and the equality “=” holds as long as $X^\alpha = X^{\alpha(k)}$.

Proof. The proof is similar to that of Proposition 3. \square

Remark 4. From Eqs. (42) and (43), $H(X|X^{(k)})$ can be rewritten as the sum of $H_i^\alpha(X_i^\alpha|X^{(k)})$:

$$H(X|X^{(k)}) = \sum_{\alpha \in \mathcal{A}} \sum_{i=1}^{n_\alpha} H_i^\alpha(X_i^\alpha|X^{(k)}) + F(X^{(k)}),$$

where each $H_i^\alpha(X_i^\alpha|X^{(k)})$ relies on a single pose $X_i^\alpha \in SE(d) \subset \mathbb{R}^{d \times (d+1)}$. In Sections VII to IX, we will exploit this decomposition of $H(X|X^{(k)})$ to improve the computational efficiency of distributed PGO.

Note that $G^\alpha(X^\alpha|X^{(k)})$ and $H^\alpha(X^\alpha|X^{(k)})$ in Eqs. (37) and (44) rely on $\nabla_{X^\alpha} F(X^{(k)})$, i.e., the Euclidean gradient of $F(X)$ with respect to $X^\alpha \in \mathcal{X}^\alpha$. From Eqs. (18) to (20), $\nabla_{X^\alpha} F(X)$ is related with $F_{ij}^{\alpha\alpha}(X)$, $F_{ij}^{\alpha\beta}(X)$ and $F_{ji}^{\beta\alpha}(X)$, which suggests

$$\begin{aligned} \nabla_{X^\alpha} F(X^{(k)}) \triangleq & \sum_{(i,j) \in \vec{\mathcal{E}}^{\alpha\alpha}} \nabla_{X^\alpha} F_{ij}^{\alpha\alpha}(X^{(k)}) + \\ & \sum_{\beta \in \mathcal{N}^\alpha} \sum_{(i,j) \in \vec{\mathcal{E}}^{\alpha\beta}} \nabla_{X^\alpha} F_{ij}^{\alpha\beta}(X^{(k)}) + \\ & \sum_{\beta \in \mathcal{N}_+^\alpha} \sum_{(j,i) \in \vec{\mathcal{E}}^{\beta\alpha}} \nabla_{X^\alpha} F_{ji}^{\beta\alpha}(X^{(k)}). \end{aligned} \quad (49)$$

As a result of Eqs. (19) and (20), $F_{ij}^{\alpha\alpha}(X)$ depends on X_i^α and X_j^α while $F_{ij}^{\alpha\beta}(X)$ and $F_{ji}^{\beta\alpha}(X)$ on X_i^α and X_j^β . Therefore, $\nabla_{X^\alpha} F(X^{(k)})$ in Eq. (49) can be evaluated with one inter-node communication round between node α and its neighbors $\beta \in \mathcal{N}^\alpha$. Furthermore, if we have $\nabla_{X^\alpha} F(X^{(k)})$ for each node $\alpha \in \mathcal{A}$, $\nabla F(X^{(k)}) \triangleq [\nabla_{X^1} F(X^{(k)}) \ \dots \ \nabla_{X^{|\mathcal{A}|}} F(X^{(k)})]$ is immediately known. Then, we conclude from Eqs. (38) and (46) that $G(X|X^{(k)})$ and $H(X|X^{(k)})$ can be constructed

in a distributed setting with one inter-node communication round between neighboring nodes α and β .

In the next sections, we will present MM methods for distributed PGO using $G(X|X^{(k)})$ and $H(X|X^{(k)})$ that are guaranteed to converge to first-order critical points.

VII. THE MAJORIZATION MINIMIZATION METHOD FOR DISTRIBUTED POSE GRAPH OPTIMIZATION

In distributed optimization, MM methods are one of the most popular first-order optimization methods [29], [30]. As mentioned before, MM methods solve an optimization problem by iteratively minimizing an upper bound of the objective function such that the objective value is either decreased or unchanged.

A. Update Rule

In Section VI, it has been proved that $G(X|X^{(k)})$ and $H(X|X^{(k)})$ are proximal operators of $F(X)$ such that

$$H(X|X^{(k)}) \geq G(X|X^{(k)}) \geq F(X),$$

and

$$H(X^{(k)}|X^{(k)}) = G(X^{(k)}|X^{(k)}) = F(X^{(k)}).$$

Following the notion of MM methods [29], we implement an update rule as the following

$$X^{(k+\frac{1}{2})} \leftarrow \arg \min_{X \in \mathcal{X}} H(X|X^{(k)}), \quad (50)$$

and

$$X^{(k+1)} \leftarrow \arg \min_{X \in \mathcal{X}} G(X|X^{(k)}) \quad (51)$$

which results in

$$F(X^{(k)}) = H(X^{(k)}|X^{(k)}) \geq H(X^{(k+\frac{1}{2})}|X^{(k)}) \geq F(X^{(k+\frac{1}{2})}), \quad (52)$$

and

$$F(X^{(k)}) = G(X^{(k)}|X^{(k)}) \geq G(X^{(k+1)}|X^{(k)}) \geq F(X^{(k+1)}) \quad (53)$$

respectively. From Eq. (42), Eq. (50) is equivalent to

$$X^{\alpha(k+\frac{1}{2})} \leftarrow \arg \min_{X^\alpha \in \mathcal{X}^\alpha} H^\alpha(X^\alpha|X^{(k)}), \quad \forall \alpha \in \mathcal{A}. \quad (54)$$

Similarly, from Eq. (36), Eq. (51) is equivalent to

$$X^{\alpha(k+1)} \leftarrow \arg \min_{X^\alpha \in \mathcal{X}^\alpha} G^\alpha(X^\alpha|X^{(k)}), \quad \forall \alpha \in \mathcal{A}. \quad (55)$$

Note that both Eqs. (54) and (55) can be independently solved within a single node $\alpha \in \mathcal{A}$. Recalling $H^\alpha(X^\alpha|X^{(k)}) = \sum_{i=1}^{n_\alpha} H_i^\alpha(X_i^\alpha|X^{(k)})$ from Eq. (43), we conclude that Eq. (54) can be further reduced to $n \triangleq \sum_{\alpha \in \mathcal{A}} n_\alpha$ independent optimization problems on $X_i^\alpha \in SE(d)$

$$X_i^{\alpha(k+\frac{1}{2})} \leftarrow \arg \min_{X_i^\alpha \in SE(d)} H_i^\alpha(X_i^\alpha|X^{(k)}), \quad \forall \alpha \in \mathcal{A} \text{ and } i \in \{1, \dots, n_\alpha\}. \quad (56)$$

In particular, as is shown in Appendix K, Eq. (56) admits a closed-form solution that only involves matrix multiplication and singular value decomposition [46].

Algorithm 1 The MM–PGO Method

- 1: **Input:** An initial iterate $X^{(0)} \in \mathcal{X}$ and $\zeta \geq \xi \geq 0$.
 - 2: **Output:** A sequence of iterates $\{X^{(k)}\}$ and $\{X^{(k+\frac{1}{2})}\}$.
 - 3: **for** $k \leftarrow 0, 1, 2, \dots$ **do**
 - 4: **for** node $\alpha \leftarrow 1, \dots, |\mathcal{A}|$ **do**
 - 5: retrieve $X^{\beta(k)}$ from $\beta \in \mathcal{N}_\alpha$
 - 6: evaluate $\omega_{ij}^{\alpha\beta(k)}$ and $\omega_{ji}^{\beta\alpha(k)}$ using Eq. (25)
 - 7: evaluate $\nabla_{X^\alpha} F(X^{(k)})$ using Eq. (49)
 - 8: $X^{\alpha(k+\frac{1}{2})} \leftarrow \arg \min_{X^\alpha \in \mathcal{X}^\alpha} H^\alpha(X^\alpha | X^{(k)})$ using Algorithm 2
 - 9: $X^{\alpha(k+1)} \leftarrow \text{improve } \arg \min_{X^\alpha \in \mathcal{X}^\alpha} G^\alpha(X^\alpha | X^{(k)})$
with $X^{\alpha(k+\frac{1}{2})}$ as the initial guess
 - 10: **end for**
 - 11: **end for**
-

Algorithm 2 Solve $X^{\alpha(k+\frac{1}{2})} \leftarrow \arg \min_{X^\alpha \in \mathcal{X}^\alpha} H^\alpha(X^\alpha | X^{(k)})$

- 1: **Input:** $X^{\alpha(k)}$ and $\nabla_{X^\alpha} F(X^{(k)})$.
 - 2: **Output:** $X^{\alpha(k+\frac{1}{2})}$.
 - 3: **for** $i \leftarrow 1, \dots, n_\alpha$ **do**
 - 4: $X_i^{\alpha(k+\frac{1}{2})} \leftarrow \arg \min_{X_i^\alpha \in SE(d)} H_i^\alpha(X_i^\alpha | X^{(k)})$ using Appendix K
 - 5: **end for**
 - 6: retrieve $X^{\alpha(k+\frac{1}{2})}$ from $X_i^{\alpha(k+\frac{1}{2})}$ in which $i = 1, \dots, n_\alpha$
-

As a result of Eqs. (52) and (53), we conclude that iteratively minimizing $H^\alpha(X^\alpha | X^{(k)})$ and $G^\alpha(X^\alpha | X^{(k)})$ improves the estimates and reduces the objective values. In our previous works, we have shown that Eq. (54) can be exactly and efficiently solved in closed form [31], and a local instead of global optimal solution to Eq. (55) is sufficient to guarantee the convergence [32]. Nevertheless, Eq. (54) fails to make full use of the information within a single node and usually induce more iterations, whereas Eq. (55) is still time-consuming to solve locally, both of which restrict the overall performance of distributed PGO.

To address these issues, we propose a novel update rule exploiting both Eqs. (54) and (55) to enhance the overall computational efficiency, in which we precompute an initial estimate from Eq. (54) and then refine the initial estimate with Eq. (55) to get the final estimate.

B. Algorithm

The proposed update rule results in the MM–PGO method for distributed PGO (Algorithm 1). The outline of the MM–PGO method is as follows:

- 1) In line 5 of Algorithm 1, each node α performs one inter-node communication round to retrieve $X^{\beta(k)}$ from its neighbors $\beta \in \mathcal{N}_\alpha$. We remark that no other inter-node communication is required.
- 2) In lines 6, 7 of Algorithm 1, each node α evaluates $\omega_{ij}^{\alpha\beta(k)}$, $\omega_{ji}^{\beta\alpha(k)}$, $\nabla_{X^\alpha} F(X)$ using $X^{\alpha(k)}$ and $X^{\beta(k)}$ where $\beta \in \mathcal{N}_\alpha$ are the neighbors of node α .

- 3) In line 8 of Algorithm 1, we obtain the intermediate solution $X^{\alpha(k+\frac{1}{2})}$ using Algorithm 2. We have proved that the resulting $X^{\alpha(k+\frac{1}{2})}$ is already sufficient to guarantee the convergence to first-order critical points.
- 4) In line 4 of Algorithm 2, there exists an exact and efficient closed-form solution to $X^{\alpha(k+\frac{1}{2})}$ using Appendix K.
- 5) In line 9 of Algorithm 1, we use $X^{\alpha(k+\frac{1}{2})}$ to initialize Eq. (55), and improve the final solution $X^{\alpha(k+1)}$ through iterative optimization such that $G^\alpha(X^{\alpha(k+1)} | X^{(k)}) \leq G^\alpha(X^{\alpha(k+\frac{1}{2})} | X^{(k)})$. Note that $X^{\alpha(k+1)}$ does not have to be a local optimal solution to Eq. (55), nevertheless, $X^{\alpha(k+1)}$ is still expected to have a faster convergence than $X^{\alpha(k+\frac{1}{2})}$.

Remark 5. The MM–PGO method requires no inter-node communication except for lines 6 and 7 of Algorithm 1 that evaluate $\omega_{ij}^{\alpha\beta(k)}$, $\omega_{ji}^{\beta\alpha(k)}$ and $\nabla_{X^\alpha} F(X^{(k)})$ using Eqs. (25) and (49), which, as mentioned before, can be distributed with one inter-node communication round between neighboring nodes α and β without introducing any additional computation.

Since $X^{\alpha(k+\frac{1}{2})}$ in Eq. (54) has a closed-form solution that can be efficiently computed, and Eq. (55) does not require $X^{\alpha(k+1)}$ to be a local optimal solution, the overall computational efficiency of the MM–PGO method is significantly improved in contrast to [31], [32]. More importantly, the MM–PGO method still converges to first-order critical points as long as the following assumption holds.

Assumption 3. For $X^{\alpha(k+1)}$ and $X^{\alpha(k+\frac{1}{2})}$, it is assumed that

$$G^\alpha(X^{\alpha(k+1)} | X^{(k)}) \leq G^\alpha(X^{\alpha(k+\frac{1}{2})} | X^{(k)}) \quad (57)$$

for each node $\alpha = 1, 2, \dots, |\mathcal{A}|$.

It is known from Proposition 4 that $H^\alpha(X^\alpha | X^{(k)}) \geq G^\alpha(X^\alpha | X^{(k)})$ and $H^\alpha(X^{\alpha(k)} | X^{(k)}) = 0$, and thus, Assumption 3 can be satisfied with ease as long as line 9 of Algorithm 1 is initialized with $X^{\alpha(k+\frac{1}{2})}$. Then, the MM–PGO method in Algorithm 1 is guaranteed to converge to first-order critical points as the following proposition states.

Proposition 5. For a sequence of $\{X^{(k)}\}$ generated by the MM–PGO method in Algorithm 1, we have the following results if Assumptions 1 to 3 hold:

- (a) $F(X^{(k)})$ is nonincreasing as $k \rightarrow \infty$;
- (b) $F(X^{(k)}) \rightarrow F^\infty$ as $k \rightarrow \infty$;
- (c) $\|X^{(k+1)} - X^{(k)}\| \rightarrow 0$ as $k \rightarrow \infty$ if $\xi > 0$;
- (d) $\|X^{(k+\frac{1}{2})} - X^{(k)}\| \rightarrow 0$ as $k \rightarrow \infty$ if $\zeta > \xi > 0$;
- (e) if $\zeta > \xi > 0$, then there exists $\epsilon > 0$ such that

$$\min_{0 \leq k < K} \|\text{grad } F(X^{(k+\frac{1}{2})})\| \leq \sqrt{\frac{2}{\epsilon} \cdot \frac{F(X^{(0)}) - F^\infty}{K+1}}$$

for any $K \geq 0$;

- (f) if $\zeta > \xi > 0$, then $\text{grad } F(X^{(k)}) \rightarrow \mathbf{0}$ and $\text{grad } F(X^{(k+\frac{1}{2})}) \rightarrow \mathbf{0}$ as $k \rightarrow \infty$.

Proof. See Appendix E. \square

Remark 6. Even though the MM–PGO method is guaranteed to converge to first-order critical points as long as $\zeta > \xi > 0$ in Eqs. (35) and (41), $\xi > 0$ and $\zeta > 0$ are recommended to

be set close to zero such that $G(X|X^{(k)})$ and $H(X|X^{(k)})$ are tighter upper bounds of $F(X)$ and yield faster convergence.

Remark 7. In contrast to other distributed PGO algorithms [36]–[39], the MM–PGO method has mildest the conditions for convergence and apply to a broad class of loss kernels.

VIII. THE ACCELERATED MAJORIZATION MINIMIZATION METHOD FOR DISTRIBUTED POSE GRAPH OPTIMIZATION WITH MASTER NODE

In the last several decades, a number of accelerated first-order optimization methods have been proposed [33], [34]. Even though most of them were originally developed for convex optimization, it has been recently found that these accelerated methods achieve good performance for nonconvex optimization as well [47]–[49]. In our previous works [31], [32], we proposed to use Nesterov’s method to accelerate distributed PGO, which in practice result in much faster convergence. Since the MM–PGO method is a first-order optimization method, it is possible to exploit Nesterov’s method for acceleration as well.

In this and next sections, we will propose the accelerated MM methods for distributed PGO with and without master node, respectively, both of which significantly improve the convergence compared to the MM–PGO method.

A. Nesterov’s Method

From Eqs. (38) and (46), it is obvious that $G(X|X^{(k)})$ and $H(X|X^{(k)})$ are proximal operators of $F(X)$. Then, the implementation of Nesterov’s method [33], [34] results in the following update rule of $X^{\alpha(k+\frac{1}{2})}$ and $X^{\alpha(k+1)}$:

$$s^{\alpha(k+1)} = \frac{\sqrt{4s^{\alpha(k)^2} + 1} + 1}{2}, \quad (58)$$

$$\lambda^{\alpha(k)} = \frac{s^{\alpha(k)} - 1}{s^{\alpha(k+1)}}, \quad (59)$$

$$Y^{\alpha(k)} = X^{\alpha(k)} + \lambda^{\alpha(k)} \cdot (X^{\alpha(k)} - X^{\alpha(k-1)}), \quad (60)$$

$$X^{\alpha(k+\frac{1}{2})} = \arg \min_{X^{\alpha} \in \mathcal{X}^{\alpha}} H^{\alpha}(X^{\alpha}|Y^{\alpha(k)}), \quad (61)$$

$$X^{\alpha(k+1)} = \arg \min_{X^{\alpha} \in \mathcal{X}^{\alpha}} G^{\alpha}(X^{\alpha}|Y^{\alpha(k)}). \quad (62)$$

In Eqs. (61) and (62), $G^{\alpha}(\cdot|Y^{\alpha(k)}) : \mathcal{X}^{\alpha} \rightarrow \mathbb{R}$ and $H^{\alpha}(\cdot|Y^{\alpha(k)}) : \mathcal{X}^{\alpha} \rightarrow \mathbb{R}$ are proximal operators at $Y^{\alpha(k)}$:

$$G^{\alpha}(X^{\alpha}|Y^{\alpha(k)}) = \frac{1}{2} \|X^{\alpha} - Y^{\alpha(k)}\|_{\Gamma^{\alpha(k)}}^2 + \langle \nabla_{X^{\alpha}} F(Y^{\alpha(k)}), X^{\alpha} - Y^{\alpha(k)} \rangle \quad (63)$$

and

$$H^{\alpha}(X^{\alpha}|Y^{\alpha(k)}) = \frac{1}{2} \|X^{\alpha} - Y^{\alpha(k)}\|_{\Pi^{\alpha(k)}}^2 + \langle \nabla_{X^{\alpha}} F(Y^{\alpha(k)}), X^{\alpha} - Y^{\alpha(k)} \rangle, \quad (64)$$

where $\Gamma^{\alpha(k)}$ and $\Pi^{\alpha(k)}$ are the same as these in $G^{\alpha}(\cdot|X^{(k)})$ and $H^{\alpha}(\cdot|X^{(k)})$ in Eqs. (37) and (44).

The key idea of Nesterov’s method is to exploit the momentum $X^{\alpha(k)} - X^{\alpha(k-1)}$ for acceleration, which is essentially governed by Eqs. (58) to (60). Note that Nesterov’s method

using Eqs. (58) to (62) is equivalent to Eqs. (54) and (55) when $s^{\alpha(k)} = 1$ and $\lambda^{\alpha(k)} = 0$, and then increasingly affected by the momentum as $s^{\alpha(k)}$ and $\lambda^{\alpha(k)}$ increase.

Nesterov’s method is known to converge quadratically for convex optimization while the unaccelerated MM method only has linear convergence [33], [34]. Even though distributed PGO is a nonconvex optimization problem, similar to [31], [32], Eqs. (58) to (62) using Nesterov’s method for acceleration empirically have significant speedup while introducing almost no extra computation or communication compared to the MM–PGO method. Thus, it is preferable to adopt Nesterov’s method to accelerate distributed PGO.

B. Adaptive Restart

In spite of faster convergence, Nesterov’s accelerated distributed PGO using Eqs. (58) to (62) is no longer nonincreasing, and might fail to converge due to the nonconvexity of PGO. Fortunately, such a problem can be remedied with an adaptive restart scheme [31], [32], [35].

In the adaptive restart scheme, we recursively define $\bar{F}^{(k)}$ that is an exponential moving averaging of $F(X^{(0)})$, $F(X^{(1)})$, \dots , $F(X^{(k)})$ [31], [49], [50]:

$$\bar{F}^{(k)} \triangleq \begin{cases} F(X^{(0)}), & k = 0, \\ (1 - \eta) \cdot \bar{F}^{(k-1)} + \eta \cdot F(X^{(k)}), & \text{otherwise} \end{cases} \quad (65)$$

where $\eta \in (0, 1]$. Then, $X^{\alpha(k+\frac{1}{2})}$ and $X^{\alpha(k+1)}$ are updated using the following steps:

- 1) Update $X^{\alpha(k+\frac{1}{2})}$ and $X^{\alpha(k+1)}$ by solving Eqs. (61) and (62) for each node $\alpha \in \mathcal{A}$;
- 2) If $F(X^{\alpha(k+\frac{1}{2})}) > \bar{F}^{(k)}$, update $X^{\alpha(k+\frac{1}{2})}$ again by solving Eq. (54) for each node $\alpha \in \mathcal{A}$;
- 3) If $F(X^{\alpha(k+1)}) > \bar{F}^{(k)}$, update $X^{\alpha(k+1)}$ again by solving Eq. (55) and reduce $s^{\alpha(k+1)}$ for each node $\alpha \in \mathcal{A}$.

Remark 8. Since $\eta \in (0, 1]$ in Eq. (65), $\bar{F}^{(k+1)} \leq \bar{F}^{(k)}$ as long as $F(X^{\alpha(k+1)}) \leq \bar{F}^{(k)}$. In Appendix F, we have proved $F(X^{\alpha(k+1)}) \leq \bar{F}^{(k)}$ if $X^{\alpha(k+\frac{1}{2})}$ and $X^{\alpha(k+1)}$ are updated with Eqs. (54) and (55) for each node $\alpha \in \mathcal{A}$. Therefore, such an adaptive restart scheme is guaranteed to result in a nonincreasing sequence of $\bar{F}^{(k)}$.

Note that one has to aggregate information across the network to evaluate $\bar{F}^{(k)}$, $F(X^{\alpha(k+\frac{1}{2})})$, $F(X^{\alpha(k+1)})$ using Eqs. (18) and (65) and a master node capable of communicating with each node $\alpha \in \mathcal{A}$ is required. Thus, we make the following assumption about the existence of such a master node in the rest of this section.

Assumption 4. There is a master node to retrieve $X^{\alpha(k)}$ and $X^{\alpha(k+\frac{1}{2})}$ from each node $\alpha \in \mathcal{A}$ and evaluate $\bar{F}^{(k)}$, $F(X^{\alpha(k+\frac{1}{2})})$, $F(X^{\alpha(k+1)})$.

C. Algorithm

From Nesterov’s method and the adaptive restart scheme in Eqs. (58) to (62) and (65), we obtain the AMM–PGO* method for distributed PGO (Algorithm 3), where “*” indicates the existence of a master node.

Algorithm 3 The AMM–PGO* Method

1: **Input:** An initial iterate $X^{(0)} \in \mathcal{X}$, and $\zeta \geq \xi \geq 0$, and $\eta \in (0, 1]$, and $\psi > 0$, and $\phi > 0$.

2: **Output:** A sequence of iterates $\{X^{(k)}\}$ and $\{X^{(k+\frac{1}{2})}\}$.

3: **for** node $\alpha \leftarrow 1, \dots, |\mathcal{A}|$ **do**

4: $X^{\alpha(-1)} \leftarrow X^{\alpha(0)}$ and $s^{\alpha(0)} \leftarrow 1$

5: send $X^{\alpha(0)}$ to the master node

6: **end for**

7: evaluate $F(X^{(0)})$ using Eq. (17) at the master node

8: $\bar{F}^{(-1)} \leftarrow F(X^{(0)})$ at the master node

9: **for** $k \leftarrow 0, 1, 2, \dots$ **do**

10: **for** node $\alpha \leftarrow 1, \dots, |\mathcal{A}|$ **do**

11: $s^{\alpha(k+1)} \leftarrow \frac{\sqrt{4s^{\alpha(k)^2+1}+1}}{2}$, $\lambda^{\alpha(k)} \leftarrow \frac{s^{\alpha(k)}-1}{s^{\alpha(k+1)}}$

12: $Y^{\alpha(k)} \leftarrow X^{\alpha(k)} + \lambda^{\alpha(k)} \cdot (X^{\alpha(k)} - X^{\alpha(k-1)})$

13: **end for**

14: $\bar{F}^{(k)} \leftarrow (1-\eta) \cdot \bar{F}^{(k-1)} + \eta \cdot F(X^{(k)})$ at the master node

15: update $X^{(k+\frac{1}{2})}$ and $X^{(k+1)}$ using Algorithm 4

16: **end for**

The outline of the AMM–PGO* method is as follows:

- 1) In lines 11, 12 of Algorithm 3, each node α computes $Y^{(k)}$ for Nesterov’s acceleration that is related with $s^{\alpha(k)} \in [1, \infty)$ and $\lambda^{\alpha(k)} \in [0, 1)$.
- 2) In line 2 of Algorithm 4, each node α performs one inter-node communication round to retrieve $X^{\beta(k)}$ and $Y^{\beta(k)}$ from its neighbors $\beta \in \mathcal{N}^\alpha$.
- 3) In line 5 of Algorithm 3 and lines 7, 13, 21 of Algorithm 4, each node α performs one inter-node communication round to send $X^{\alpha(k+\frac{1}{2})}$ and $X^{\alpha(k+1)}$ to the master node.
- 4) In lines 3, 4 of Algorithm 4, each node α evaluates $\omega_{ij}^{\alpha\beta(k)}$, $\omega_{ji}^{\beta\alpha(k)}$, $\nabla_{X^\alpha} F(X^{(k)})$, $\nabla_{X^\alpha} F(Y^{(k)})$ using $X^{\alpha(k)}$, $Y^{\alpha(k)}$, $X^{\beta(k)}$, $Y^{\beta(k)}$ where $\beta \in \mathcal{N}^\alpha$ are the neighbors of node α .
- 5) In lines 8, 14 of Algorithm 3 and lines 9, 15, 23 of Algorithm 4, the master node evaluates $\bar{F}^{(k)}$, $F(X^{(k+\frac{1}{2})})$, $F(X^{(k+1)})$ that are used for adaptive restart.
- 6) In lines 10 to 24 of Algorithm 4, the master node performs adaptive restart to keep $F(X^{(k+\frac{1}{2})}) \leq \bar{F}^{(k)}$ and $F(X^{(k+1)}) \leq \bar{F}^{(k)}$, which yields a nonincreasing sequence of $\bar{F}^{(k)}$ to guarantee the convergence.
- 7) In lines 6, 19 of Algorithm 4, note that $X^{\alpha(k+1)}$ does not have to be a local optimal solution to Eq. (55).
- 8) In lines 25 to 27 of Algorithm 4, $F(X^{(k+1)})$ is guaranteed to yield sufficient improvement over $\bar{F}^{(k)}$ compared to $F(X^{(k+\frac{1}{2})})$.

In spite of acceleration, the AMM–PGO* method is guaranteed to converge to first-order critical points under mild conditions as the following proposition states.

Proposition 6. If Assumptions 1 to 4 hold, then for a sequence of iterates $\{X^{(k)}\}$ generated by Algorithm 3, we obtain

- (a) $\bar{F}^{(k)}$ is nonincreasing;
- (b) $F(X^{(k)}) \rightarrow F^\infty$ and $\bar{F}^{(k)} \rightarrow F^\infty$ as $k \rightarrow \infty$;

Algorithm 4 Updates for the AMM–PGO* Method

1: **for** node $\alpha \leftarrow 1, \dots, |\mathcal{A}|$ **do**

2: retrieve $X^{\beta(k)}$ and $Y^{\beta(k)}$ from $\beta \in \mathcal{N}_\alpha$

3: evaluate $\omega_{ij}^{\alpha\beta(k)}$ and $\omega_{ji}^{\beta\alpha(k)}$ using Eq. (25)

4: evaluate $\nabla_{X^\alpha} F(X^{(k)})$ and $\nabla_{X^\alpha} F(Y^{(k)})$ using Eq. (49)

5: $X^{\alpha(k+\frac{1}{2})} \leftarrow \arg \min_{X^\alpha \in \mathcal{X}^\alpha} H^\alpha(X^\alpha|Y^{(k)})$ using Algorithm 2

6: $X^{\alpha(k+1)} \leftarrow \text{improve } \arg \min_{X^\alpha \in \mathcal{X}^\alpha} G^\alpha(X^\alpha|Y^{(k)})$ with $X^{\alpha(k+\frac{1}{2})}$ as the initial guess

7: send $X^{\alpha(k+\frac{1}{2})}$ and $X^{\alpha(k+1)}$ to the master node

8: **end for**

9: evaluate $F(X^{(k+\frac{1}{2})})$ and $F(X^{(k+1)})$ using Eq. (17) at the master node

10: **if** $F(X^{(k+\frac{1}{2})}) > \bar{F}^{(k)} - \psi \cdot \|X^{(k+\frac{1}{2})} - X^{(k)}\|^2$ **then**

11: **for** node $\alpha \leftarrow 1, \dots, |\mathcal{A}|$ **do**

12: $X^{\alpha(k+\frac{1}{2})} \leftarrow \arg \min_{X^\alpha \in \mathcal{X}^\alpha} H^\alpha(X^\alpha|X^{(k)})$ using Algorithm 2

13: send $X^{\alpha(k+\frac{1}{2})}$ to the master node

14: **end for**

15: evaluate $F(X^{(k+\frac{1}{2})})$ using Eq. (17) at the master node

16: **end if**

17: **if** $F(X^{(k+1)}) > \bar{F}^{(k)} - \psi \cdot \|X^{(k+1)} - X^{(k)}\|^2$ **then**

18: **for** node $\alpha \leftarrow 1, \dots, |\mathcal{A}|$ **do**

19: $X^{\alpha(k+1)} \leftarrow \text{improve } \arg \min_{X^\alpha \in \mathcal{X}^\alpha} G^\alpha(X^\alpha|X^{(k)})$ with $X^{\alpha(k+\frac{1}{2})}$ as the initial guess

20: $s^{\alpha(k+1)} \leftarrow \max\{\frac{1}{2}s^{\alpha(k+1)}, 1\}$

21: send $X^{\alpha(k+1)}$ to the master node

22: **end for**

23: evaluate $F(X^{(k+1)})$ using Eq. (17) at the master node

24: **end if**

25: **if** $\bar{F}^{(k)} - F(X^{(k+1)}) < \phi \cdot (\bar{F}^{(k)} - F(X^{(k+\frac{1}{2})}))$ **then**

26: $X^{(k+1)} \leftarrow X^{(k+\frac{1}{2})}$ and $F(X^{(k+1)}) \leftarrow F(X^{(k+\frac{1}{2})})$

27: **end if**

- (c) $\|X^{(k+1)} - X^{(k)}\| \rightarrow 0$ as $k \rightarrow \infty$ if $\xi > 0$ and $\zeta > 0$;
- (d) $\|X^{(k+\frac{1}{2})} - X^{(k)}\| \rightarrow 0$ as $k \rightarrow \infty$ if $\zeta \geq \xi > 0$;
- (e) if $\zeta \geq \xi > 0$, then there exists $\epsilon > 0$ such that

$$\min_{0 \leq k < K} \|\text{grad } F(X^{(k+\frac{1}{2})})\| \leq 2\sqrt{\frac{1}{\epsilon} \cdot \frac{F(X^{(0)}) - F^\infty}{K+1}}$$

for any $K \geq 0$;

- (f) if $\zeta > \xi > 0$, then $\text{grad } F(X^{(k)}) \rightarrow \mathbf{0}$ and $\text{grad } F(X^{(k+\frac{1}{2})}) \rightarrow \mathbf{0}$ as $k \rightarrow \infty$.

Proof. See Appendix F. □

Remark 9. If $\eta = 1$ in Eq. (65), $F(X^{(k)}) = \bar{F}^{(k)}$, and $F(X^{(k)})$ is also nonincreasing according to Proposition 6(a). While $F(X^{(k)})$ might fail to be nonincreasing, we still recommend to choose $\eta \ll 1$ that empirically yields fewer adaptive restarts and faster convergence for distributed PGO.

Remark 10. In Algorithm 4, $\psi > 0$ and $\phi > 0$ guarantee that $F(X^{(k+\frac{1}{2})})$ and $F(X^{(k+1)})$ yield sufficient improvement over $\bar{F}^{(k)}$ in terms of $\|X^{(k+\frac{1}{2})} - X^{(k)}\|$ and $\|X^{(k+1)} - X^{(k)}\|$, and are recommended to set close to zero to avoid unnecessary adaptive restarts and make better use of Nesterov's acceleration.

IX. THE ACCELERATED MAJORIZATION MINIMIZATION METHOD FOR DISTRIBUTED POSE GRAPH OPTIMIZATION WITHOUT MASTER NODE

In this section, we will propose accelerated MM methods for distributed PGO without master node. The resulting accelerated MM method not only is guaranteed to converge to first-order critical points with limited local communication but also has almost no loss of computational efficiency in contrast to the AMM-PGO* method with master node (see Section X).

A. Adaptive Restart

The adaptive restart is essential for the convergence of accelerated MM methods. In the AMM-PGO* method (Algorithm 3), the adaptive restart scheme needs a master node to evaluate $F(X^{(k)})$ and $\bar{F}^{(k)}$ and guarantee the convergence. However, in the case of no master node, such an adaptive restart scheme requires substantial amount of inter-node communication across the network, making the AMM-PGO* method unscalable for large-scale distributed PGO. Recently, we developed an adaptive restart scheme for distributed PGO that does not require a master node but still generates convergent iterates with limited local communication [32]. In spite of that, the adaptive restart scheme in [32] is conservative and suffers from unnecessary restarts that hinder Nesterov's acceleration and yield slower convergence than the AMM-PGO* method. Thus, we need to redesign the adaptive restart scheme to boost the performance of distributed PGO without master node.

Recall that the AMM-PGO* method's adaptive restart scheme is for the purpose of $F(X^{(k+1)}) \leq \bar{F}^{(k)}$. In this section, we propose the following adaptive restart scheme that keeps $F(X^{(k+1)}) \leq \bar{F}^{(k)}$ for distributed PGO without master node such that the convergence is guaranteed for decentralized accelerated MM methods.

For notational simplicity, we introduce $\Delta G^\alpha(X|X^{(k)}) : \mathcal{X} \rightarrow \mathbb{R}$ that is related to the gap between the objective and surrogate functions:

$$\begin{aligned} \Delta G^\alpha(X|X^{(k)}) &\triangleq \\ &\frac{1}{2} \sum_{\beta \in \mathcal{N}_\alpha^-} \sum_{(i,j) \in \vec{\mathcal{E}}^{\alpha\beta}} \left(F_{ij}^{\alpha\beta}(X) - E_{ij}^{\alpha\beta}(X|X^{(k)}) \right) + \\ &\frac{1}{2} \sum_{\beta \in \mathcal{N}_\alpha^+} \sum_{(i,j) \in \vec{\mathcal{E}}^{\beta\alpha}} \left(F_{ij}^{\beta\alpha}(X) - E_{ij}^{\beta\alpha}(X|X^{(k)}) \right) - \\ &\frac{\xi}{2} \|X^\alpha - X^{\alpha(k)}\|^2, \quad (66) \end{aligned}$$

where $F_{ij}^{\alpha\beta}(X)$, $F_{ij}^{\beta\alpha}(X)$, $E_{ij}^{\alpha\beta}(X|X^{(k)})$, $E_{ij}^{\beta\alpha}(X|X^{(k)})$ are given in Eqs. (20) and (33). From $\Delta G^\alpha(X|X^{(k)})$ in Eq. (66), we recursively define $F^{\alpha(k)}$, $\bar{F}^{\alpha(k)}$, $G^{\alpha(k)}$ according to:

$$\begin{aligned} 1) \text{ If } k = -1, \text{ each node } \alpha \text{ initializes } F^{\alpha(-1)} \text{ and } \bar{F}^{\alpha(-1)} \text{ with} \\ F^{\alpha(-1)} &\triangleq \sum_{(i,j) \in \vec{\mathcal{E}}^{\alpha\alpha}} F_{ij}^{\alpha\alpha}(X^{(0)}) + \\ &\frac{1}{2} \sum_{\beta \in \mathcal{N}_\alpha^-} \sum_{(i,j) \in \vec{\mathcal{E}}^{\alpha\beta}} F_{ij}^{\alpha\beta}(X^{(0)}) + \frac{1}{2} \sum_{\beta \in \mathcal{N}_\alpha^+} \sum_{(i,j) \in \vec{\mathcal{E}}^{\beta\alpha}} F_{ij}^{\beta\alpha}(X^{(0)}) \quad (67) \end{aligned}$$

and

$$\bar{F}^{\alpha(-1)} \triangleq F^{\alpha(-1)}. \quad (68)$$

2) If $k \geq 0$, each node α recursively updates $G^{\alpha(k)}$, $F^{\alpha(k)}$ and $\bar{F}^{\alpha(k)}$ according to

$$G^{\alpha(k)} \triangleq G^\alpha(X^{\alpha(k)}|X^{(k-1)}) + F^{\alpha(k-1)}, \quad (69)$$

$$F^{\alpha(k)} \triangleq G^{\alpha(k)} + \Delta G^\alpha(X^{(k)}|X^{(k-1)}), \quad (70)$$

$$\bar{F}^{\alpha(k)} \triangleq (1 - \eta) \cdot \bar{F}^{\alpha(k-1)} + \eta \cdot F^{\alpha(k)} \quad (71)$$

where $\eta \in (0, 1]$.

From the definitions of $F_{ij}^{\alpha\alpha}(X)$, $F_{ij}^{\alpha\beta}(X)$, $F_{ij}^{\beta\alpha}(X)$, $G^\alpha(X^\alpha|X^{(k)})$, $\Delta G^\alpha(X|X^{(k)})$ in Eqs. (19), (20), (37) and (66), it is tedious but straightforward to show that $G^{\alpha(k)}$, $F^{\alpha(k)}$, $\bar{F}^{\alpha(k)}$ in Eqs. (67) to (71) can be explicitly evaluated with one inter-node communication round between node α and its neighbors $\beta \in \mathcal{N}_\alpha$. Furthermore, we have the following proposition about $F^{\alpha(k)}$, $\bar{F}^{\alpha(k)}$, $G^{\alpha(k)}$ that is important for the adaptive restart scheme without master node.

Proposition 7. For any $k \geq 0$, we have

- (a) $F(X^{(k)}) = \sum_{\alpha \in \mathcal{A}} F^{\alpha(k)}$ where $F(X^{(k)})$ is given in Eq. (17);
- (b) $\bar{F}^{(k)} = \sum_{\alpha \in \mathcal{A}} \bar{F}^{\alpha(k)}$ where $\bar{F}^{(k)}$ is given in Eq. (65);
- (c) $F^{\alpha(k+1)} \leq \bar{F}^{\alpha(k+1)} \leq \bar{F}^{\alpha(k)}$ if $G^{\alpha(k+1)} \leq \bar{F}^{\alpha(k)}$.

Proof. See Appendix G. \square

In Algorithms 3 and 4, the AMM-PGO* method's adaptive restart scheme requires a master node to evaluate and compare $F(X^{(k+1)})$ and $\bar{F}^{(k)}$ in order to keep $F(X^{(k+1)}) \leq \bar{F}^{(k)}$. In spite of local communication, we remark it is still possible to result in $F(X^{(k+1)}) \leq \bar{F}^{(k)}$ using $G^{\alpha(k)}$, $F^{\alpha(k)}$, $\bar{F}^{\alpha(k)}$ for distributed PGO without master node as follows:

1) From Propositions 7(a) and 7(b), we obtain $F(X^{(k+1)}) = \sum_{\alpha \in \mathcal{A}} F^{\alpha(k+1)}$ and $\bar{F}^{(k)} = \sum_{\alpha \in \mathcal{A}} \bar{F}^{\alpha(k)}$, and as a result,

$$F(X^{(k+1)}) = \sum_{\alpha \in \mathcal{A}} F^{\alpha(k+1)} \leq \sum_{\alpha \in \mathcal{A}} \bar{F}^{\alpha(k)} = \bar{F}^{(k)} \quad (72)$$

as long as

$$F^{\alpha(k+1)} \leq \bar{F}^{\alpha(k)} \quad (73)$$

for each node $\alpha \in \mathcal{A}$. In addition, Proposition 7(c) indicates that $G^{\alpha(k+1)} \leq \bar{F}^{\alpha(k)}$ leads to Eq. (73). Therefore, $F(X^{(k+1)}) \leq \bar{F}^{(k)}$ is reduced to requiring

$$G^{\alpha(k+1)} \leq \bar{F}^{\alpha(k)} \quad (74)$$

for each node $\alpha \in \mathcal{A}$.

2) In terms of $G^{\alpha(k+1)}$ and $\bar{F}^{\alpha(k)}$, we obtain from Eq. (69) that Eq. (74) is equivalent to

$$G^{\alpha(k+1)} = G^{\alpha}(X^{\alpha(k+1)}|X^{(k)}) + F^{\alpha(k)} \leq \bar{F}^{\alpha(k)}. \quad (75)$$

From Eqs. (72) to (75), we conclude $F^{\alpha(k+1)} \leq \bar{F}^{\alpha(k)}$ and $F(X^{(k+1)}) \leq \bar{F}^{(k)}$ as long as

$$G^{\alpha}(X^{\alpha(k+1)}|X^{(k)}) \leq 0 \quad (76)$$

and

$$F^{\alpha(k)} \leq \bar{F}^{\alpha(k)} \quad (77)$$

for each node $\alpha \in \mathcal{A}$.

3) Recall from Eq. (37) that $G^{\alpha}(X^{\alpha(k)}|X^{(k)}) = 0$. Then, if X^{α} in Eqs. (54) and (55) is initialized with $X^{\alpha(k)}$, the resulting $X^{\alpha(k+1)}$ has

$$G^{\alpha}(X^{\alpha(k+1)}|X^{(k)}) \leq G^{\alpha}(X^{\alpha(k)}|X^{(k)}) = 0, \quad (78)$$

which yields Eq. (76).

4) In Appendix H, it can be shown by induction that Eq. (77) holds for distributed PGO without master node.

From the discussion above, we conclude that Eqs. (76) and (77) can be always satisfied, and more importantly, result in $F(X^{(k+1)}) \leq \bar{F}^{(k)}$ for distributed PGO without master node. This suggests an adaptive restart scheme that evaluates and compares $G^{\alpha(k+1)}$ and $\bar{F}^{\alpha(k)}$ independently at each node $\alpha \in \mathcal{A}$ to keep $F(X^{(k+1)}) \leq \bar{F}^{(k)}$. We emphasize that the resulting adaptive restart scheme requires no master node and evaluates neither $F(X^{(k+1)})$ nor $\bar{F}^{(k)}$. Therefore, such an adaptive restart scheme differs from these in the AMM-PGO* method and [31], [49], [50] that rely on a master node to evaluate and compare $F(X^{(k+1)})$ and $\bar{F}^{(k)}$. In addition, the adaptive restart scheme takes at most one inter-node communication round among neighboring nodes at each iteration, which is well suited for distributed PGO without master node.

B. Algorithm

Following the adaptive restart scheme using $G^{\alpha(k+1)}$ and $\bar{F}^{\alpha(k)}$ to keep $F(X^{(k+1)}) \leq \bar{F}^{(k)}$, we obtain the AMM-PGO# method (Algorithm 5) for distributed PGO, where “#” indicates that no master node is needed.

The outline of the AMM-PGO# method is similar to the AMM-PGO* method and the key difference is the adaptive restart scheme:

- 1) In lines 5, 14 of Algorithm 5, each node α performs one inter-node communication round to retrieve $X^{\beta(k)}$ and $Y^{\beta(k)}$ from its neighbors $\beta \in \mathcal{N}^{\alpha}$. We remark that no other inter-node communication is required.
- 2) In lines 6, 7, 15, 16 of Algorithm 5 and lines 4, 6, 9, 13 of Algorithm 6, each node α evaluates $F^{\alpha(k)}$, $\bar{F}^{\alpha(k)}$, $G^{\alpha(k+\frac{1}{2})}$, $G^{\alpha(k+1)}$ that are used for adaptive restart. Note that $X^{\beta(k)}$ and $X^{\beta(k-1)}$ from node α 's neighbors $\beta \in \mathcal{N}^{\alpha}$ are needed.
- 3) In lines 7 to 15 of Algorithm 6, each node α performs independent adaptive restart such that $G^{\alpha(k+\frac{1}{2})} \leq \bar{F}^{\alpha(k)}$ and $G^{\alpha(k+1)} \leq \bar{F}^{\alpha(k)}$, which also results in $F(X^{(k+1)}) \leq$

Algorithm 5 The AMM-PGO# Method

- 1: **Input:** An initial iterate $X^{(0)} \in \mathcal{X}$, and $\eta \in (0, 1]$, and $\zeta \geq \xi \geq 0$, and $\psi > 0$, and $\phi > 0$.
 - 2: **Output:** A sequence of iterates $\{X^{(k)}\}$ and $\{X^{(k+\frac{1}{2})}\}$.
 - 3: **for** node $\alpha \leftarrow 1, \dots, |\mathcal{A}|$ **do**
 - 4: $X^{\alpha(-1)} \leftarrow X^{\alpha(0)}$ and $s^{\alpha(0)} \leftarrow 1$
 - 5: retrieve $X^{\beta(-1)}$ and $X^{\beta(0)}$ from $\beta \in \mathcal{N}_{\alpha}$
 - 6: evaluate $F^{\alpha(-1)}$ using Eq. (67)
 - 7: evaluate $\bar{F}^{\alpha(-1)}$ using Eq. (68)
 - 8: $G^{\alpha(0)} \leftarrow G^{\alpha}(X^{\alpha(0)}|X^{(-1)}) + F^{\alpha(-1)}$
 - 9: **end for**
 - 10: **for** $k \leftarrow 0, 1, 2, \dots$ **do**
 - 11: **for** node $\alpha \leftarrow 1, \dots, |\mathcal{A}|$ **do**
 - 12: $s^{\alpha(k+1)} \leftarrow \frac{\sqrt{4s^{\alpha(k)2}+1}+1}{2}$, $\lambda^{\alpha(k)} \leftarrow \frac{s^{\alpha(k)}-1}{s^{\alpha(k+1)}}$
 - 13: $Y^{\alpha(k)} \leftarrow X^{\alpha(k)} + \lambda^{\alpha(k)} \cdot (X^{\alpha(k)} - X^{\alpha(k-1)})$
 - 14: retrieve $X^{\beta(k)}$ and $Y^{\beta(k)}$ from $\beta \in \mathcal{N}_{\alpha}$
 - 15: $F^{\alpha(k)} \leftarrow G^{\alpha(k)} + \Delta G^{\alpha}(X^{(k)}|X^{(k-1)})$ using Eqs. (66) and (69)
 - 16: $\bar{F}^{\alpha(k)} \leftarrow (1-\eta) \cdot \bar{F}^{\alpha(k-1)} + \eta \cdot F^{\alpha(k)}$
 - 17: update $X^{\alpha(k+\frac{1}{2})}$ and $X^{\alpha(k+1)}$ using Algorithm 6
 - 18: **end for**
 - 19: **end for**
-

$\bar{F}^{(k)}$ and a nonincreasing sequence of $\bar{F}^{(k)}$ for distributed PGO without master node.

4) In lines 16 to 18 of Algorithm 6, $G^{\alpha(k+1)}$ is guaranteed to yield sufficient improvement over $\bar{F}^{\alpha(k+1)}$ compared to $G^{\alpha(k+\frac{1}{2})}$.

The AMM-PGO# method is guaranteed to converge to first-order critical points under mild conditions as the following propositions states.

Proposition 8. If Assumptions 1 to 3 hold, then for a sequence of iterates $\{X^{(k)}\}$ generated by Algorithm 5, we obtain

- (a) $\bar{F}^{(k)}$ is nonincreasing;
- (b) $F(X^{(k)}) \rightarrow F^{\infty}$ and $\bar{F}^{(k)} \rightarrow F^{\infty}$ as $k \rightarrow \infty$;
- (c) $\|X^{(k+1)} - X^{(k)}\| \rightarrow 0$ as $k \rightarrow \infty$ if $\zeta > \xi > 0$;
- (d) $\|X^{(k+\frac{1}{2})} - X^{(k)}\| \rightarrow 0$ as $k \rightarrow \infty$ if $\zeta > \xi > 0$;
- (e) if $\zeta > \xi > 0$, then there exists $\epsilon > 0$ such that

$$\min_{0 \leq k < K} \|\text{grad } F(X^{(k+\frac{1}{2})})\| \leq 2\sqrt{\frac{1}{\epsilon} \cdot \frac{F(X^{(0)}) - F^{\infty}}{K+1}}$$

for any $K \geq 0$;

- (f) if $\zeta > \xi > 0$, then $\text{grad } F(X^{(k)}) \rightarrow \mathbf{0}$ and $\text{grad } F(X^{(k+\frac{1}{2})}) \rightarrow \mathbf{0}$ as $k \rightarrow \infty$.

Proof. See Appendix H. □

In spite of no master node, Proposition 8 indicates that the AMM-PGO# method has provable convergence as long as each node $\alpha \in \mathcal{A}$ can communicate with its neighbors $\beta \in \mathcal{N}^{\alpha}$. Thus, the AMM-PGO# method eliminates the bottleneck of communication for distributed PGO without master node. In addition, the AMM-PGO# method also reduces unnecessary

Algorithm 6 Updates for the AMM–PGO[#] Method

- 1: evaluate $\omega_{ij}^{\alpha\beta(k)}$ and $\omega_{ji}^{\beta\alpha(k)}$ using Eq. (25)
 - 2: evaluate $\nabla_{X^\alpha} F(X^{(k)})$ and $\nabla_{X^\alpha} F(Y^{(k)})$ using Eq. (49)
 - 3: $X^{\alpha(k+\frac{1}{2})} \leftarrow \arg \min_{X^\alpha \in \mathcal{X}^\alpha} H^\alpha(X^\alpha|Y^{(k)})$ using Algorithm 2
 - 4: $G^{\alpha(k+\frac{1}{2})} \leftarrow G^\alpha(X^{\alpha(k+\frac{1}{2})}|X^{(k)}) + F^{\alpha(k)}$
 - 5: $X^{\alpha(k+1)} \leftarrow \text{improve } \arg \min_{X^\alpha \in \mathcal{X}^\alpha} G^\alpha(X^\alpha|Y^{(k)})$ with $X^{\alpha(k+\frac{1}{2})}$ as the initial guess
 - 6: $G^{\alpha(k+1)} \leftarrow G^\alpha(X^{\alpha(k+1)}|X^{(k)}) + F^{\alpha(k)}$
 - 7: **if** $G^{\alpha(k+\frac{1}{2})} > \bar{F}^{\alpha(k)} - \psi \cdot \|X^{\alpha(k+\frac{1}{2})} - X^{\alpha(k)}\|^2$ **then**
 - 8: $X^{\alpha(k+\frac{1}{2})} \leftarrow \arg \min_{X^\alpha \in \mathcal{X}^\alpha} H^\alpha(X^\alpha|X^{(k)})$ using Algorithm 2
 - 9: $G^{\alpha(k+\frac{1}{2})} \leftarrow G^\alpha(X^{\alpha(k+\frac{1}{2})}|X^{(k)}) + F^{\alpha(k)}$
 - 10: **end if**
 - 11: **if** $G^{\alpha(k+1)} > \bar{F}^{\alpha(k)}$ **then**
 - 12: $X^{\alpha(k+1)} \leftarrow \text{improve } \arg \min_{X^\alpha \in \mathcal{X}^\alpha} G^\alpha(X^\alpha|X^{(k)})$ with $X^{\alpha(k+\frac{1}{2})}$ as the initial guess
 - 13: $G^{\alpha(k+1)} \leftarrow G^\alpha(X^{\alpha(k+1)}|X^{(k)}) + F^{\alpha(k)}$
 - 14: $s^{\alpha(k+1)} \leftarrow \max\{\frac{1}{2}s^{\alpha(k+1)}, 1\}$
 - 15: **end if**
 - 16: **if** $\bar{F}^{\alpha(k)} - G^{\alpha(k+1)} < \phi \cdot (\bar{F}^{\alpha(k)} - G^{\alpha(k+\frac{1}{2})})$ **then**
 - 17: $X^{\alpha(k+1)} \leftarrow X^{\alpha(k+\frac{1}{2})}$ and $G^{\alpha(k+1)} \leftarrow G^{\alpha(k+\frac{1}{2})}$
 - 18: **end if**
-

adaptive restarts compared to [32], and thus makes better of Nesterov’s acceleration and has faster convergence.

X. EXPERIMENTS

In this section, we evaluate the performance of our MM methods (MM–PGO, AMM–PGO* and AMM–PGO[#]) for distributed PGO on the simulated Cube datasets and a number of 2D and 3D SLAM benchmark datasets [8]. In terms of MM–PGO, AMM–PGO* and AMM–PGO[#], η , ξ , ζ , ψ and ϕ in Algorithms 1, 3 and 5 are 5×10^{-4} , 1×10^{-10} , 1.5×10^{-10} , 1×10^{-10} and 1×10^{-6} , respectively, for all the experiments. In addition, MM–PGO, AMM–PGO* and AMM–PGO[#] can take at most one iteration when solving Eqs. (55) and (62) to improve the estimates. All the experiments have been performed on a laptop with an Intel Xeon(R) CPU E3-1535M v6 and 64GB of RAM running Ubuntu 18.04.

A. Cube Datasets

In this section, we test and evaluate our MM methods for distributed PGO on 20 simulated Cube datasets (see Fig. 2) with 5, 10 and 50 robots.

In the experiment, a simulated Cube dataset has $12 \times 12 \times 12$ cube grids with 1 m side length, a path of 3600 poses along the rectilinear edge of the cube grid, odometric measurements between all the pairs of sequential poses, and loop-closure measurements between nearby but non-sequential poses that are randomly available with a probability of 0.1. We generate the odometric and loop-closure measurements according to the noise models in [8] with an expected translational RMSE of

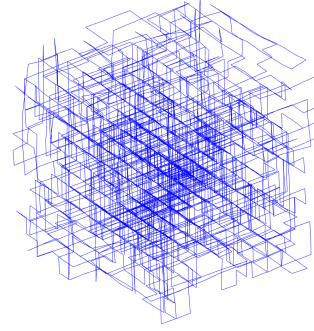


Fig. 2: A Cube dataset has $12 \times 12 \times 12$ grids of side length of 1 m, 3600 poses, probability of loop closure of 0.1, an translational RSME of $\sigma_t = 0.02$ m and an angular RSME of $\sigma_R = 0.02\pi$ rad.

$\sigma_t = 0.02$ m and an expected angular RMSE of $\sigma_R = 0.02\pi$ rad. The centralized chordal initialization [40] is implemented such that distributed PGO with different number of robots have the same initial estimate. The maximum number of iterations is 1000.

We evaluate the convergence of MM–PGO, AMM–PGO* and AMM–PGO[#] in terms of the relative suboptimality gap and Riemannian gradient norm. For reference, we also make comparisons against AMM–PGO [32]. Note that AMM–PGO is the original accelerated MM method for distributed PGO whose adaptive restart scheme is conservative and might prohibit Nesterov’s acceleration.

Relative Suboptimality Gap. We implement the certifiably-correct SE–Sync [8] to get the globally optimal objective value F^* for distributed PGO with the trivial loss kernel (Example 1), making it possible to compute the relative suboptimality gap $(F - F^*)/F^*$ where F is the objective value for each iteration. The results are in Fig. 3.

Riemannian Gradient Norm. We also compute the Riemannian gradient norm for distributed PGO with the trivial (Example 1) and nontrivial—Huber (Example 2) and Welsch (Example 3)—losses kernels for evaluation. Note that it is difficult to find the globally optimal solution to distributed PGO if nontrivial loss kernels are used. The results are in Figs. 4 to 6.

In Figs. 3 to 6, it can be seen that MM–PGO, AMM–PGO*, AMM–PGO[#] and AMM–PGO have a faster convergence if the number of robots (nodes) decreases. This is expected since $G(X|X^{(k)})$ and $H(X|X^{(k)})$ in Eqs. (35) and (41) result in tighter approximations for distributed PGO with fewer robots (nodes). In addition, Figs. 4 to 6 suggest that the convergence rate of MM–PGO, AMM–PGO*, AMM–PGO[#] and AMM–PGO also relies on the type of loss kernels. Nevertheless, AMM–PGO*, AMM–PGO[#] and AMM–PGO accelerated by Nesterov’s method outperform the unaccelerated MM–PGO method by a large margin for any number of robots and any types of loss kernels, which means that Nesterov’s method improves the convergence of distributed PGO. In particular, Figs. 3(a), 4(a), 5(a) and 6(a) indicate that AMM–PGO[#] with 50 robot still converges faster than MM–PGO with 5 robots despite that the later has a much smaller number of robots. Therefore, we conclude that the im-

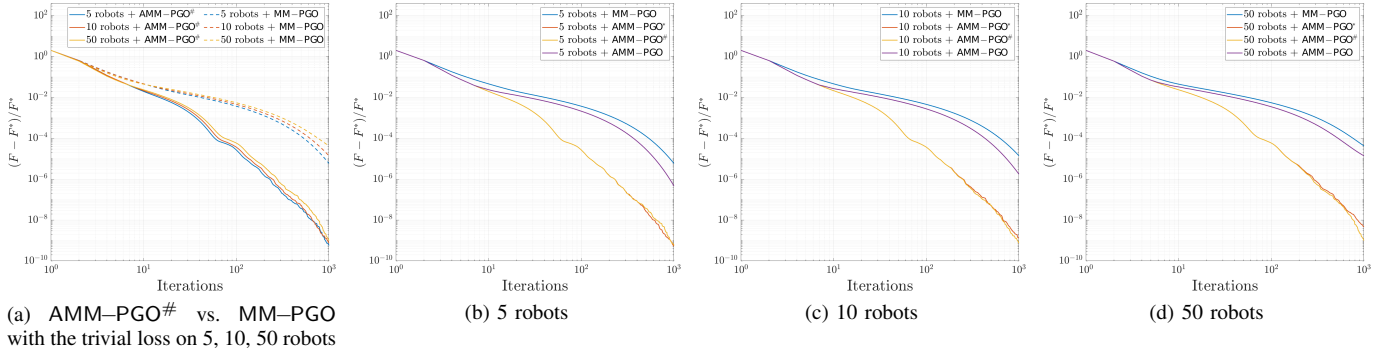


Fig. 3: The relative suboptimality gaps of the MM-PGO, AMM-PGO^{*}, AMM-PGO[#] and AMM-PGO [32] methods for distributed PGO with the trivial loss kernel on 5, 10 and 50 robots. The results are averaged over 20 Monte Carlo runs.

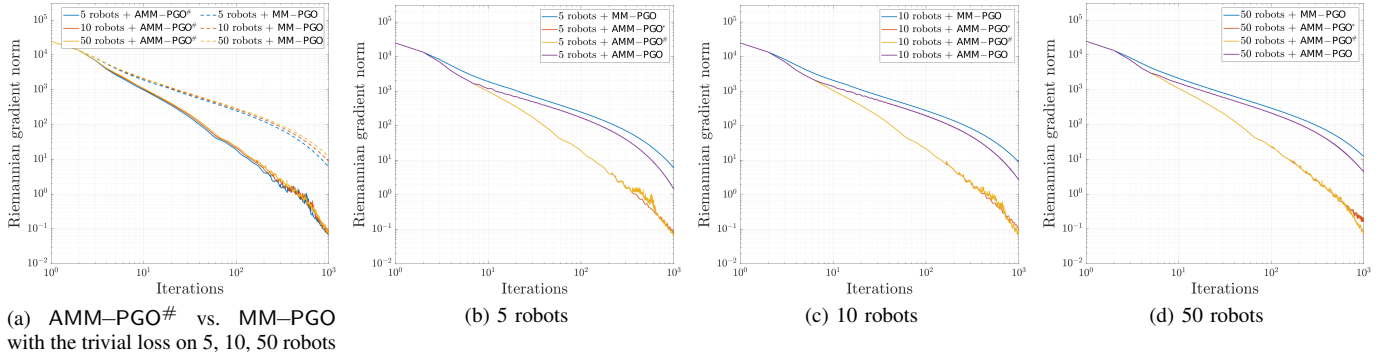


Fig. 4: The Riemannian gradient norms of the MM-PGO, AMM-PGO^{*}, AMM-PGO[#] and AMM-PGO [32] methods for distributed PGO with the trivial loss kernel on 5, 10 and 50 robots. The results are averaged over 20 Monte Carlo runs.

plementation of Nesterov’s method accelerate the convergence of distributed PGO.

Furthermore, we emphasize the convergence comparisons of AMM-PGO^{*}, AMM-PGO[#] and AMM-PGO, which are all accelerated with Nesterov’s method while differing from each other by the adaptive restart schemes—AMM-PGO^{*} has an additional master node to aggregate information from all the robots (nodes), whereas AMM-PGO[#] and AMM-PGO are restricted to one inter-node communication round per iteration among neighboring robots (nodes). Notwithstanding limited local communication, as is shown in Figs. 3 to 6, AMM-PGO[#] has a convergence rate comparable to that of AMM-PGO^{*} using a master node while being significantly faster than AMM-PGO. In particular, AMM-PGO[#] reduces adaptive restarts by 80% to 95% compared to AMM-PGO on the Cube datasets, and thus, is expected to make better use of Nesterov’s acceleration. Since AMM-PGO[#] and AMM-PGO differ in the adaptive restart schemes, we attribute the faster convergence of AMM-PGO[#] to its redesigned adaptive restart scheme. These results suggest that AMM-PGO[#] is advantageous over other methods for very large-scale distributed PGO where computational and communicational efficiency are equally important.

B. Benchmark Datasets

In this section, we evaluate our MM methods (MM-PGO, AMM-PGO^{*} and AMM-PGO[#]) for distributed PGO on a

TABLE I: 2D and 3D SLAM benchmark datasets.

| Dataset | 2D/3D | # Poses | # Measurements | Simulated Dataset |
|------------|-------|---------|----------------|-------------------|
| ais2klinik | 2D | 15115 | 16727 | No |
| city | 2D | 10000 | 20687 | Yes |
| CSAIL | 2D | 1045 | 1172 | No |
| M3500 | 2D | 3500 | 5453 | Yes |
| intel | 2D | 1728 | 2512 | No |
| MITb | 2D | 808 | 827 | No |
| sphere | 3D | 2500 | 4949 | Yes |
| torus | 3D | 5000 | 9048 | Yes |
| grid | 3D | 8000 | 22236 | Yes |
| garage | 3D | 1661 | 6275 | No |
| cubicle | 3D | 5750 | 16869 | No |
| rim | 3D | 10195 | 29743 | No |

number of 2D and 3D SLAM benchmark datasets (see Table I) [8]. We use the trivial loss kernel and assume there are no outliers such that the globally optimal solution can be exactly computed with SE-Sync [8]. For each dataset, we also make comparisons against SE-Sync [8], distributed Gauss-Seidel (DGS) [36] and the Riemannian block coordinate descent (RBCD) [37] method, all of which are the state-of-the-art algorithms for centralized and distributed PGO. The SE-Sync and DGS methods use the recommended settings in [8], [36]. We implement two Nesterov’s accelerated variants of RBCD [37], i.e., one with greedy selection rule and adaptive restart (RBCD++*) and the other with uniform selection

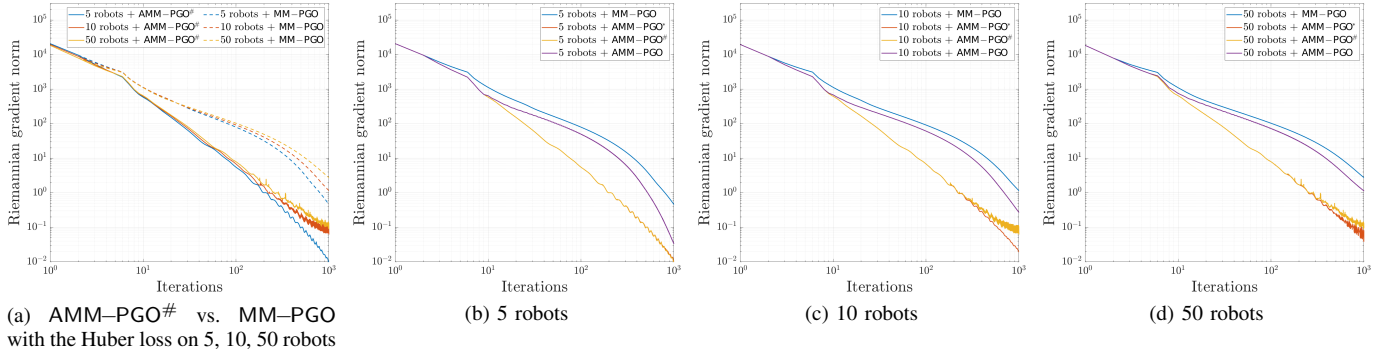


Fig. 5: The Riemannian gradient norms of the MM-PGO, AMM-PGO^{*}, AMM-PGO[#] and AMM-PGO [32] methods for distributed PGO with the Huber loss kernel on 5, 10 and 50 robots. The results are averaged over 20 Monte Carlo runs.

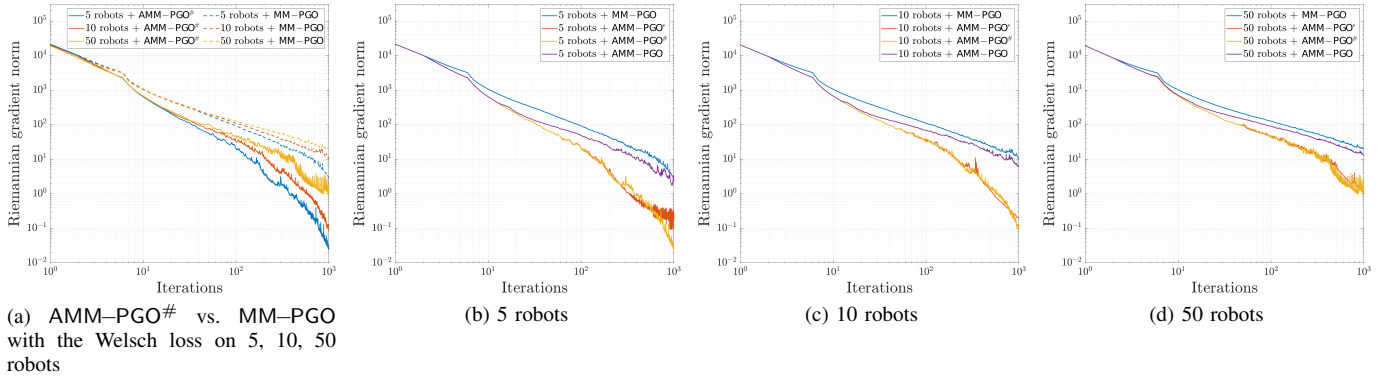


Fig. 6: The Riemannian gradient norms of the MM-PGO, AMM-PGO^{*}, AMM-PGO[#] and AMM-PGO [32] methods for distributed PGO with the Welsch loss kernel on 5, 10 and 50 robots. The results are averaged over 20 Monte Carlo runs.

TABLE II: An overview of the state-of-the-art algorithms for distributed and centralized PGO. Note that AMM-PGO^{*} and RBCD++^{*} require a master node for distributed PGO, and AMM-PGO[#] is the only accelerated method with provable convergence for distributed PGO without master node.

| Method | Distributed | Accelerated | Masterless | Converged |
|--------------------------|-------------|-------------|------------|-----------|
| SE-Sync [8] | No | N/A | N/A | Yes |
| DGS [36] | Yes | No | Yes | No |
| RBCD++ [*] [37] | Yes | Yes | No | Yes |
| RBCD++ [#] [37] | Yes | Yes | Yes | No |
| MM-PGO | Yes | No | Yes | Yes |
| AMM-PGO [*] | Yes | Yes | No | Yes |
| AMM-PGO [#] | Yes | Yes | Yes | Yes |

rule and fixed restart (RBCD++[#])². As mentioned before, AMM-PGO^{*} and AMM-PGO[#] can take at most one iteration when updating $X^{\alpha(k+1)}$ using Eqs. (55) and (62), which is similar to RBCD++^{*} and RBCD++[#]. An overview of the aforementioned methods is given in Table II.

Number of Iterations. First, we examine the convergence of MM-PGO, AMM-PGO^{*}, AMM-PGO[#], DGS [36], RBCD++^{*} [37] and RBCD++[#] [37] w.r.t. the number of iterations. The distributed PGO has 10 robots and all the meth-

²In the experiments, we run RBCD++[#] [37] with fixed restart frequencies of 30, 50 and 100 iterations for each dataset and select the one with the best performance.

ods are initialized with the distributed Nesterov’s accelerated chordal initialization [32].

The objective values of each method with 100, 250 and 1000 iterations are reported in Table III and the reconstruction results using AMM-PGO[#] are shown in Figs. 7 and 8. For almost all the benchmark datasets, AMM-PGO^{*} and AMM-PGO[#] outperform the other methods (MM-PGO, DGS, RBCD++^{*} and RBCD++[#]). While RBCD++^{*} and RBCD++[#] have similar performances in four comparatively simple datasets—CSAIL, sphere, torus and grid—we remark that AMM-PGO^{*} and AMM-PGO[#] achieve much better results in the other more challenging datasets in particular if there are no more than 250 iterations. As discussed later, AMM-PGO^{*} and AMM-PGO[#] have faster convergence to more accurate estimates without any extra computation and communication in contrast to RBCD++^{*} and RBCD++[#]. Last but not the least, Table III demonstrates that the accelerated AMM-PGO^{*} and AMM-PGO[#] converge significantly faster than the unaccelerated MM-PGO, which further validates the usefulness of Nesterov’s method.

We also compute the performance profiles [51] based on the number of iterations. Given a tolerance $\Delta \in (0, 1]$, the objective value threshold $F_{\Delta}(p)$ for PGO problem p is defined to be

$$F_{\Delta}(p) = F^* + \Delta \cdot (F^{(0)} - F^*), \quad (79)$$

where $F^{(0)}$ and F^* are the initial and globally optimal

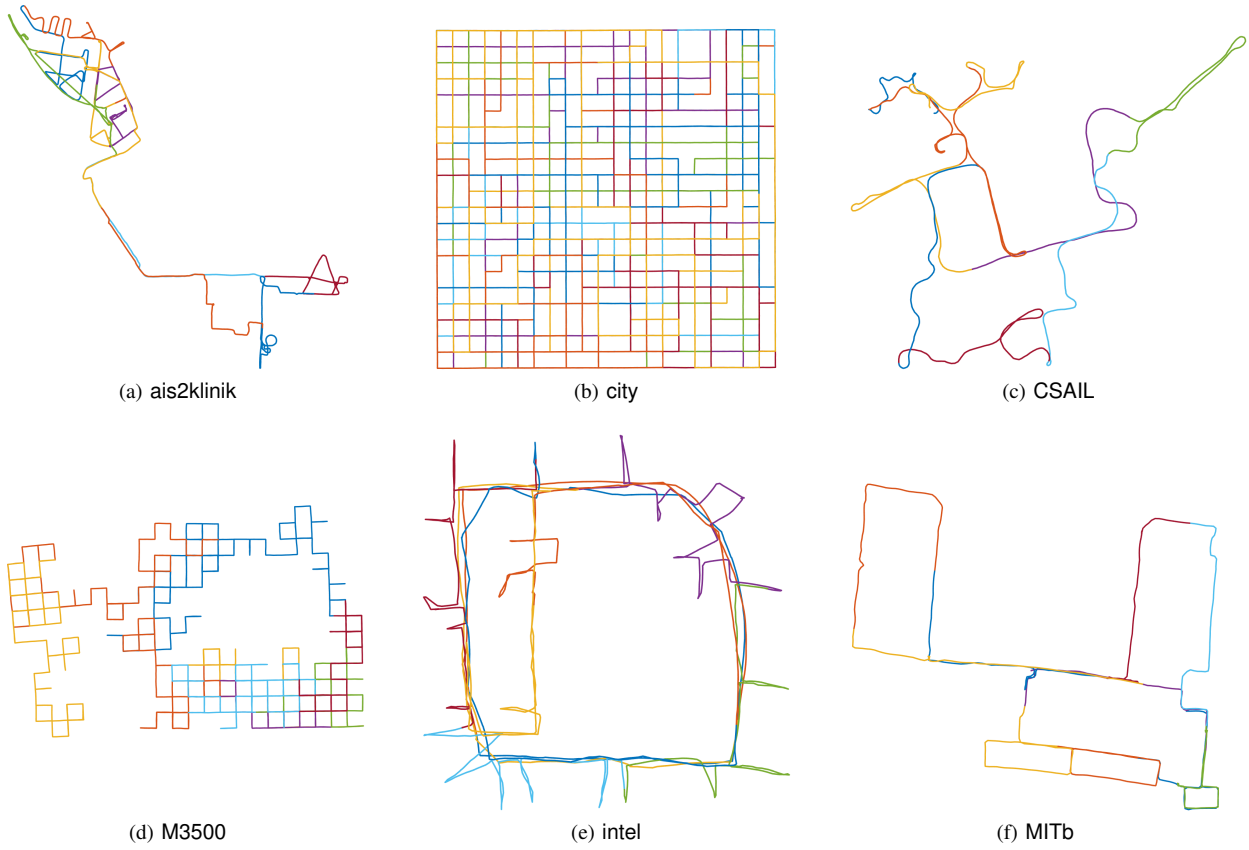


Fig. 7: AMM-PGO[#] results on the 2D SLAM benchmark datasets where the different colors denote the odometries of different robots. The distributed PGO has 10 robots and is initialized with the distributed Nesterov's accelerated chordal initialization [32]. The number of iterations is 1000.

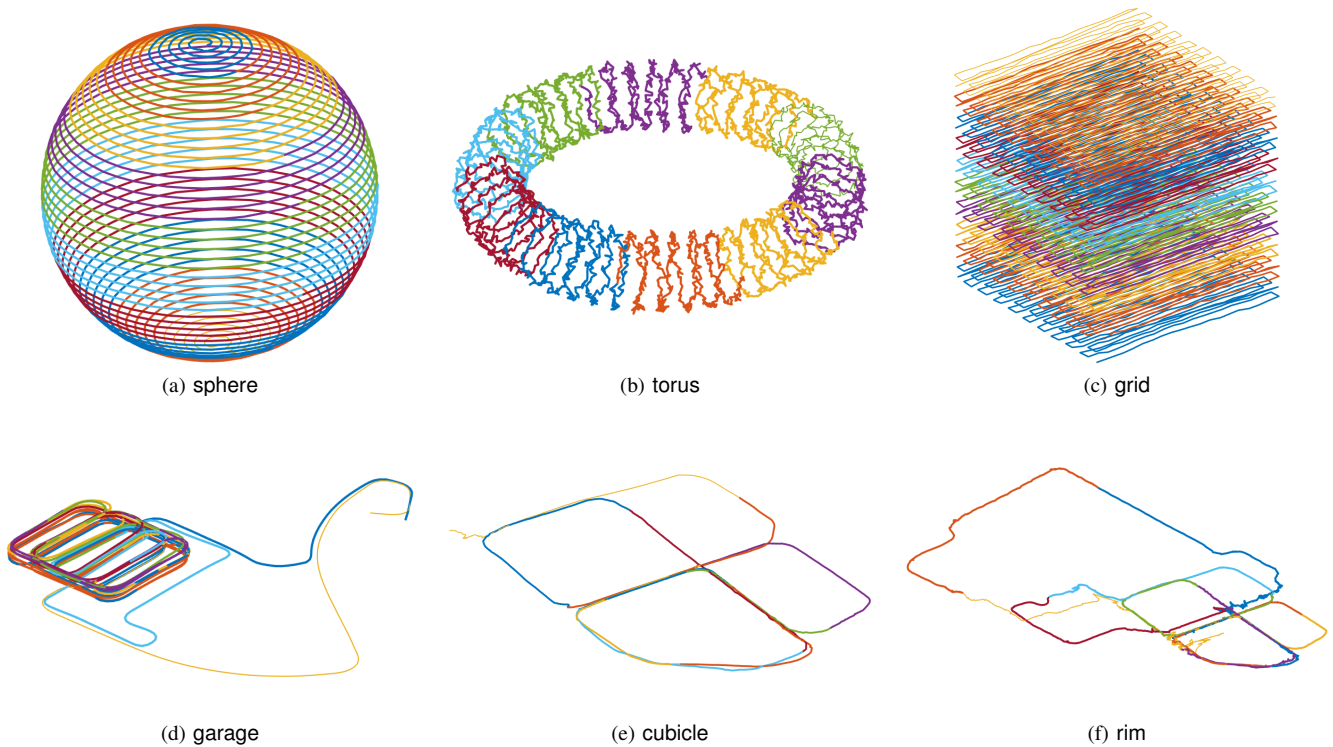


Fig. 8: AMM-PGO[#] results on the 3D SLAM benchmark datasets where the different colors denote the odometries of different robots. The distributed PGO has 10 robots and is initialized with the distributed Nesterov's accelerated chordal initialization [32]. The number of iterations is 1000.

TABLE III: Results of distributed PGO on the 2D and 3D SLAM Benchmark datasets (see Table I). The distributed PGO has 10 robots and is initialized with the distributed Nesterov’s accelerated chordal initialization [32]. We report the objective values of each method with 100, 250 and 1000 iterations. $F^{(k)}$ and F^* are the objective value at iteration k and globally optimal objective value, respectively. The best results are colored in red and the second best in blue if no methods tie for the best.

| Dataset | $F^{(0)}$ | F^* | k | $F^{(k)}$ | | | | | |
|----------------------------|----------------------|----------------------|------|------------------------|----------------------|-------------------------|----------------------|----------------------|----------------------|
| | | | | Methods w/ Master Node | | Methods w/o Master Node | | | |
| | | | | AMM-PGO* | RBCD++* [37] | MM-PGO | AMM-PGO# | DGS [36] | RBCD++# [37] |
| 2D SLAM Benchmark Datasets | | | | | | | | | |
| ais2klinik | 3.8375×10^2 | 1.8850×10^2 | 100 | 2.0372×10^2 | 2.1079×10^2 | 2.1914×10^2 | 2.0371×10^2 | 8.4701×10^2 | 2.1715×10^2 |
| | | | 250 | 1.9447×10^2 | 2.0077×10^2 | 2.1371×10^2 | 1.9446×10^2 | 9.1623×10^1 | 2.1084×10^2 |
| | | | 1000 | 1.8973×10^2 | 1.9074×10^2 | 2.0585×10^2 | 1.8936×10^2 | 3.8968×10^2 | 2.0253×10^2 |
| city | 7.0404×10^2 | 6.3862×10^2 | 100 | 6.4327×10^2 | 6.5138×10^2 | 6.5061×10^2 | 6.4327×10^2 | 7.7745×10^2 | 6.5396×10^2 |
| | | | 250 | 6.3899×10^2 | 6.4732×10^2 | 6.4850×10^2 | 6.3899×10^2 | 7.0063×10^2 | 6.5122×10^2 |
| | | | 1000 | 6.3862×10^2 | 6.3935×10^2 | 6.4461×10^2 | 6.3863×10^2 | 6.5583×10^2 | 6.4768×10^2 |
| CSAIL | 3.1719×10^1 | 3.1704×10^1 | 100 | 3.1704×10^1 | 3.1704×10^1 | 3.1706×10^1 | 3.1704×10^1 | 3.2479×10^1 | 3.1705×10^1 |
| | | | 250 | 3.1704×10^1 | 3.1704×10^1 | 3.1706×10^1 | 3.1704×10^1 | 3.1792×10^1 | 3.1704×10^1 |
| | | | 1000 | 3.1704×10^1 | 3.1704×10^1 | 3.1705×10^1 | 3.1704×10^1 | 3.1712×10^1 | 3.1704×10^1 |
| M3500 | 2.2311×10^2 | 1.9386×10^2 | 100 | 1.9446×10^2 | 1.9511×10^2 | 1.9560×10^2 | 1.9447×10^2 | 1.9557×10^2 | 1.9551×10^2 |
| | | | 250 | 1.9414×10^2 | 1.9443×10^2 | 1.9516×10^2 | 1.9414×10^2 | 1.9445×10^2 | 1.9511×10^2 |
| | | | 1000 | 1.9388×10^2 | 1.9392×10^2 | 1.9461×10^2 | 1.9388×10^2 | 1.9415×10^2 | 1.9455×10^2 |
| intel | 5.3269×10^1 | 5.2348×10^1 | 100 | 5.2397×10^1 | 5.2496×10^1 | 5.2517×10^1 | 5.2397×10^1 | 5.2541×10^1 | 5.2526×10^1 |
| | | | 250 | 5.2352×10^1 | 5.2415×10^1 | 5.2483×10^1 | 5.2351×10^1 | 5.2441×10^1 | 5.2489×10^1 |
| | | | 1000 | 5.2348×10^1 | 5.2349×10^1 | 5.2421×10^1 | 5.2348×10^1 | 5.2381×10^1 | 5.2425×10^1 |
| MITb | 8.8430×10^1 | 6.1154×10^1 | 100 | 6.1331×10^1 | 6.1518×10^1 | 6.3657×10^1 | 6.1330×10^1 | 9.5460×10^1 | 6.1997×10^1 |
| | | | 250 | 6.1157×10^1 | 6.1187×10^1 | 6.2335×10^1 | 6.1165×10^1 | 7.8273×10^1 | 6.1599×10^1 |
| | | | 1000 | 6.1154×10^1 | 6.1154×10^1 | 6.1454×10^1 | 6.1154×10^1 | 7.2450×10^1 | 6.1209×10^1 |
| 3D SLAM Benchmark Datasets | | | | | | | | | |
| sphere | 1.9704×10^3 | 1.6870×10^3 | 100 | 1.6870×10^3 | 1.6870×10^3 | 1.6901×10^3 | 1.6870×10^3 | 1.6875×10^3 | 1.6870×10^3 |
| | | | 250 | 1.6870×10^3 | 1.6870×10^3 | 1.6874×10^3 | 1.6870×10^3 | 1.6872×10^3 | 1.6870×10^3 |
| | | | 1000 | 1.6870×10^3 | 1.6870×10^3 | 1.6870×10^3 | 1.6870×10^3 | 1.6872×10^3 | 1.6870×10^3 |
| torus | 2.4654×10^4 | 2.4227×10^4 | 100 | 2.4227×10^4 | 2.4227×10^4 | 2.4234×10^4 | 2.4227×10^4 | 2.4248×10^4 | 2.4227×10^4 |
| | | | 250 | 2.4227×10^4 | 2.4227×10^4 | 2.4227×10^4 | 2.4227×10^4 | 2.4243×10^4 | 2.4227×10^4 |
| | | | 1000 | 2.4227×10^4 | 2.4227×10^4 | 2.4227×10^4 | 2.4227×10^4 | 2.4236×10^4 | 2.4227×10^4 |
| grid | 2.8218×10^5 | 8.4319×10^4 | 100 | 8.4323×10^4 | 8.4320×10^4 | 1.0830×10^5 | 8.4399×10^4 | 1.4847×10^5 | 8.4920×10^4 |
| | | | 250 | 8.4319×10^4 | 8.4319×10^4 | 8.6054×10^4 | 8.4321×10^4 | 1.4066×10^5 | 8.4319×10^4 |
| | | | 1000 | 8.4319×10^4 | 8.4319×10^4 | 8.4319×10^4 | 8.4319×10^4 | 1.4654×10^5 | 8.4319×10^4 |
| garage | 1.5470×10^0 | 1.2625×10^0 | 100 | 1.3105×10^0 | 1.3282×10^0 | 1.3396×10^0 | 1.3105×10^0 | 1.3170×10^0 | 1.3364×10^0 |
| | | | 250 | 1.2872×10^0 | 1.3094×10^0 | 1.3288×10^0 | 1.2872×10^0 | 1.2867×10^0 | 1.3276×10^0 |
| | | | 1000 | 1.2636×10^0 | 1.2681×10^0 | 1.3145×10^0 | 1.2636×10^0 | 1.2722×10^0 | 1.3124×10^0 |
| cubicle | 8.3514×10^2 | 7.1713×10^2 | 100 | 7.1812×10^2 | 7.2048×10^2 | 7.2300×10^2 | 7.1812×10^2 | 7.3185×10^2 | 7.2210×10^2 |
| | | | 250 | 7.1714×10^2 | 7.1794×10^2 | 7.2082×10^2 | 7.1715×10^2 | 7.2308×10^2 | 7.2081×10^2 |
| | | | 1000 | 7.1713×10^2 | 7.1713×10^2 | 7.2082×10^2 | 7.1713×10^2 | 7.2044×10^2 | 7.1845×10^2 |
| rim | 8.1406×10^4 | 5.4609×10^3 | 100 | 5.5044×10^3 | 5.7184×10^3 | 5.8138×10^3 | 5.5044×10^3 | 6.1840×10^3 | 5.7810×10^3 |
| | | | 250 | 5.4648×10^3 | 5.5050×10^3 | 5.7197×10^3 | 5.4648×10^3 | 6.1184×10^3 | 5.7195×10^3 |
| | | | 1000 | 5.4609×10^3 | 5.4617×10^3 | 5.5509×10^3 | 5.4609×10^3 | 6.0258×10^3 | 5.5373×10^3 |

objective values, respectively. Let $I_{\Delta}(p)$ denote the minimum number of iterations that a PGO method takes to reduce the objective value to $F_{\Delta}(p)$, i.e.,

$$I_{\Delta}(p) \triangleq \min_k \{k \geq 0 | F^{(k)} \leq F_{\Delta}(p)\},$$

where $F^{(k)}$ is the objective value at iteration k. Then, for a problem set \mathcal{P} , the performance profiles of a PGO method is the percentage of problems solved w.r.t. the number of iterations k:

$$\text{percentage of problems solved at iteration k} \triangleq \frac{|\{p \in \mathcal{P} | I_{\Delta}(p) \leq k\}|}{|\mathcal{P}|}.$$

The performance profiles based on the number of iterations over a variety of 2D and 3D SLAM benchmark datasets (see Table I) are shown in Fig. 9. The tolerances evaluated are $\Delta = 1 \times 10^{-2}$, 5×10^{-3} , 1×10^{-3} and 1×10^{-4} . We report the performance of MM-PGO, AMM-PGO*, AMM-PGO#, DGS [36], RBCD++* [37] and RBCD++# [37] for distributed PGO with 10 robots (nodes). As expected, AMM-PGO* and AMM-PGO# dominates the other methods (MM-PGO, DGS, RBCD++* and RBCD++#) in terms of the convergence for all the tolerances Δ , which means that AMM-PGO* and AMM-PGO# are better choices for distributed PGO.

In Table III and Fig. 9, we emphasize that AMM-PGO#

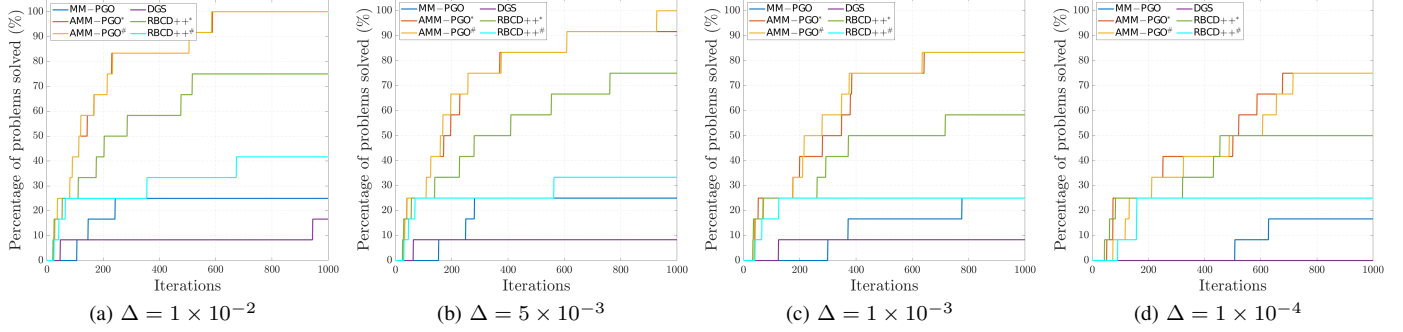


Fig. 9: Performance profiles for MM-PGO, AMM-PGO*, AMM-PGO#, DGS [36], RBCD++* [37] and RBCD++# [37] over a variety of 2D and 3D SLAM Benchmark datasets (see Table I). The performance is based on the number of iterations k and the evaluation tolerances are $\Delta = 1 \times 10^{-2}$, 5×10^{-3} , 1×10^{-3} and 1×10^{-4} . The distributed PGO has 10 robots (nodes) and is initialized with the distributed Nesterov’s accelerated chordal initialization [32]. Note that AMM-PGO* and RBCD++* [37] require a master node, whereas MM-PGO, AMM-PGO#, DGS [36] and RBCD++# [37] do not.

requiring no master node achieves comparable performance to that of AMM-PGO* using a master node, and is a lot better than all the other methods with a master node (RBCD++*) and without (MM-PGO, DGS and RBCD++#). Even though RBCD++* and RBCD++# are similarly accelerated with Nesterov’s method, we remark that RBCD++# without a master node suffers a great performance drop compared to RBCD++*, and more importantly, RBCD++# has no convergence guarantees to first-order critical points. These results reverify that AMM-PGO# is more suitable for very large-scale distributed PGO with limited local communication.

Note that all of MM-PGO, AMM-PGO*, AMM-PGO#, DGS [36], RBCD++* [37] and RBCD++# [37] have to exchange poses of inter-node measurements with the neighbors, and thus, need almost the same amount of communication per iteration. However, Fig. 9 indicates that AMM-PGO* and AMM-PGO# have much faster convergence in terms of the number of iterations, which also means less communication for the same level of accuracy. In addition, RBCD++* and RBCD++# have to keep part of the nodes in idle during optimization and rely on red-black coloring for block aggregation and random sampling for block selection, which induce additional computation and communication. In contrast, neither AMM-PGO* nor AMM-PGO# has any extra practical restrictions except those in Assumptions 1 to 4.

Optimization Time. In addition, we evaluate the speedup of AMM-PGO* and AMM-PGO# with different numbers of robots (nodes) against the state-of-the-art centralized algorithm SE-Sync [8]. To improve the optimization time efficiency of AMM-PGO* and AMM-PGO#, $X^{\alpha(k+1)}$ in Eqs. (55) and (62) uses the same rotation as $X^{\alpha(k+\frac{1}{2})}$ and only updates the translation. Since the number of robots varies in the experiments, the centralized chordal initialization [40] is adopted for all the methods.

Similar to the number of iterations, we also use the performance profiles to evaluate AMM-PGO* and AMM-PGO# in terms of the optimization time. Recall from Eq. (79) the objective value threshold $F_{\Delta}(p)$ where p is the PGO problem and $\Delta \in (0, 1]$ is the tolerance. Since the average optimization time per node is directly related with the speedup, we measure

the efficiency of a distributed PGO method with N nodes by computing the average optimization time $T_{\Delta}(p, N)$ that each node takes to reduce the objective value to $F_{\Delta}(p)$:

$$T_{\Delta}(p, N) = \frac{T_{\Delta}(p)}{N},$$

where $T_{\Delta}(p)$ denotes the total optimization time of all the N nodes. We remark that the centralized optimization method has $N = 1$ node and $T_{\Delta}(p, N) = T_{\Delta}(p)$. Let $T_{\text{SE-Sync}}$ denote the optimization time that SE-Sync needs to find the globally optimal solution. The performance profiles assume a distributed PGO method solves problem p for some $\mu \in [0, +\infty)$ if $T_{\Delta}(p, N) \leq \mu \cdot T_{\text{SE-Sync}}$. Note that μ is the scaled average optimization time per node and SE-Sync solves problem p globally at $\mu = 1$. Then, as a result of [51], the performance profiles evaluate the speedup of distributed PGO methods for a given optimization problem set \mathcal{P} using the percentage of problems solved w.r.t. the scaled average optimization time per node $\mu \in [0, +\infty)$:

$$\text{percentage of problems solved at } \mu \triangleq \frac{|\{p \in \mathcal{P} | T_{\Delta}(p, N) \leq \mu \cdot T_{\text{SE-Sync}}\}|}{|\mathcal{P}|}.$$

Fig. 10 shows the performance profiles based on the scaled average optimization time per node. The tolerances evaluated are $\Delta = 1 \times 10^{-2}$, 1×10^{-3} , 1×10^{-4} and 1×10^{-5} . We report the performance of AMM-PGO* and AMM-PGO# with 10, 25 and 100 robots (nodes). For reference, we also evaluate the performance profile of the centralized PGO baseline SE-Sync [8]. As the results demonstrate, AMM-PGO* and AMM-PGO# are significantly faster than SE-Sync [8] in most cases for modest accuracies of $\Delta = 1 \times 10^{-2}$ and $\Delta = 1 \times 10^{-3}$, for which the only challenging case is the CSAIL dataset, whose chordal initialization is already very close to the globally optimal solution. In spite of the performance decline for smaller tolerances of $\Delta = 1 \times 10^{-4}$ and $\Delta = 1 \times 10^{-5}$, AMM-PGO* and AMM-PGO# with 100 robots (nodes) still achieve a 2.5 ~ 20x speedup of optimization time over SE-Sync for more than 70% of the benchmark datasets, not to mention that the average optimization time per node of AMM-PGO* and AMM-PGO# decreases with

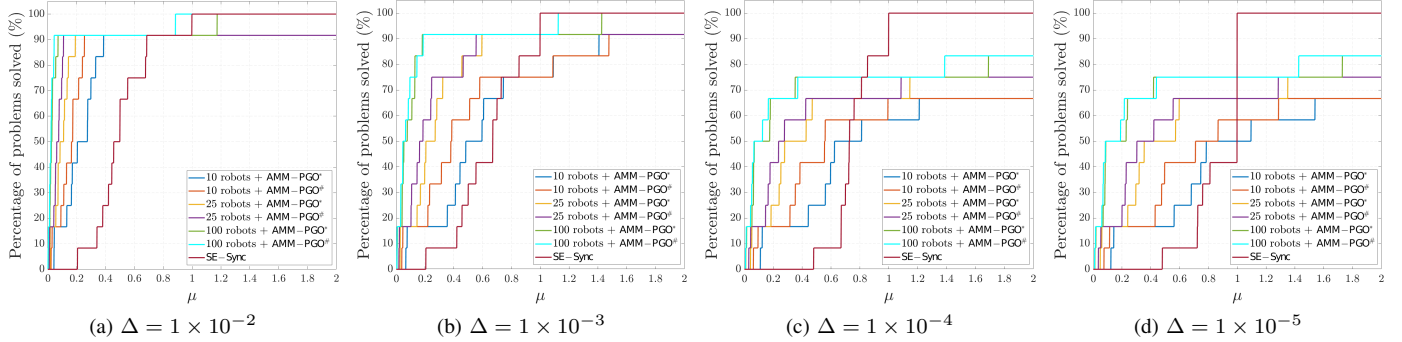


Fig. 10: Performance profiles for AMM-PGO^{*}, AMM-PGO[#] and SE-Sync [8] over a variety of 2D and 3D SLAM Benchmark datasets (see Table I). The performance is based on the scaled average optimization time per node $\mu \in [0, +\infty)$ and the evaluation tolerances are $\Delta = 1 \times 10^{-2}$, 1×10^{-3} , 1×10^{-4} and 1×10^{-5} . The distributed PGO has 10, 25 and 100 robots (nodes) and is initialized with the classic chordal initialization [40]. Note that SE-Sync [8] solves all the PGO problems globally at $\mu = 1$.

the number of robots (nodes). Note that the communication overhead is not considered in the experiments. Nevertheless Fig. 10 indicates that AMM-PGO^{*} and AMM-PGO[#] are promising as fast parallel backends for very large-scale PGO and real-time multi-robot SLAM.

In summary, AMM-PGO^{*} and AMM-PGO[#] not only achieves the state-of-the-art performance for distributed PGO, but also enjoys a significant multi-node speedup compared to the centralized baseline [8] for modestly accurate estimates that are sufficient for practical use.

C. Robust Distributed PGO

In this section, we evaluate the robustness of AMM-PGO[#] against the outlier inter-node loop closures. Similar to [24], [27], we first use the distributed pairwise consistent measurement set maximization algorithm (PCM) [52] to reject spurious inter-node loop closures and then solve the resulting distributed PGO using AMM-PGO[#] with the trivial (Example 1), Huber (Example 2) and Welsch (Example 3) loss kernels.

We implement AMM-PGO[#] on the 2D *intel* and 3D *garage* datasets (see Table I) with 10 robots (nodes). For each dataset, we add false inter-node loop closures with uniformly random rotation and translation errors in the range of $[0, \pi]$ rad and $[0, 5]$ m, respectively. In addition, after the initial outlier rejection using the PCM algorithm [52], we initialize AMM-PGO[#] with the distributed Nesterov’s accelerated chordal initialization [32] for all the loss kernels.

The absolute trajectory errors (ATE) of AMM-PGO[#] for different outlier thresholds of inter-node loop closures are reported in Fig. 11. The ATEs are computed against the outlier-free results of SE-Sync [8] and averaged over 10 Monte Carlo runs.

In Fig. 11(a), PCM [52] rejects most of the outlier inter-node loop closure for the *intel* dataset and AMM-PGO[#] solves the distributed PGO problems regardless of the loss kernel types and outlier thresholds. Note that AMM-PGO[#] with the Welsch loss kernel has larger ATEs (avg. 0.057 m) against SE-Sync [8] than those with the trivial and Huber loss kernels (avg. 0.003 m), and we argue that this is related

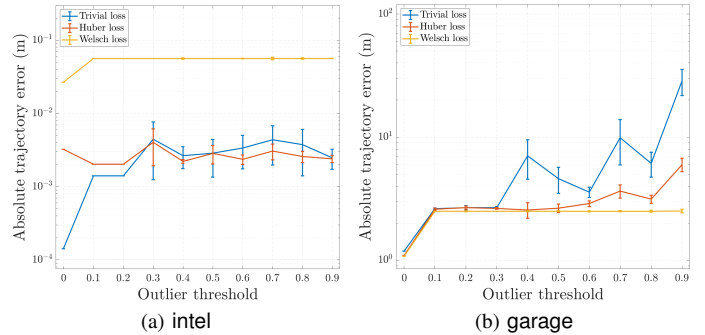


Fig. 11: Absolute trajectory errors (ATE) of distributed PGO using AMM-PGO[#] with the trivial, Huber and Welsch loss kernels on the 2D *intel* and 3D *garage* datasets. The outlier thresholds of inter-node loop closures are $0 \sim 0.9$. The ATEs are computed against the outlier-free results of SE-Sync [8] and are averaged over 10 Monte Carlo runs. The distributed PGO has 10 robots (nodes) and is initialized with the distributed Nesterov’s accelerated chordal initialization [32]. The PCM algorithm [52] is used to initially reject spurious inter-robot loop closures.

to the loss kernel types. The ATEs are evaluated based on SE-Sync using the trivial loss kernel, which is in fact identical or similar to distributed PGO with the trivial and Huber loss kernels but different from that with the Welsch loss kernel. Therefore, the estimates from the trivial and Huber loss kernels are expected to be more close to those of SE-Sync, which result in smaller ATEs compared to the Welsch loss kernel if there are no outliers.

For the more challenging *garage* dataset, as is shown in Fig. 11(b), PCM fails for outlier thresholds over 0.4, and further, distributed PGO with the trivial and Huber loss kernels results in ATEs as large as 65 m. In contrast, distributed PGO with the Welsch loss kernel still successfully estimates the poses with an average ATE of 2.5 m despite the existence of outliers—note that the *garage* dataset has a trajectory over 7 km. For the *garage* dataset, a qualitative comparison of distributed PGO with different loss kernels is also presented in Fig. 12, where the Welsch loss kernel still has the best

performance. The results are not surprising since the Welsch loss kernel is known to be more robust against outliers than the other two loss kernels [45].

The results above indicate that our MM methods can be applied to distributed PGO in the presence of outlier inter-node loop closures when combined with robust loss kernels like Welsch and other outlier rejection techniques like PCM [52]. In addition, we emphasize again that our MM methods have provable convergence to first-order critical points for a broad class of robust loss kernels, whereas the convergence guarantees of existing distributed PGO methods [36]–[39] are restricted to the trivial loss kernel.

XI. CONCLUSION AND FUTURE WORK

We presented majorization minimization (MM) methods for distributed PGO that has important applications in multi-robot SLAM. Our MM methods had provable convergence for a broad class of robust loss kernels in robotics and computer vision. Furthermore, we elaborated on the use of Nesterov’s method and adaptive restart for acceleration and developed accelerated MM methods AMM–PGO* and AMM–PGO# without sacrifice of convergence guarantees. In particular, we designed a novel adaptive restart scheme making the AMM–PGO# method without a master node comparable to the AMM–PGO* method using a master node for information aggregation. The extensive experiments on numerous 2D and 3D SLAM datasets indicated that our MM methods outperformed existing state-of-the-art methods and robustly handled distributed PGO with outlier inter-node loop closures.

Our MM methods for distributed PGO can be improved as follows. A more tractable and robust initialization technique is definitely beneficial to the accuracy and efficiency of distributed PGO. Even though our MM methods have reliable performances against outliers, a more complete theoretical analysis for robust distributed PGO is still necessary. In addition, our MM methods can be implemented as local solvers for distributed certifiably correct PGO [37] to handle poor or random initialization. Since all the nodes are now assumed to be synchronized, it is necessary and useful to extend our MM methods for asynchronous distributed PGO. Lastly, real multi-robot tests might make the results of our MM methods more convincing where not only the optimization time but also the communication overhead can be validated.

XII. ACKNOWLEDGMENT

This material is partially based upon work supported by the National Science Foundation under award DCSD-1662233. Any opinions, findings, and conclusions or recommendations expressed in this material are those of the authors and do not necessarily reflect the views of the National Science Foundation. We thank Yulun Tian for kindly sharing us with the code of Riemannian block coordinate descent method (RBCD) for distributed PGO [37].

REFERENCES

[1] C. Cadena, L. Carlone, H. Carrillo, Y. Latif, D. Scaramuzza, J. Neira, I. Reid, and J. J. Leonard, “Past, present, and future of simultaneous localization and mapping: Toward the robust-perception age,” *IEEE Transactions on robotics*, vol. 32, no. 6, pp. 1309–1332, 2016.

[2] D. M. Rosen, K. J. Doherty, A. Terán Espinoza, and J. J. Leonard, “Advances in inference and representation for simultaneous localization and mapping,” *Annual Review of Control, Robotics, and Autonomous Systems*, vol. 4, pp. 215–242, 2021.

[3] S. Thrun, W. Burgard, and D. Fox, *Probabilistic Robotics*. MIT press, 2005.

[4] A. Geiger, P. Lenz, and R. Urtasun, “Are we ready for autonomous driving? The kitti vision benchmark suite,” in *IEEE Conference on Computer Vision and Pattern Recognition*, 2012, pp. 3354–3361.

[5] A. Singer, “Angular synchronization by eigenvectors and semidefinite programming,” *Applied and computational harmonic analysis*, vol. 30, no. 1, pp. 20–36, 2011.

[6] A. Singer and Y. Shkolnisky, “Three-dimensional structure determination from common lines in cryo-em by eigenvectors and semidefinite programming,” *SIAM journal on imaging sciences*, vol. 4, no. 2, pp. 543–572, 2011.

[7] D. M. Rosen, M. Kaess, and J. J. Leonard, “Rise: An incremental trust-region method for robust online sparse least-squares estimation,” *IEEE Transactions on Robotics*, vol. 30, no. 5, pp. 1091–1108, 2014.

[8] D. M. Rosen, L. Carlone, A. S. Bandeira, and J. J. Leonard, “SE-Sync: A certifiably correct algorithm for synchronization over the special euclidean group,” *The International Journal of Robotics Research*, vol. 38, no. 2-3, pp. 95–125, 2019.

[9] D. M. Rosen, “Scalable low-rank semidefinite programming for certifiably correct machine perception,” in *Intl. Workshop on the Algorithmic Foundations of Robotics (WAFR)*, vol. 3, 2020.

[10] F. Dellaert, “Factor graphs and GTSAM: A hands-on introduction,” Georgia Institute of Technology, Tech. Rep., 2012.

[11] T. Fan, H. Wang, M. Rubenstein, and T. Murphey, “Efficient and guaranteed planar pose graph optimization using the complex number representation,” in *2019 IEEE/RSJ International Conference on Intelligent Robots and Systems (IROS)*, 2019, pp. 1904–1911.

[12] L. Carlone, G. C. Calafiore, C. Tommolillo, and F. Dellaert, “Planar pose graph optimization: Duality, optimal solutions, and verification,” *IEEE Transactions on Robotics*, vol. 32, no. 3, pp. 545–565, 2016.

[13] L. Carlone, D. M. Rosen, G. Calafiore, J. J. Leonard, and F. Dellaert, “Lagrangian duality in 3D SLAM: Verification techniques and optimal solutions,” in *IEEE/RSJ International Conference on Intelligent Robots and Systems (IROS)*, 2015.

[14] G. Grisetti, C. Stachniss, and W. Burgard, “Nonlinear constraint network optimization for efficient map learning,” *IEEE Transactions on Intelligent Transportation Systems*, vol. 10, no. 3, pp. 428–439, 2009.

[15] T. Fan, H. Wang, M. Rubenstein, and T. Murphey, “CPL-SLAM: Efficient and certifiably correct planar graph-based slam using the complex number representation,” *IEEE Transactions on Robotics*, vol. 36, no. 6, pp. 1719–1737, 2020.

[16] J. Briales and J. Gonzalez-Jimenez, “Cartan-sync: Fast and global se (d)-synchronization,” *IEEE Robotics and Automation Letters*, vol. 2, no. 4, pp. 2127–2134, 2017.

[17] L. Li, A. Bayuelo, L. Bobadilla, T. Alam, and D. A. Shell, “Coordinated multi-robot planning while preserving individual privacy,” in *2019 International Conference on Robotics and Automation (ICRA)*, 2019, pp. 2188–2194.

[18] Y. Zhang and D. A. Shell, “Complete characterization of a class of privacy-preserving tracking problems,” *The International Journal of Robotics Research*, vol. 38, no. 2-3, pp. 299–315, 2019.

[19] A. Cunningham, M. Paluri, and F. Dellaert, “DDF-SAM: Fully distributed SLAM using constrained factor graphs,” in *IEEE/RSJ International Conference on Intelligent Robots and Systems*, 2010.

[20] R. Aragues, L. Carlone, G. Calafiore, and C. Sagues, “Multi-agent localization from noisy relative pose measurements,” in *IEEE International Conference on Robotics and Automation*, 2011, pp. 364–369.

[21] A. Cunningham, V. Indelman, and F. Dellaert, “DDF-SAM 2.0: Consistent distributed smoothing and mapping,” in *IEEE International Conference on Robotics and Automation*, 2013, pp. 5220–5227.

[22] S. Saedi, M. Trentini, M. Seto, and H. Li, “Multiple-robot simultaneous localization and mapping: A review,” *Journal of Field Robotics*, vol. 33, no. 1, pp. 3–46, 2016.

[23] J. Dong, E. Nelson, V. Indelman, N. Michael, and F. Dellaert, “Distributed real-time cooperative localization and mapping using an uncertainty-aware expectation maximization approach,” in *IEEE International Conference on Robotics and Automation (ICRA)*, 2015.

[24] P.-Y. Lajoie, B. Ramtoula, Y. Chang, L. Carlone, and G. Beltrame, “Door-slam: Distributed, online, and outlier resilient slam for robotic teams,” *IEEE Robotics and Automation Letters*, vol. 5, no. 2, pp. 1656–1663, 2020.

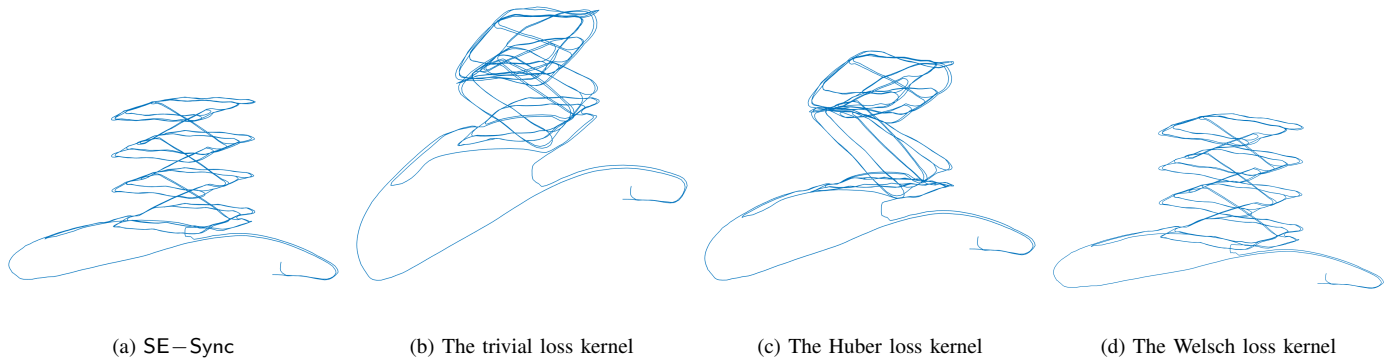


Fig. 12: A qualitative comparison of distributed PGO with the trivial, Huber and Welsch loss kernels for the garage dataset with spurious inter-node loop closures. The outlier-free result of SE-Sync [8] is shown in Fig. 12(a) for reference. The outlier threshold of inter-node loop closures is 0.6 and PCM [52] is used for initial outlier rejection.

- [25] T. Cieslewski, S. Choudhary, and D. Scaramuzza, "Data-efficient decentralized visual SLAM," in *IEEE International Conference on Robotics and Automation (ICRA)*, 2018.
- [26] V. Tchuiev and V. Indelman, "Distributed consistent multi-robot semantic localization and mapping," *IEEE Robotics and Automation Letters*, vol. 5, no. 3, pp. 4649–4656, 2020.
- [27] Y. Chang, Y. Tian, J. P. How, and L. Carlone, "Kimera-multi: a system for distributed multi-robot metric-semantic simultaneous localization and mapping," *arXiv preprint arXiv:2011.04087*, 2020.
- [28] Y. Tian, Y. Chang, F. H. Arias, C. Nieto-Granda, J. P. How, and L. Carlone, "Kimera-multi: Robust, distributed, dense metric-semantic slam for multi-robot systems," *arXiv preprint arXiv:2106.14386*, 2021.
- [29] D. R. Hunter and K. Lange, "A tutorial on MM algorithms," *The American Statistician*, vol. 58, no. 1, pp. 30–37, 2004.
- [30] Y. Sun, P. Babu, and D. P. Palomar, "Majorization-minimization algorithms in signal processing, communications, and machine learning," *IEEE Transactions on Signal Processing*, vol. 65, no. 3, pp. 794–816, 2016.
- [31] T. Fan and T. Murphey, "Generalized proximal methods for pose graph optimization," in *International Symposium on Robotics Research (ISRR)*, 2019.
- [32] —, "Majorization minimization methods for distributed pose graph optimization with convergence guarantees," in *IEEE/RSJ International Conference on Intelligent Robots and Systems*, 2020.
- [33] Y. Nesterov, "A method for unconstrained convex minimization problem with the rate of convergence $O(1/k^2)$," in *Doklady AN USSR*, vol. 269, 1983, pp. 543–547.
- [34] —, *Introductory lectures on convex optimization: A basic course*. Springer Science & Business Media, 2013, vol. 87.
- [35] B. O’donoghue and E. Candes, "Adaptive restart for accelerated gradient schemes," *Foundations of computational mathematics*, vol. 15, no. 3, pp. 715–732, 2015.
- [36] S. Choudhary, L. Carlone, C. Nieto, J. Rogers, H. I. Christensen, and F. Dellaert, "Distributed mapping with privacy and communication constraints: Lightweight algorithms and object-based models," *The International Journal of Robotics Research*, vol. 36, no. 12, pp. 1286–1311, 2017.
- [37] Y. Tian, K. Khosoussi, D. M. Rosen, and J. P. How, "Distributed certifiably correct pose-graph optimization," *arXiv preprint arXiv:1911.03721*, 2019.
- [38] R. Tron and R. Vidal, "Distributed 3-d localization of camera sensor networks from 2-d image measurements," *IEEE Transactions on Automatic Control*, vol. 59, no. 12, pp. 3325–3340, 2014.
- [39] E. Cristofalo, E. Montijano, and M. Schwager, "Geod: Consensus-based geodesic distributed pose graph optimization," *arXiv preprint arXiv:2010.00156*, 2020.
- [40] L. Carlone, R. Tron, K. Daniilidis, and F. Dellaert, "Initialization techniques for 3D SLAM: a survey on rotation estimation and its use in pose graph optimization," in *IEEE International Conference on Robotics and Automation (ICRA)*, 2015.
- [41] Y. Tian, A. Koppel, A. S. Bedi, and J. P. How, "Asynchronous and parallel distributed pose graph optimization," *IEEE Robotics and Automation Letters*, vol. 5, no. 4, pp. 5819–5826, 2020.
- [42] H. Yang, P. Antonante, V. Tzoumas, and L. Carlone, "Graduated non-convexity for robust spatial perception: From non-minimal solvers to global outlier rejection," *IEEE Robotics and Automation Letters*, vol. 5, no. 2, pp. 1127–1134, 2020.
- [43] P. Agarwal, G. D. Tipaldi, L. Spinello, C. Stachniss, and W. Burgard, "Robust map optimization using dynamic covariance scaling," in *2013 IEEE International Conference on Robotics and Automation*, 2013, pp. 62–69.
- [44] L. Carlone and G. C. Calafiore, "Convex relaxations for pose graph optimization with outliers," *IEEE Robotics and Automation Letters*, vol. 3, no. 2, pp. 1160–1167, 2018.
- [45] J. T. Barron, "A general and adaptive robust loss function," in *Proceedings of the IEEE/CVF Conference on Computer Vision and Pattern Recognition (CVPR)*, June 2019.
- [46] S. Umeyama, "Least-squares estimation of transformation parameters between two point patterns," *IEEE Transactions on Pattern Analysis & Machine Intelligence*, no. 4, pp. 376–380, 1991.
- [47] S. Ghadimi and G. Lan, "Accelerated gradient methods for nonconvex nonlinear and stochastic programming," *Mathematical Programming*, vol. 156, no. 1-2, pp. 59–99, 2016.
- [48] C. Jin, P. Netrapalli, and M. I. Jordan, "Accelerated gradient descent escapes saddle points faster than gradient descent," in *Conference On Learning Theory*, 2018.
- [49] H. Li and Z. Lin, "Accelerated proximal gradient methods for nonconvex programming," in *Advances in neural information processing systems*, 2015, pp. 379–387.
- [50] H. Zhang and W. W. Hager, "A nonmonotone line search technique and its application to unconstrained optimization," *SIAM Journal on Optimization*, vol. 14, no. 4, pp. 1043–1056, 2004.
- [51] E. D. Dolan and J. J. Moré, "Benchmarking optimization software with performance profiles," *Mathematical Programming*, vol. 91, no. 2, pp. 201–213, 2002.
- [52] J. G. Mangelson, D. Dominic, R. M. Eustice, and R. Vasudevan, "Pairwise consistent measurement set maximization for robust multi-robot map merging," in *2018 IEEE International Conference on Robotics and Automation (ICRA)*. IEEE, 2018, pp. 2916–2923.
- [53] P.-A. Absil, R. Mahony, and R. Sepulchre, *Optimization algorithms on matrix manifolds*. Princeton University Press, 2009.
- [54] A. McAdams, A. Selle, R. Tamstorf, J. Teran, and E. Sifakis, "Computing the singular value decomposition of 3×3 matrices with minimal branching and elementary floating point operations," University of Wisconsin-Madison Department of Computer Sciences, Tech. Rep., 2011.

APPENDIX A. NOTATION

| Symbol | Description | Equation |
|---|--|--------------------|
| Inner Products, Norms and Gradients | | |
| $\langle \cdot, \cdot \rangle_M$ | $\langle X, Y \rangle_M \triangleq \text{trace}(XMY^\top)$ | Eq. (1) |
| $\langle \cdot, \cdot \rangle$ | $\langle X, Y \rangle \triangleq \text{trace}(XY^\top)$ | Eq. (2) |
| $\ \cdot \ $ | The Frobenius norm of matrices and vectors | |
| $\ \cdot \ _2$ | The induced 2-norm of matrices and vectors | |
| $\ \cdot \ _M$ | $\ X\ _M \triangleq \sqrt{\text{trace}(XMX^\top)}$ | Eq. (3) |
| $\nabla F(X)$ | The Euclidean gradient of $F(X)$ | |
| $\text{grad } F(X)$ | The Riemannian gradient of $F(X)$ | |
| Graph Theory | | |
| $\vec{\mathcal{G}} = (\mathcal{V}, \vec{\mathcal{E}})$ | The directed graph whose vertices are ordered pairs | |
| $\vec{\mathcal{E}}^{\alpha\beta}$ | The set of edges between node α and β | Eq. (4) |
| \mathcal{N}_-^α | The set of nodes with edges from node α | Eq. (5) |
| \mathcal{N}_+^α | The set of nodes with edges to node α | Eq. (6) |
| \mathcal{N}^α | The set of neighbors of node α | Eq. (7) |
| Poses | | |
| X_i^α | The i -th pose of node α | Eq. (13) |
| t_i^α | The translational part for X_i^α | |
| R_i^α | The rotational part for X_i^α | |
| X^α | The poses of node α | Eq. (14) |
| X | All the poses of distributed pose graph optimization | Eq. (15) |
| $\tilde{t}_{ij}^\alpha, \tilde{t}_{ij}^{\alpha\beta}$ | The translational part of the noisy intra- and inter-node relative pose measurements | |
| $\tilde{R}_{ij}^{\alpha\alpha}, \tilde{R}_{ij}^{\alpha\beta}$ | The rotational part of the noisy intra- and inter-node relative pose measurements | |
| Objective Functions | | |
| $F(X)$ | The objective function for distributed pose graph optimization | Eq. (18) |
| $F_{ij}^{\alpha\alpha}(X)$ | The sub-objective function related to intra-node measurements | Eq. (19) |
| $F_{ij}^{\alpha\beta}(X)$ | The sub-objective function related to inter-node measurements | Eq. (20) |
| Surrogate Functions | | |
| $E_{ij}^{\alpha\beta}(X X^{(k)})$ | The surrogate function of $F_{ij}^{\alpha\beta}(X)$ | Eq. (33) |
| $G(X X^{(k)})$ | The surrogate function of $F(X)$ | Eq. (35) |
| $G^\alpha(X^\alpha X^{(k)})$ | The sub-surrogate function in $G(X X^{(k)})$ that is related to poses of node α | Eq. (37) |
| $H(X X^{(k)})$ | The surrogate function of $F(X)$ | Eq. (41) |
| $H^\alpha(X^\alpha X^{(k)})$ | The sub-surrogate function in $H(X X^{(k)})$ that is related to poses of node α | Eq. (44) |
| $H_i^\alpha(X_i^\alpha X^{(k)})$ | The sub-surrogate function in $H(X X^{(k)})$ and $H^\alpha(X^\alpha X^{(k)})$ that is related to a single pose X_i^α of node α | Eq. (45) |
| Nesterov's Acceleration | | |
| $s^{\alpha(k)}, \lambda^{\alpha(k)}$ | The scalars related to the extrapolation of Nesterov's acceleration | Eqs. (58) and (59) |
| $Y^{\alpha(k)}$ | The extrapolation of $X^{\alpha(k)}$ and $X^{\alpha(k-1)}$ | Eq. (60) |
| Adaptive Restart | | |
| $\bar{F}^{(k)}$ | The exponential moving average of $F(X^{(0)}), F(X^{(1)}), \dots, F(X^{(k)})$ | Eq. (65) |
| $\Delta G^\alpha(X X^{(k)})$ | The function computing the gap between $F(X)$ and $G^\alpha(X X^{(k)})$ related to poses of node α | Eq. (66) |
| $G^{\alpha(k)}, F^{\alpha(k)}$ | The intermediates for the adaptive restart scheme without a master node | Eqs. (69) and (70) |
| $\bar{F}^{\alpha(k)}$ | The exponential moving average of $F^{\alpha(0)}, F^{\alpha(1)}, \dots, F^{\alpha(k)}$ | Eq. (71) |
| Constant Scalars | | |
| ξ | The regularizer for $G(X X^{(k)})$ | Eq. (35) |
| ζ | The regularizer for $H(X X^{(k)})$ | Eq. (41) |
| η | The exponential moving average parameter for $\bar{F}^{(k)}$ and $\bar{F}^{\alpha(k)}$ | Eqs. (65) and (71) |
| ψ and ϕ | The parameters for the adaptive restart | |

APPENDIX B. PROOF OF PROPOSITION 1

For any nodes $\alpha, \beta \in \mathcal{A}$, it should be noted that

$$\frac{1}{2}\|X\|_{M_{ij}^{\alpha\beta}}^2 = \frac{1}{2}\|X - X^{(k)}\|_{M_{ij}^{\alpha\beta}}^2 + \langle X^{(k)} M_{ij}^{\alpha\beta}, X - X^{(k)} \rangle + \frac{1}{2}\|X^{(k)}\|_{M_{ij}^{\alpha\beta}}^2 \quad (80)$$

always holds. Then, we will prove Proposition 1 considering cases of $\alpha = \beta$ and $\alpha \neq \beta$, respectively.

- 1) If $\alpha = \beta$, Eq. (22) indicates $\nabla F_{ij}^{\alpha\beta}(X^{(k)}) = X^{(k)} M_{ij}^{\alpha\beta}$. From Eqs. (22), (25) and (80), it is immediate to conclude that Eq. (24) holds for any X and $X^{(k)} \in \mathbb{R}^{d \times (d+1)n}$ as long as $\alpha = \beta$.
- 2) If $\alpha \neq \beta$, as a result of Assumption 2(c), $\rho(s)$ is a concave function, which suggests

$$\rho(s') \leq \rho(s) + \nabla \rho(s) \cdot (s' - s).$$

If we let $s = \|X\|_{M_{ij}^{\alpha\beta}}^2$ and $s' = \|X\|_{M_{ij}^{\alpha\beta}}^2$, the equation above can be written as

$$\frac{1}{2}\rho(\|X\|_{M_{ij}^{\alpha\beta}}^2) \leq \frac{1}{2}\rho(\|X^{(k)}\|_{M_{ij}^{\alpha\beta}}^2) + \frac{1}{2}\nabla \rho(\|X^{(k)}\|_{M_{ij}^{\alpha\beta}}^2) \cdot (\|X\|_{M_{ij}^{\alpha\beta}}^2 - \|X^{(k)}\|_{M_{ij}^{\alpha\beta}}^2). \quad (81)$$

From Eq. (80), it can be shown that

$$\frac{1}{2}\|X\|_{M_{ij}^{\alpha\beta}}^2 - \frac{1}{2}\|X^{(k)}\|_{M_{ij}^{\alpha\beta}}^2 = \frac{1}{2}\|X - X^{(k)}\|_{M_{ij}^{\alpha\beta}}^2 + \langle X^{(k)} M_{ij}^{\alpha\beta}, X - X^{(k)} \rangle. \quad (82)$$

Then, applying Eq. (82) on the right-hand side of Eq. (81) results in

$$\begin{aligned} & \frac{1}{2}\rho(\|X\|_{M_{ij}^{\alpha\beta}}^2) \\ & \leq \frac{1}{2}\nabla \rho(\|X^{(k)}\|_{M_{ij}^{\alpha\beta}}^2) \cdot \|X - X^{(k)}\|_{M_{ij}^{\alpha\beta}}^2 + \\ & \quad \nabla \rho(\|X^{(k)}\|_{M_{ij}^{\alpha\beta}}^2) \cdot \langle X^{(k)} M_{ij}^{\alpha\beta}, X - X^{(k)} \rangle + \\ & \quad \frac{1}{2}\rho(\|X^{(k)}\|_{M_{ij}^{\alpha\beta}}^2). \end{aligned} \quad (83)$$

From Eqs. (23) and (25), we obtain

$$F_{ij}^{\alpha\beta}(X^{(k)}) = \frac{1}{2}\rho(\|X^{(k)}\|_{M_{ij}^{\alpha\beta}}^2),$$

$$\nabla F_{ij}^{\alpha\beta}(X^{(k)}) = \nabla \rho(\|X^{(k)}\|_{M_{ij}^{\alpha\beta}}^2) \cdot X^{(k)} M_{ij}^{\alpha\beta},$$

$$\omega_{ij}^{\alpha\beta(k)} = \nabla \rho(\|X^{(k)}\|_{M_{ij}^{\alpha\beta}}^2),$$

with which Eq. (83) is simplified to

$$\begin{aligned} & \frac{1}{2}\omega_{ij}^{\alpha\beta(k)}\|X - X^{(k)}\|_{M_{ij}^{\alpha\beta}}^2 + \langle \nabla F_{ij}^{\alpha\beta}(X^{(k)}), X - X^{(k)} \rangle + \\ & \quad F_{ij}^{\alpha\beta}(X^{(k)}) \geq F_{ij}^{\alpha\beta}(X). \end{aligned}$$

Thus, Eq. (24) for $\alpha \neq \beta$ as well.

The proof is completed.

APPENDIX C. PROOF OF PROPOSITION 2

From Eqs. (32) and (33), we obtain

$$E_{ij}^{\alpha\beta}(X|X^{(k)}) \geq \frac{1}{2}\omega_{ij}^{\alpha\beta(k)}\|X - X^{(k)}\|_{M_{ij}^{\alpha\beta}}^2 + \langle \nabla F_{ij}^{\alpha\beta}(X^{(k)}), X - X^{(k)} \rangle + F_{ij}^{\alpha\beta}(X^{(k)}), \quad (84)$$

in which the equality “=” holds as long as $X = X^{(k)}$. From Proposition 1, we obtain

$$\frac{1}{2}\omega_{ij}^{\alpha\beta(k)}\|X - X^{(k)}\|_{M_{ij}^{\alpha\beta}}^2 + \langle \nabla F_{ij}^{\alpha\beta}(X^{(k)}), X - X^{(k)} \rangle + F_{ij}^{\alpha\beta}(X^{(k)}) \geq F_{ij}^{\alpha\beta}(X). \quad (85)$$

Then, as a result of Eqs. (84) and (85), it is straightforward to show

$$E_{ij}^{\alpha\beta}(X|X^{(k)}) \geq F_{ij}^{\alpha\beta}(X)$$

for any $X \in \mathbb{R}^{d \times (d+1)n}$, in which the equality “=” holds as long as $X = X^{(k)}$. The proof is completed.

APPENDIX D. PROOF OF PROPOSITION 3

Proof of (a). From Eq. (31), it can be concluded that

$$\begin{aligned} \frac{1}{2}\|X - X^{(k)}\|_{\Omega_{ij}^{\alpha\beta}}^2 &= \kappa_{ij}^{\alpha\beta}\|R_i^\alpha - R_i^{\alpha(k)}\|^2 + \\ &\tau_{ij}^{\alpha\beta}\|(R_i^\alpha - R_i^{\alpha(k)})\tilde{t}_{ij}^{\alpha\beta} + t_i^\alpha - t_i^{\alpha(k)}\|^2 + \\ &\kappa_{ij}^{\alpha\beta}\|R_j^\beta - R_j^{\beta(k)}\|^2 + \tau_{ij}^{\alpha\beta}\|t_j^\beta - t_j^{\beta(k)}\|^2. \end{aligned} \quad (86)$$

From Eq. (19), it is by definition that $F_{ij}^{\alpha\beta}(X)$ is a function related with $X^\alpha \in \mathcal{X}^\alpha$ and $X^\beta \in \mathcal{X}^\beta$ only, and thus, $\nabla F_{ij}^{\alpha\beta}(X)$ is sparse, which suggests

$$\begin{aligned} \langle \nabla F_{ij}^{\alpha\beta}(X^{(k)}), X - X^{(k)} \rangle &= \\ &\langle \nabla_{X^\alpha} F_{ij}^{\alpha\beta}(X^{(k)}), X^\alpha - X^{\alpha(k)} \rangle + \\ &\langle \nabla_{X^\beta} F_{ij}^{\alpha\beta}(X^{(k)}), X^\beta - X^{\beta(k)} \rangle. \end{aligned} \quad (87)$$

In Eq. (87), $\nabla_{X^\alpha} F_{ij}^{\alpha\beta}(X^{(k)})$ is the Euclidean gradient of $F_{ij}^{\alpha\beta}(X)$ with respect to $X^\alpha \in \mathcal{X}^\alpha$ at $X^{(k)} \in \mathcal{X}$. Substituting Eqs. (86) and (87) into Eq. (33), we obtain

$$\begin{aligned} E_{ij}^{\alpha\beta}(X|X^{(k)}) &= \omega_{ij}^{\alpha\beta(k)} \cdot \left(\kappa_{ij}^{\alpha\beta}\|R_i^\alpha - R_i^{\alpha(k)}\|^2 + \right. \\ &\tau_{ij}^{\alpha\beta}\|(R_i^\alpha - R_i^{\alpha(k)})\tilde{t}_{ij}^{\alpha\beta} + t_i^\alpha - t_i^{\alpha(k)}\|^2 + \\ &\kappa_{ij}^{\alpha\beta}\|R_j^\beta - R_j^{\beta(k)}\|^2 + \tau_{ij}^{\alpha\beta}\|t_j^\beta - t_j^{\beta(k)}\|^2 \left. \right) + \\ &\langle \nabla_{X^\alpha} F_{ij}^{\alpha\beta}(X^{(k)}), X^\alpha - X^{\alpha(k)} \rangle + \\ &\langle \nabla_{X^\beta} F_{ij}^{\alpha\beta}(X^{(k)}), X^\beta - X^{\beta(k)} \rangle + F_{ij}^{\alpha\beta}(X^{(k)}). \end{aligned} \quad (88)$$

In a similar way, $F_{ij}^{\alpha\alpha}(X)$ in Eq. (19) can be rewritten as

$$\begin{aligned} F_{ij}^{\alpha\alpha}(X) &= \frac{1}{2}\kappa_{ij}^{\alpha\alpha}\|(R_i^\alpha - R_i^{\alpha(k)})\tilde{R}_{ij}^{\alpha\alpha} - (R_j^\alpha - R_j^{\alpha(k)})\|^2 + \\ &\frac{1}{2}\tau_{ij}^{\alpha\alpha}\|(R_i^\alpha - R_i^{\alpha(k)})\tilde{t}_{ij}^{\alpha\alpha} + t_i^\alpha - t_i^{\alpha(k)} - (t_j^\alpha - t_j^{\alpha(k)})\|^2 + \\ &\langle \nabla_{X^\alpha} F_{ij}^{\alpha\alpha}(X^{(k)}), X^\alpha - X^{\alpha(k)} \rangle + F_{ij}^{\alpha\alpha}(X^{(k)}). \end{aligned} \quad (89)$$

Substituting Eqs. (88) and (89) into Eq. (35) and simplifying the resulting equation with Eq. (49), we obtain

$$G(X|X^{(k)}) = \sum_{\alpha \in \mathcal{A}} G^\alpha(X^\alpha|X^{(k)}) + F(X^{(k)}),$$

in which $G^\alpha(X^\alpha|X^{(k)})$ is a function that is related with $X^\alpha \in \mathcal{X}^\alpha$ only. Furthermore, a tedious but straightforward mathematical manipulation from Eqs. (87) to (89) indicates that there exists positive-semidefinite matrices $\Gamma^{\alpha(k)} \in \mathbb{R}^{(d+1)n_\alpha \times (d+1)n_\alpha}$ such that $G^\alpha(X^\alpha|X^{(k)})$ in the equation above can be written as

$$\begin{aligned} G^\alpha(X^\alpha|X^{(k)}) &= \frac{1}{2}\|X^\alpha - X^{\alpha(k)}\|_{\Gamma^{\alpha(k)}}^2 + \\ &\langle \nabla_{X^\alpha} F(X^{(k)}), X^\alpha - X^{\alpha(k)} \rangle, \end{aligned}$$

in which the formulation of $\Gamma^{\alpha(k)}$ is given in Appendix I. The proof is completed.

Proof of (b). If we substitute Eq. (37) into Eq. (36), the result is

$$\begin{aligned} G(X|X^{(k)}) &= \sum_{\alpha \in \mathcal{A}} \left[\frac{1}{2}\|X^\alpha - X^{\alpha(k)}\|_{\Gamma^{\alpha(k)}}^2 + \right. \\ &\left. \langle \nabla_{X^\alpha} F(X^{(k)}), X^\alpha - X^{\alpha(k)} \rangle \right] + F(X^{(k)}). \end{aligned} \quad (90)$$

Furthermore, it can be shown that

$$\frac{1}{2}\|X - X^{(k)}\|_{\Gamma^{(k)}}^2 = \sum_{\alpha \in \mathcal{A}} \frac{1}{2}\|X^\alpha - X^{\alpha(k)}\|_{\Gamma^{\alpha(k)}}^2,$$

in which $\Gamma^{(k)} \in \mathbb{R}^{(d+1)n \times (d+1)n}$ is defined as Eq. (39), and

$$\begin{aligned} \langle \nabla F(X^{(k)}), X - X^{(k)} \rangle &= \\ &\sum_{\alpha \in \mathcal{A}} \langle \nabla_{X^\alpha} F(X^{(k)}), X^\alpha - X^{\alpha(k)} \rangle. \end{aligned}$$

Thus, Eq. (90) is equivalent to Eq. (38), i.e.,

$$\begin{aligned} G(X|X^{(k)}) &= \frac{1}{2}\|X - X^{(k)}\|_{\Gamma^{(k)}}^2 + \\ &\langle \nabla F(X^{(k)}), X - X^{(k)} \rangle + F(X^{(k)}). \end{aligned} \quad (91)$$

From Proposition 2, it is known that $E_{ij}^{\alpha\beta}(X|X^{(k)})$ majorizes $F_{ij}^{\alpha\beta}(X)$ and $E_{ij}^{\alpha\beta}(X|X^{(k)}) = F_{ij}^{\alpha\beta}(X^{(k)})$ if $X = X^{(k)}$. Then, as a result of Eqs. (18) and (35), it can be concluded that $G(X|X^{(k)})$ majorizes $F(X)$ and $G(X|X^{(k)}) = F(X)$ if $X = X^{(k)}$. The proof is completed.

Proof of (c). From Eqs. (22), (33), (35) and (91), we rewrite $\Gamma^{(k)} \in \mathbb{R}^{(d+1)n \times (d+1)n}$ as

$$\begin{aligned} \Gamma^{(k)} &= \sum_{\alpha \in \mathcal{A}} \sum_{(i,j) \in \bar{\mathcal{E}}^{\alpha\alpha}} M_{ij}^{\alpha\alpha} + \\ &\sum_{\substack{\alpha, \beta \in \mathcal{A}, \\ \alpha \neq \beta}} \sum_{(i,j) \in \bar{\mathcal{E}}^{\alpha\beta}} \omega_{ij}^{\alpha\beta(k)} \cdot \Omega_{ij}^{\alpha\beta} + \xi \cdot \mathbf{I}, \end{aligned} \quad (92)$$

in which $\Omega_{ij}^{\alpha\beta} \succeq M_{ij}^{\alpha\beta}$ by Eq. (32) and $\xi \geq 0$. Then, as a result of Eqs. (27), (32) and (92), it is straightforward to conclude that

$$\Gamma^{(k)} \succeq M^{(k)} + \xi \cdot \mathbf{I} \succeq M^{(k)}. \quad (93)$$

The proof is completed.

Proof of (d). Let $\Gamma \in \mathbb{R}^{(d+1)n \times (d+1)n}$ be defined as

$$\Gamma \triangleq \sum_{\alpha \in \mathcal{A}} \sum_{(i,j) \in \mathcal{E}^{\alpha}} M_{ij}^{\alpha} + \sum_{\substack{\alpha, \beta \in \mathcal{A}, \\ \alpha \neq \beta}} \sum_{(i,j) \in \mathcal{E}^{\alpha\beta}} \Omega_{ij}^{\alpha\beta} + \xi \cdot \mathbf{I}. \quad (94)$$

From Assumption 2(d) and Eq. (25), it can be concluded that

$$0 \leq \omega_{ij}^{\alpha\beta(k)} \leq 1 \quad (95)$$

for any $X^{(k)} \in \mathbb{R}^{d \times (d+1)n}$. Furthermore, it is known that $\Omega_{ij}^{\alpha\beta} \succeq 0$, then Eqs. (92), (94) and (95) result in $\Gamma \succeq \Gamma^{(k)}$ for any $X^{(k)} \in \mathbb{R}^{d \times (d+1)n}$. The proof is completed.

APPENDIX E. PROOF OF PROPOSITION 5

Proof of (a). From Assumption 3 and line 8 of Algorithm 1, we obtain

$$G^{\alpha}(X^{\alpha(k+1)}|X^{(k)}) \leq G^{\alpha}(X^{\alpha(k+\frac{1}{2})}|X^{(k)}) \quad (96)$$

and

$$H^{\alpha}(X^{\alpha(k+\frac{1}{2})}|X^{(k)}) \leq H^{\alpha}(X^{\alpha(k)}|X^{(k)}). \quad (97)$$

From Eqs. (36), (42), (96) and (97), it can be concluded that

$$G(X^{(k+1)}|X^{(k)}) \leq G(X^{(k+\frac{1}{2})}|X^{(k)}) \quad (98)$$

and

$$H(X^{(k+\frac{1}{2})}|X^{(k)}) \leq H(X^{(k)}|X^{(k)}). \quad (99)$$

Note that Eq. (48) suggests

$$F(X^{(k+1)}) \leq G(X^{(k+1)}|X^{(k)}) \quad (100)$$

and

$$G(X^{(k+\frac{1}{2})}|X^{(k)}) \leq H(X^{(k+\frac{1}{2})}|X^{(k)}). \quad (101)$$

Then, Eqs. (98) to (101) result in

$$\begin{aligned} F(X^{(k+1)}) &\leq G(X^{(k+1)}|X^{(k)}) \leq \\ &G(X^{(k+\frac{1}{2})}|X^{(k)}) \leq H(X^{(k+\frac{1}{2})}|X^{(k)}) \leq \\ &H(X^{(k)}|X^{(k)}) = F(X^{(k)}), \end{aligned} \quad (102)$$

which indicates that $F(X^{(k)})$ is nonincreasing. The proof is completed.

Proof of (b). From Proposition 5(a), it has been proved that $F(X^{(k)})$ is nonincreasing. From Eq. (17) and Assumption 2, $F(X^{(k)}) \geq 0$, i.e., $F(X^{(k)})$ is bounded below. As a result, there exists $F^{\infty} \in \mathbb{R}$ such that $F(X^{(k)}) \rightarrow F^{\infty}$. The proof is completed.

Proof of (c). From Eq. (102), it is known that $F(X^{(k)}) \geq G(X^{(k+1)}|X^{(k)})$, which suggests

$$F(X^{(k)}) - F(X^{(k+1)}) \geq G(X^{(k+1)}|X^{(k)}) - F(X^{(k+1)}). \quad (103)$$

From Eqs. (26) and (38), we obtain

$$\begin{aligned} F(X^{(k+1)}) &\leq \frac{1}{2} \|X^{(k+1)} - X^{(k)}\|_{M^{(k)}}^2 + \\ &\langle \nabla F(X^{(k)}), X - X^{(k)} \rangle + F(X^{(k)}) \end{aligned} \quad (104)$$

and

$$\begin{aligned} G(X^{(k+1)}|X^{(k)}) &= \frac{1}{2} \|X^{(k+1)} - X^{(k)}\|_{\Gamma^{(k)}}^2 + \\ &\langle \nabla F(X^{(k)}), X - X^{(k)} \rangle + F(X^{(k)}), \end{aligned} \quad (105)$$

respectively. Substituting Eqs. (104) and (105) into the right-hand side of Eq. (103), we obtain

$$\begin{aligned} F(X^{(k)}) - F(X^{(k+1)}) &\geq \\ &\frac{1}{2} \|X^{(k+1)} - X^{(k)}\|_{\Gamma^{(k)}}^2 - \frac{1}{2} \|X^{(k+1)} - X^{(k)}\|_{M^{(k)}}^2. \end{aligned} \quad (106)$$

From Eqs. (93) and (106), there exists a constant scalar $\delta > 0$ such that

$$F(X^{(k)}) - F(X^{(k+1)}) \geq \frac{\delta}{2} \|X^{(k+1)} - X^{(k)}\|^2 \quad (107)$$

as long as $\xi > 0$. From Proposition 5(b), we obtain

$$F(X^{(k)}) - F(X^{(k+1)}) \rightarrow 0, \quad (108)$$

and thus, it can be concluded from Eqs. (107) and (108) that

$$\|X^{(k+1)} - X^{(k)}\| \rightarrow 0. \quad (109)$$

The proof is completed.

Proof of (d). From Eq. (102), it is known that $F(X^{(k)}) \geq H(X^{(k+\frac{1}{2})}|X^{(k)})$ and $G(X^{(k+\frac{1}{2})}|X^{(k)}) \geq G(X^{(k+1)}|X^{(k)}) \geq F(X^{(k+1)})$, which suggests

$$\begin{aligned} F(X^{(k)}) - F(X^{(k+1)}) &\geq \\ &H(X^{(k+\frac{1}{2})}|X^{(k)}) - G(X^{(k+\frac{1}{2})}|X^{(k)}). \end{aligned}$$

From Eqs. (38) and (46), the equation above is equivalent to

$$\begin{aligned} F(X^{(k)}) - F(X^{(k+1)}) &\geq \\ &\frac{1}{2} \|X^{(k+\frac{1}{2})} - X^{(k)}\|_{\Pi^{(k)}}^2 - \frac{1}{2} \|X^{(k+\frac{1}{2})} - X^{(k)}\|_{\Gamma^{(k)}}^2. \end{aligned} \quad (110)$$

A similar procedure to the derivation of Eq. (93) results in

$$\Pi^{(k)} \succeq \Gamma^{(k)} + (\zeta - \xi) \cdot \mathbf{I}, \quad (111)$$

which suggests there exists a constant scalar $\delta' > 0$ such that

$$\Pi^{(k)} \succeq \Gamma^{(k)} + \delta' \cdot \mathbf{I}$$

if $\zeta > \xi > 0$. Then, similar to the proof of Proposition 5(c), we obtain

$$F(X^{(k)}) - F(X^{(k+1)}) \geq \frac{\delta'}{2} \|X^{(k+\frac{1}{2})} - X^{(k)}\|^2. \quad (112)$$

Thus, it can be concluded that

$$\|X^{(k+\frac{1}{2})} - X^{(k)}\| \rightarrow 0. \quad (113)$$

The proof is completed.

Proof of (e). The following proposition about $\nabla F(X)$ is needed in this proof.

Proposition 9. If Assumption 2(e) holds, then the Euclidean gradient $\nabla F(\cdot) : \mathbb{R}^{d \times (d+1)n} \rightarrow \mathbb{R}^{d \times (d+1)n}$ of $F(X)$ in Eq. (18) is Lipschitz continuous, i.e., there exists a constant $\mu > 0$ such that $\|\nabla F(X) - \nabla F(X')\| \leq \mu \cdot \|X - X'\|$.

Proof. From Assumption 2(e), it is known that $\rho(\|X\|^2)$ has Lipschitz continuous gradient, which suggests that $F_{ij}^{\alpha\beta}(X) = \frac{1}{2}\rho(\|X\|_{M_{ij}^{\alpha\beta}}^2)$ in Eq. (23) has Lipschitz continuous gradient. Note that $F_{ij}^{\alpha\alpha}(X) = \frac{1}{2}\|X\|_{M_{ij}^{\alpha\alpha}}^2$ in Eq. (22) has Lipschitz continuous gradient as well. Then, from Eq. (18), it can be concluded that $F(X)$ has Lipschitz continuous gradient. The proof is completed. \square

It is straightforward to show that the Riemannian gradient $\text{grad} F(X)$ takes the form as

$$\text{grad} F(X) = [\text{grad}_1 F(X) \quad \cdots \quad \text{grad}_{|\mathcal{A}|} F(X)] \in T_X \mathcal{X}.$$

In the equation above, $\text{grad}_\alpha F(X)$ is the Riemannian gradient of $F(X)$ with respect to $X^\alpha \in \mathcal{X}^\alpha$ for node $\alpha \in \mathcal{A}$, and can be written as

$$\text{grad}_\alpha F(X) = [\text{grad}_{t^\alpha} F(X) \quad \text{grad}_{R^\alpha} F(X)] \in T_{X^\alpha} \mathcal{X}^\alpha \quad (114)$$

in which recall that

$$T_{X^\alpha} \mathcal{X}^\alpha \triangleq \mathbb{R}^{d \times n_\alpha} \times T_{R^\alpha} SO(d)^{n_\alpha}.$$

From [8], [53], it can be shown that $\text{grad}_{t^\alpha} F(X)$ and $\text{grad}_{R^\alpha} F(X)$ in Eq. (114) are

$$\text{grad}_{t^\alpha} F(X) = \nabla_{t^\alpha} F(X) \quad (115)$$

and

$$\text{grad}_{R^\alpha} F(X) = \nabla_{R^\alpha} F(X) - R^\alpha \text{SymBlockDiag}_d^\alpha (R^{\alpha\top} \nabla_{R^\alpha} F(X)). \quad (116)$$

In Eq. (116), $\text{SymBlockDiag}_d^\alpha : \mathbb{R}^{d n_\alpha \times d n_\alpha} \rightarrow \mathbb{R}^{d n_\alpha \times d n_\alpha}$ is a linear operator

$$\text{SymBlockDiag}_d^\alpha(Z) \triangleq \frac{1}{2} \text{BlockDiag}_d^\alpha(Z + Z^\top), \quad (117)$$

in which $\text{BlockDiag}_d^\alpha : \mathbb{R}^{d n_\alpha \times d n_\alpha} \rightarrow \mathbb{R}^{d n_\alpha \times d n_\alpha}$ extracts the $d \times d$ -block diagonals of a matrix, i.e.,

$$\text{BlockDiag}_d^\alpha(Z) \triangleq \begin{bmatrix} Z_{11} & & \\ & \ddots & \\ & & Z_{n_\alpha n_\alpha} \end{bmatrix} \in \mathbb{R}^{d n_\alpha \times d n_\alpha}.$$

As a result of Eqs. (114) to (117), there exists a linear operator

$$\mathcal{Q}_X : \mathbb{R}^{d \times d(n+1)} \rightarrow \mathbb{R}^{d \times d(n+1)} \quad (118)$$

that continuously depends on $X \in \mathcal{X}$ such that

$$\text{grad} F(X) = \mathcal{Q}_X(\nabla F(X)). \quad (119)$$

From Eq. (46), it is straightforward to show that

$$\begin{aligned} & \nabla H(X^{(k+\frac{1}{2})}|X^{(k)}) \\ &= \nabla F(X^{(k)}) + (X^{(k+\frac{1}{2})} - X^{(k)})\Pi^{(k)} \\ &= \nabla F(X^{(k+\frac{1}{2})}) + (X^{(k+\frac{1}{2})} - X^{(k)})\Pi^{(k)} + \\ & \quad (\nabla F(X^{(k)}) - \nabla F(X^{(k+\frac{1}{2})})). \end{aligned} \quad (120)$$

Note that Eq. (119) applies to any functions on \mathcal{X} . As a result of Eqs. (119) and (120), we obtain

$$\begin{aligned} & \text{grad} H(X^{(k+\frac{1}{2})}|X^{(k)}) \\ &= \text{grad} F(X^{(k+\frac{1}{2})}) + \\ & \quad \mathcal{Q}_{X^{(k+\frac{1}{2})}}((X^{(k+\frac{1}{2})} - X^{(k)})\Pi^{(k)}) + \\ & \quad \mathcal{Q}_{X^{(k+\frac{1}{2})}}(\nabla F(X^{(k)}) - \nabla F(X^{(k+\frac{1}{2})})). \end{aligned} \quad (121)$$

From line 8 of Algorithm 1, we obtain.

$$\text{grad} H^\alpha(X^{\alpha(k+\frac{1}{2})}|X^{(k)}) = \mathbf{0}.$$

In addition, it is by definition that

$$\begin{aligned} & \text{grad} H(X|X^{(k)}) = \\ & \quad [\text{grad} H^1(X^1|X^{(k)}) \quad \cdots \quad \text{grad} H^{|\mathcal{A}|}(X^{|\mathcal{A}|}|X^{(k)})], \end{aligned}$$

which suggests

$$\text{grad} H(X^{(k+\frac{1}{2})}|X^{(k)}) = \mathbf{0}. \quad (122)$$

From Eqs. (121) and (122), we obtain

$$\begin{aligned} \text{grad} F(X^{(k+\frac{1}{2})}) &= \mathcal{Q}_{X^{(k+\frac{1}{2})}}((X^{(k)} - X^{(k+\frac{1}{2})})\Pi^{(k)}) + \\ & \quad \mathcal{Q}_{X^{(k+\frac{1}{2})}}(\nabla F(X^{(k+\frac{1}{2})}) - \nabla F(X^{(k)})). \end{aligned}$$

From the equation above, it can be shown that

$$\begin{aligned} & \|\text{grad} F(X^{(k+\frac{1}{2})})\| \\ &= \|\mathcal{Q}_{X^{(k+\frac{1}{2})}}((X^{(k)} - X^{(k+\frac{1}{2})})\Pi^{(k)}) + \\ & \quad \mathcal{Q}_{X^{(k+\frac{1}{2})}}(\nabla F(X^{(k+\frac{1}{2})}) - \nabla F(X^{(k)}))\| \\ &\leq \|\mathcal{Q}_{X^{(k+\frac{1}{2})}}((X^{(k)} - X^{(k+\frac{1}{2})})\Pi^{(k)})\| + \\ & \quad \|\mathcal{Q}_{X^{(k+\frac{1}{2})}}(\nabla F(X^{(k+\frac{1}{2})}) - \nabla F(X^{(k)}))\| \\ &\leq \|\mathcal{Q}_{X^{(k+\frac{1}{2})}}\|_2 \cdot \|\Pi^{(k)}\|_2 \cdot \|X^{(k+\frac{1}{2})} - X^{(k)}\| + \\ & \quad \|\mathcal{Q}_{X^{(k+\frac{1}{2})}}\|_2 \cdot \|\nabla F(X^{(k+\frac{1}{2})}) - \nabla F(X^{(k)})\|, \end{aligned} \quad (123)$$

in which $\|\cdot\|_2$ denotes the induced 2-norm of linear operators. From Propositions 4(d) and 9, there exists a constant positive-semidefinite matrix $\Pi \in \mathbb{R}^{(d+1)n \times (d+1)n}$ and constant positive scalar $\mu > 0$ such that $\Pi \succeq \Pi^{(k)} \succeq 0$ and $\|\nabla F(X^{(k+\frac{1}{2})}) - \nabla F(X^{(k)})\| \leq \mu \cdot \|X^{(k+\frac{1}{2})} - X^{(k)}\|$ for any $k \geq 0$, making it possible to upper-bound the right-hand side of Eq. (123):

$$\begin{aligned} & \|\text{grad} F(X^{(k+\frac{1}{2})})\| \\ &\leq \|\mathcal{Q}_{X^{(k+\frac{1}{2})}}\|_2 \cdot \|\Pi\|_2 \cdot \|X^{(k+\frac{1}{2})} - X^{(k)}\| + \\ & \quad \|\mathcal{Q}_{X^{(k+\frac{1}{2})}}\|_2 \cdot \mu \cdot \|X^{(k+\frac{1}{2})} - X^{(k)}\|. \end{aligned} \quad (124)$$

Moreover, Eqs. (114) to (116) indicate that $\mathcal{Q}_X(\cdot)$ only depends on the rotation $R^\alpha \in SO(d)^{n_\alpha}$ for $\alpha \in \mathcal{A}$. Since $\mathcal{Q}_X(\cdot)$ is continuous and $SO(d)^{n_\alpha}$ is a compact manifold, $\|\mathcal{Q}_{X^{(k+\frac{1}{2})}}\|_2$ is bounded for any $X^{(k+\frac{1}{2})} \in \mathcal{X}$. Thus, there exists a constant scalar $\nu > 0$ such that the right-hand side of Eq. (124) can be upper-bounded as

$$\|\text{grad} F(X^{(k+\frac{1}{2})})\| \leq \nu \|X^{(k+\frac{1}{2})} - X^{(k)}\|. \quad (125)$$

As long as $\zeta > \xi > 0$, Eqs. (112) and (125) result in

$$\|\text{grad} F(X^{(k+\frac{1}{2})})\|^2 \leq \frac{2\nu^2}{\delta'} (F(X^{(k)}) - F(X^{(k+1)})).$$

Then, there exists a constant scalar $\epsilon = \frac{\delta'}{\nu^2} > 0$ with which the equation above can be rewritten as

$$F(X^{(k)}) - F(X^{(k+1)}) \geq \frac{\epsilon}{2} \|\text{grad } F(X^{(k+\frac{1}{2})})\|^2. \quad (126)$$

As a result of Eq. (126), we obtain

$$\begin{aligned} F(X^{(0)}) - F(X^{(K+1)}) &\geq \frac{\epsilon}{2} \sum_{k=0}^K \|\text{grad } F(X^{(k+\frac{1}{2})})\|^2 \\ &\geq \frac{\epsilon(K+1)}{2} \min_{0 \leq k \leq K} \|\text{grad } F(X^{(k+\frac{1}{2})})\|^2. \end{aligned} \quad (127)$$

From Propositions 5(a) and 5(b), it can be concluded that $F(X^{(k+1)}) \geq F^\infty$ for any $k \geq 0$, which and Eq. (127) suggest

$$\min_{0 \leq k < K} \|\text{grad } F(X^{(k+\frac{1}{2})})\| \leq \sqrt{\frac{2}{\epsilon} \cdot \frac{F(X^{(0)}) - F^\infty}{K+1}}.$$

The proof is completed.

Proof of (f). As a result of Propositions 5(c) and 5(d), it is known that

$$\|X^{(k+1)} - X^{(k)}\| \rightarrow 0$$

and

$$\|X^{(k+\frac{1}{2})} - X^{(k)}\| \rightarrow 0$$

as long as $\zeta > \xi > 0$. Thus, it can be concluded from Eq. (125) that

$$\text{grad } F(X^{(k+\frac{1}{2})}) \rightarrow \mathbf{0}$$

if $\zeta > \xi > 0$. In addition, Assumption 2(b) indicates that $\text{grad } F(X^{(k)})$ is continuous, which suggests

$$\text{grad } F(X^{(k)}) \rightarrow \text{grad } F(X^{(k+\frac{1}{2})}).$$

Then, we obtain

$$\text{grad } F(X^{(k)}) \rightarrow \mathbf{0}.$$

The proof is completed.

APPENDIX F. PROOF OF PROPOSITION 6

Proof of (a). In this proof, we will prove $F(X^{(k)}) \leq \bar{F}^{(k)}$ and $\bar{F}^{(k+1)} \leq \bar{F}^{(k)}$ by induction.

1) From lines 4, 8, 14 of Algorithm 3, it can be shown that

$$F(X^{(-1)}) = F(X^{(0)}) = \bar{F}^{(-1)} = \bar{F}^{(0)}. \quad (128)$$

2) Suppose $k \geq 0$ and $F(X^{(k)}) \leq \bar{F}^{(k)}$ holds at k -th iteration. In terms of $X^{(k+\frac{1}{2})}$, if the adaptive restart scheme for $X^{(k+\frac{1}{2})}$ is not triggered, it is immediate to show from line 10 of Algorithm 4 that

$$F(X^{(k+\frac{1}{2})}) \leq \bar{F}^{(k)}. \quad (129)$$

On the other hand, if the adaptive restart scheme for $X^{(k+\frac{1}{2})}$ is triggered, line 12 of Algorithm 4 results in

$$H^\alpha(X^{\alpha(k+\frac{1}{2})}|X^{(k)}) \leq H^\alpha(X^{\alpha(k)}|X^{(k)}) = 0, \quad (130)$$

where $H^\alpha(X^{\alpha(k)}|X^{(k)}) = 0$ is from Eq. (44). Then, Eqs. (42), (48) and (130) indicate

$$F(X^{(k+\frac{1}{2})}) \leq H(X^{(k+\frac{1}{2})}|X^{(k)}) \leq F(X^{(k)}) \leq \bar{F}^{(k)}. \quad (131)$$

Therefore, no matter whether the adaptive restart scheme is triggered or not, we conclude from Eqs. (129) and (131) that

$$F(X^{(k+\frac{1}{2})}) \leq \bar{F}^{(k)} \quad (132)$$

always holds.

Furthermore, as a result of lines 25 to 27 of Algorithm 4, we obtain

$$F(X^{(k+1)}) - \bar{F}^{(k)} \leq \phi \cdot (F(X^{(k+\frac{1}{2})}) - \bar{F}^{(k)}) \leq 0. \quad (133)$$

From line 14 of Algorithm 3 and $F(X^{(k+1)}) - \bar{F}^{(k)} \leq 0$ in Eq. (133), we obtain

$$F(X^{(k+1)}) - \bar{F}^{(k+1)} = (1 - \eta) \cdot (F(X^{(k+1)}) - \bar{F}^{(k)}) \leq 0$$

and

$$\bar{F}^{(k+1)} - \bar{F}^{(k)} = \eta \cdot (F(X^{(k+1)}) - \bar{F}^{(k)}) \leq 0,$$

which suggest $F(X^{(k+1)}) \leq \bar{F}^{(k+1)} \leq \bar{F}^{(k)}$.

3) Therefore, it can be concluded that $F(X^{(k)}) \leq \bar{F}^{(k)}$ and $\bar{F}^{(k+1)} \leq \bar{F}^{(k)}$, which suggests that $\bar{F}^{(k)}$ is nonincreasing. The proof is completed.

Proof of (b). From line 14 of Algorithm 3, we obtain

$$\bar{F}^{(k+1)} = (1 - \eta) \cdot \bar{F}^{(k)} + \eta \cdot F(X^{(k+1)}), \quad (134)$$

which and Eq. (128) suggest that $\bar{F}^{(k)}$ is a convex combination of $F(X^{(0)})$, $F(X^{(1)})$, \dots , $F(X^{(k)})$ as long as $\eta \in (0, 1]$. Since $F(X^{(k)}) \geq 0$, we obtain $\bar{F}^{(k)} \geq 0$ as well, i.e., $\bar{F}^{(k)}$ is bounded below. Proposition 6(a) indicates that $\bar{F}^{(k)}$ is nonincreasing, and thus, there exists F^∞ such that $\bar{F}^{(k)} \rightarrow F^\infty$. Then, it can be still concluded from Eq. (134) that $F(X^{(k)}) \rightarrow F^\infty$.

Proof of (c). If $k = -1$, line 4 of Algorithm 3 and Eq. (65) suggest $X^{(-1)} = X^{(0)}$ and $\bar{F}^{(-1)} = \bar{F}^{(0)} = F(X^{(0)})$, respectively, from which we conclude

$$\bar{F}^{(-1)} - \bar{F}^{(0)} = \|X^{(-1)} - X^{(0)}\|^2. \quad (135)$$

If $k \geq 0$, there exists three possible cases for $X^{(k+1)}$:

1) If $X^{(k+1)}$ is from line 6 of Algorithm 4, then the adaptive restart scheme is not triggered and line 10 of Algorithm 4 results in

$$\bar{F}^{(k)} - F(X^{(k+1)}) \geq \psi \cdot \|X^{(k+1)} - X^{(k)}\|^2. \quad (136)$$

2) If $X^{(k+1)}$ is from line 19 of Algorithm 4, then the adaptive restart scheme is triggered and Eq. (110) holds as well, from which and Eq. (93) we obtain

$$F(X^{(k)}) - F(X^{(k+1)}) \geq \frac{\xi}{2} \|X^{(k+1)} - X^{(k)}\|^2.$$

In the proof of Proposition 6(a), it is known that $\bar{F}^{(k)} \geq F(X^{(k)})$, then the equation above results in

$$\bar{F}^{(k)} - F(X^{(k+1)}) \geq \frac{\xi}{2} \|X^{(k+1)} - X^{(k)}\|^2. \quad (137)$$

3) If $X^{(k+1)}$ is from line 26 of Algorithm 4, then we obtain $X^{(k+1)} = X^{(k+\frac{1}{2})}$ and $F(X^{(k+1)}) = F(X^{(k+\frac{1}{2})})$. Then, similar to the derivations of Eqs. (136) and (137), lines 5 and 12 of Algorithm 4 result in

$$\bar{F}^{(k)} - F(X^{(k+\frac{1}{2})}) \geq \psi \cdot \|X^{(k+\frac{1}{2})} - X^{(k)}\|^2 \quad (138)$$

and

$$\bar{F}^{(k)} - F(X^{(k+\frac{1}{2})}) \geq \frac{\zeta}{2} \|X^{(k+\frac{1}{2})} - X^{(k)}\|^2, \quad (139)$$

respectively, from which and $X^{(k+1)} = X^{(k+\frac{1}{2})}$ and $F(X^{(k+1)}) = F(X^{(k+\frac{1}{2})})$ we obtain either

$$\bar{F}^{(k)} - F(X^{(k+1)}) \geq \psi \cdot \|X^{(k+1)} - X^{(k)}\|^2$$

or

$$\bar{F}^{(k)} - F(X^{(k+1)}) \geq \frac{\zeta}{2} \|X^{(k+1)} - X^{(k)}\|^2.$$

Therefore, if $0 < \eta \leq 1$, $0 < \psi \leq 1$, $\xi > 0$, $\zeta > 0$, it can be shown from cases 1) to 3) above that there exists a constant scalar $\sigma > 0$ such that

$$\bar{F}^{(k)} - F(X^{(k+1)}) \geq \frac{\sigma}{2} \|X^{(k+1)} - X^{(k)}\|^2 \quad (140)$$

holds for any $k \geq 0$. In addition, note that Eq. (134) is equivalent to

$$\bar{F}^{(k)} - \bar{F}^{(k+1)} = \eta \cdot (\bar{F}^{(k)} - F(X^{(k+1)})). \quad (141)$$

From Eqs. (140) and (141), we conclude that there exists $\delta > 0$ such that

$$\begin{aligned} \bar{F}^{(k)} - \bar{F}^{(k+1)} &= \eta \cdot (\bar{F}^{(k)} - F(X^{(k+1)})) \geq \\ &\frac{\eta\sigma}{2} \|X^{(k+1)} - X^{(k)}\|^2 \geq \frac{\delta}{2} \|X^{(k+1)} - X^{(k)}\|^2 \end{aligned} \quad (142)$$

for any $k \geq 0$.

As a result of Eqs. (135) and (142), we further obtain

$$\bar{F}^{(k)} - \bar{F}^{(k+1)} \geq \frac{\delta}{2} \|X^{(k+1)} - X^{(k)}\|^2 \quad (143)$$

for any $k \geq -1$. Recall $\bar{F}^{(k)} \rightarrow F^\infty$ from Proposition 6(b), which suggests

$$\bar{F}^{(k)} - \bar{F}^{(k+1)} \rightarrow 0. \quad (144)$$

Therefore, Eqs. (143) and (144) indicate that

$$\|X^{(k+1)} - X^{(k)}\| \rightarrow 0.$$

The proof is completed.

Proof of (d). Note that Eqs. (138) and (139) suggest that there exists $\sigma' > 0$ such that

$$\bar{F}^{(k)} - F(X^{(k+\frac{1}{2})}) \geq \frac{\sigma'}{2} \|X^{(k+\frac{1}{2})} - X^{(k)}\|^2 \quad (145)$$

always holds. From lines 25 to 27 of Algorithm 4, we obtain

$$\begin{aligned} \bar{F}^{(k)} - F(X^{(k+1)}) &\geq \phi \cdot (\bar{F}^{(k)} - F(X^{(k+\frac{1}{2})})) \geq \\ &\frac{\phi\sigma'}{2} \|X^{(k+\frac{1}{2})} - X^{(k)}\|^2, \end{aligned} \quad (146)$$

where the last inequality is due to Eq. (145). From Eqs. (141) and (146), it can be shown that

$$\begin{aligned} \bar{F}^{(k)} - \bar{F}^{(k+1)} &= \eta \cdot (\bar{F}^{(k)} - F(X^{(k+1)})) \geq \\ &\frac{\eta\phi\sigma'}{2} \|X^{(k+\frac{1}{2})} - X^{(k)}\|^2. \end{aligned} \quad (147)$$

The equation above suggests that there exists a constant scalar $\delta' > 0$ such that

$$\bar{F}^{(k)} - \bar{F}^{(k+1)} \geq \frac{\delta'}{2} \|X^{(k+\frac{1}{2})} - X^{(k)}\|^2. \quad (148)$$

Note that Proposition 6(b) results in $\bar{F}^{(k)} - \bar{F}^{(k+1)} \rightarrow 0$. Thus, similar to the proof of Proposition 6(c), it can be concluded from Eq. (148) that

$$\|X^{(k+\frac{1}{2})} - X^{(k)}\| \rightarrow 0$$

if $\zeta > \xi > 0$. The proof is completed.

Proof of (e). For any $k \geq 0$, there are two possible cases about $X^{\alpha(k+\frac{1}{2})} \in \mathcal{X}^\alpha$:

1) If $X^{\alpha(k+\frac{1}{2})} \in \mathcal{X}^\alpha$ is from line 5 of Algorithm 4, we obtain

$$X^{\alpha(k+\frac{1}{2})} \leftarrow \arg \min_{X^\alpha \in \mathcal{X}^\alpha} H^\alpha(X^\alpha | Y^{(k)}). \quad (149)$$

From Eq. (44), it can be shown that

$$\begin{aligned} &\nabla H^\alpha(X^{\alpha(k+\frac{1}{2})} | Y^{(k)}) \\ &= \nabla_{X^\alpha} F(Y^{(k)}) + (X^{\alpha(k+\frac{1}{2})} - Y^{\alpha(k)}) \Pi^{\alpha(k)} \\ &= \nabla_{X^\alpha} F(X^{(k+\frac{1}{2})}) + (X^{\alpha(k+\frac{1}{2})} - Y^{\alpha(k)}) \Pi^{\alpha(k)} + \\ &\quad (\nabla_{X^\alpha} F(Y^{(k)}) - \nabla_{X^\alpha} F(X^{(k+\frac{1}{2})})). \end{aligned}$$

The equation above suggests

$$\begin{aligned} &\text{grad } H^\alpha(X^{\alpha(k+\frac{1}{2})} | Y^{(k)}) \\ &= \text{grad}_\alpha F(X^{(k+\frac{1}{2})}) + \\ &\quad \mathcal{Q}_{X^{\alpha(k+\frac{1}{2})}}^\alpha ((X^{\alpha(k+\frac{1}{2})} - Y^{\alpha(k)}) \Pi^{\alpha(k)}) + \\ &\quad \mathcal{Q}_{X^{\alpha(k+\frac{1}{2})}}^\alpha (\nabla_{X^\alpha} F(Y^{(k)}) - \nabla_{X^\alpha} F(X^{(k+\frac{1}{2})})), \end{aligned} \quad (150)$$

where $\text{grad}_\alpha F(X)$ is the Riemannian gradient of $F(X)$ with respect to $X^\alpha \in \mathcal{X}^\alpha$, and $\mathcal{Q}_{X^\alpha}^\alpha : \mathbb{R}^{d \times d n_\alpha} \rightarrow \mathbb{R}^{d \times d n_\alpha}$ is a linear operator that extracts the α -th block of $\mathcal{Q}_X(\cdot)$ in Eq. (118). Since $X^{\alpha(k+\frac{1}{2})}$ is an optimal solution to Eq. (149), we obtain

$$\text{grad } H^\alpha(X^{\alpha(k+\frac{1}{2})} | Y^{(k)}) = \mathbf{0}. \quad (151)$$

From Eqs. (150) and (151), a straightforward mathematical manipulation indicates

$$\begin{aligned} &\text{grad}_\alpha F(X^{(k+\frac{1}{2})}) \\ &= \mathcal{Q}_{X^{\alpha(k+\frac{1}{2})}}^\alpha ((Y^{\alpha(k)} - X^{\alpha(k+\frac{1}{2})}) \Pi^{\alpha(k)}) + \\ &\quad \mathcal{Q}_{X^{\alpha(k+\frac{1}{2})}}^\alpha (\nabla_{X^\alpha} F(X^{(k+\frac{1}{2})}) - \nabla_{X^\alpha} F(Y^{(k)})). \end{aligned} \quad (152)$$

From Eq. (152), we further obtain

$$\begin{aligned}
& \|\text{grad}_\alpha F(X^{(k+\frac{1}{2})})\| \\
& \leq \|\mathcal{Q}_{X^{\alpha(k+\frac{1}{2})}}^\alpha\|_2 \cdot \|(Y^{\alpha(k)} - X^{\alpha(k+\frac{1}{2})})\Pi^{\alpha(k)}\| + \\
& \quad \|\mathcal{Q}_{X^{\alpha(k+\frac{1}{2})}}^\alpha\|_2 \cdot \|\nabla_{X^\alpha} F(X^{(k+\frac{1}{2})}) - \nabla_{X^\alpha} F(Y^{(k)})\| \\
& \leq \|\mathcal{Q}_{X^{\alpha(k+\frac{1}{2})}}^\alpha\|_2 \cdot \|(Y^{(k)} - X^{(k+\frac{1}{2})})\Pi^{(k)}\| + \\
& \quad \|\mathcal{Q}_{X^{\alpha(k+\frac{1}{2})}}^\alpha\|_2 \cdot \|\nabla F(X^{(k+\frac{1}{2})}) - \nabla F(Y^{(k)})\| \\
& \leq \|\mathcal{Q}_{X^{\alpha(k+\frac{1}{2})}}^\alpha\|_2 \cdot \|\Pi^{(k)}\|_2 \cdot \|X^{(k+\frac{1}{2})} - Y^{(k)}\| + \\
& \quad \|\mathcal{Q}_{X^{\alpha(k+\frac{1}{2})}}^\alpha\|_2 \cdot \|\nabla F(X^{(k+\frac{1}{2})}) - \nabla F(Y^{(k)})\|,
\end{aligned}$$

where $\|\cdot\|_2$ denotes the induced 2-norm of linear operators. As a result of Propositions 4(d) and 9, the right-hand side of the equation above can be further upper-bounded as

$$\begin{aligned}
& \|\text{grad}_\alpha F(X^{(k+\frac{1}{2})})\| \\
& \leq \|\mathcal{Q}_{X^{\alpha(k+\frac{1}{2})}}^\alpha\|_2 \cdot \|\Pi\|_2 \cdot \|X^{(k+\frac{1}{2})} - Y^{(k)}\| + \\
& \quad \|\mathcal{Q}_{X^{\alpha(k+\frac{1}{2})}}^\alpha\|_2 \cdot \mu \cdot \|X^{(k+\frac{1}{2})} - Y^{(k)}\|. \quad (153)
\end{aligned}$$

Similar to Eqs. (124) and (125), $\|\mathcal{Q}_{X^{\alpha(k+\frac{1}{2})}}^\alpha\|_2$ in Eq. (153) is bounded as well. Therefore, there exists a constant scalar $\nu^\alpha > 0$ such that the right-hand side of Eq. (153) can be upper-bounded:

$$\|\text{grad}_\alpha F(X^{(k+\frac{1}{2})})\| \leq \nu^\alpha \|X^{(k+\frac{1}{2})} - Y^{(k)}\|. \quad (154)$$

Recall that $Y^{(k)} \in \mathbb{R}^{d \times (d+1)n}$ results from line 12 of Algorithm 3:

$$Y^{(k)} = X^{(k)} + (X^{(k)} - X^{(k-1)})\lambda^{(k)}. \quad (155)$$

In Eq. (155), $\lambda^{(k)} \in \mathbb{R}^{(d+1)n \times (d+1)n}$ is a diagonal matrix $\lambda^{(k)} \triangleq \text{diag}\{\lambda^{1(k)} \cdot \mathbf{I}^1, \dots, \lambda^{|\mathcal{A}|(k)} \cdot \mathbf{I}^{|\mathcal{A}|}\} \in \mathbb{R}^{(d+1)n \times (d+1)n}$,

where $\lambda^{\alpha(k)} \in \mathbb{R}$ is given by line 11 of Algorithm 3 and $\mathbf{I}^\alpha \in \mathbb{R}^{(d+1)n_\alpha \times (d+1)n_\alpha}$ is the identity matrix. From Eqs. (154) and (155), it can be shown that

$$\begin{aligned}
& \|\text{grad}_\alpha F(X^{(k+\frac{1}{2})})\| \\
& \leq \nu^\alpha \|X^{(k+\frac{1}{2})} - X^{(k)} - (X^{(k)} - X^{(k-1)})\lambda^{(k)}\| \\
& \leq \nu^\alpha \|(X^{(k)} - X^{(k-1)})\lambda^{(k)}\| + \nu^\alpha \|X^{(k+\frac{1}{2})} - X^{(k)}\| \quad (156) \\
& \leq \nu^\alpha \|\lambda^{(k)}\|_2 \cdot \|X^{(k)} - X^{(k-1)}\| + \\
& \quad \nu^\alpha \|X^{(k+\frac{1}{2})} - X^{(k)}\|.
\end{aligned}$$

From line 11 of Algorithm 3, we obtain $s^{\alpha(k)} \geq 1$, and thus,

$$\lambda^{\alpha(k)} = \frac{\sqrt{4s^{\alpha(k)^2} + 1} - 1}{2s^{\alpha(k)}} = \frac{2s^{\alpha(k)}}{\sqrt{4s^{\alpha(k)^2} + 1} + 1} \in (0, 1),$$

which suggests $\|\lambda^{(k)}\|_2 \in (0, 1)$. Then, we upper-bound the right-hand side of Eq. (156) using $\|\lambda^{(k)}\|_2 \in (0, 1)$:

$$\begin{aligned}
& \|\text{grad}_\alpha F(X^{(k+\frac{1}{2})})\| \leq \nu^\alpha \|X^{(k)} - X^{(k-1)}\| + \\
& \quad \nu^\alpha \|X^{(k+\frac{1}{2})} - X^{(k)}\|. \quad (157)
\end{aligned}$$

2) If $X^{\alpha(k+\frac{1}{2})} \in \mathcal{X}^\alpha$ is from line 12 of Algorithm 4, we obtain

$$X^{\alpha(k+\frac{1}{2})} \leftarrow \arg \min_{X^\alpha \in \mathcal{X}^\alpha} H^\alpha(X^\alpha | X^{(k)}). \quad (158)$$

A similar procedure to the derivation of Eq. (154) yields

$$\|\text{grad}_\alpha F(X^{(k+\frac{1}{2})})\| \leq \nu^\alpha \|X^{(k+\frac{1}{2})} - X^{(k)}\|,$$

where $\nu^\alpha > 0$ is the same as that in Eq. (154). Thus, we obtain

$$\begin{aligned}
& \|\text{grad}_\alpha F(X^{(k+\frac{1}{2})})\| \leq \nu^\alpha \|X^{(k+\frac{1}{2})} - X^{(k)}\| \leq \\
& \quad \nu^\alpha \|X^{(k)} - X^{(k-1)}\| + \nu^\alpha \|X^{(k+\frac{1}{2})} - X^{(k)}\|. \quad (159)
\end{aligned}$$

Therefore, as long as $k \geq 0$, it can be concluded from Eqs. (157) and (159) that

$$\begin{aligned}
& \|\text{grad}_\alpha F(X^{(k+\frac{1}{2})})\| \leq \nu^\alpha \|X^{(k)} - X^{(k-1)}\| + \\
& \quad \nu^\alpha \|X^{(k+\frac{1}{2})} - X^{(k)}\| \quad (160)
\end{aligned}$$

holds for any node $\alpha \in \mathcal{A}$.

If $k \geq 0$, as a result of Eq. (160), there exists a constant scalar $\nu \triangleq \sum_{\alpha \in \mathcal{A}} \nu^\alpha > 0$ such that

$$\begin{aligned}
& \|\text{grad} F(X^{(k+\frac{1}{2})})\| \\
& \leq \sum_{\alpha \in \mathcal{A}} \|\text{grad}_\alpha F(X^{(k+\frac{1}{2})})\| \\
& \leq \sum_{\alpha \in \mathcal{A}} \nu^\alpha \cdot (\|X^{(k)} - X^{(k-1)}\| + \|X^{(k+\frac{1}{2})} - X^{(k)}\|) \\
& = \nu \|X^{(k)} - X^{(k-1)}\| + \nu \|X^{(k+\frac{1}{2})} - X^{(k)}\| \\
& \leq \sqrt{2\nu} \sqrt{\|X^{(k)} - X^{(k-1)}\|^2 + \|X^{(k+\frac{1}{2})} - X^{(k)}\|^2},
\end{aligned}$$

which is equivalent to

$$\begin{aligned}
& \|\text{grad} F(X^{(k+\frac{1}{2})})\|^2 \leq 2\nu^2 \cdot \|X^{(k)} - X^{(k-1)}\|^2 + \\
& \quad 2\nu^2 \cdot \|X^{(k+\frac{1}{2})} - X^{(k)}\|^2. \quad (161)
\end{aligned}$$

Note that Eqs. (143) and (148) hold as long as $\zeta > \xi > 0$, from which we might upper-bound $\|X^{(k)} - X^{(k-1)}\|^2$ and $\|X^{(k+\frac{1}{2})} - X^{(k)}\|^2$ in Eq. (161) and obtain

$$\begin{aligned}
& \|\text{grad} F(X^{(k+\frac{1}{2})})\|^2 \leq \frac{4\nu^2}{\delta} (\bar{F}^{(k-1)} - \bar{F}^{(k)}) + \\
& \quad \frac{4\nu^2}{\delta'} (\bar{F}^{(k)} - \bar{F}^{(k+1)}). \quad (162)
\end{aligned}$$

Recall from Proposition 6(a) that

$$\bar{F}^{(k-1)} - \bar{F}^{(k)} \geq 0 \quad (163)$$

and

$$\bar{F}^{(k)} - \bar{F}^{(k+1)} \geq 0. \quad (164)$$

Then, if we let $\epsilon \triangleq \min\{\frac{\delta}{2\nu^2}, \frac{\delta'}{2\nu^2}\} > 0$, Eqs. (162) to (164) lead to

$$\bar{F}^{(k-1)} - \bar{F}^{(k+1)} \geq \frac{\epsilon}{2} \|\text{grad} F(X^{(k+\frac{1}{2})})\|^2. \quad (165)$$

A telescoping sum of Eq. (165) over k from 0 to K yields

$$\bar{F}^{(-1)} + \bar{F}^{(0)} - \bar{F}^{(k)} - \bar{F}^{(k+1)} \geq \frac{\epsilon}{2} \sum_{k=0}^K \|\text{grad} F(X^{(k+\frac{1}{2})})\|^2,$$

and thus,

$$\begin{aligned} \overline{F}^{(-1)} + \overline{F}^{(0)} - \overline{F}^{(k)} - \overline{F}^{(k+1)} &\geq \\ \frac{\epsilon(K+1)}{2} \min_{0 \leq k \leq K} \|\text{grad } F(X^{(k+\frac{1}{2})})\|^2. \end{aligned} \quad (166)$$

From lines 8, 14 of Algorithm 3, we obtain

$$\overline{F}^{(-1)} = \overline{F}^{(0)} = F(X^{(0)}), \quad (167)$$

and Propositions 6(a) and 6(b) indicate

$$\overline{F}^{(k)} \geq \overline{F}^{(k+1)} \geq F^\infty. \quad (168)$$

As a result of Eqs. (166) to (168), it can be concluded that

$$F(X^{(0)}) - F^\infty \geq \frac{\epsilon(K+1)}{4} \min_{0 \leq k \leq K} \|\text{grad } F(X^{(k+\frac{1}{2})})\|^2,$$

which is equivalent to

$$\min_{0 \leq k \leq K} \|\text{grad } F(X^{(k+\frac{1}{2})})\| \leq 2\sqrt{\frac{1}{\epsilon} \cdot \frac{F(X^{(0)}) - F^\infty}{K+1}}. \quad (169)$$

The proof is completed.

Proof of (f). From Propositions 6(c) and 6(d), we obtain

$$\|X^{(k+1)} - X^{(k)}\| \rightarrow 0$$

and

$$\|X^{(k+\frac{1}{2})} - X^{(k)}\| \rightarrow 0$$

as long as $\zeta > \xi > 0$, from which and Eq. (161), it is trivial to show that

$$\text{grad } F(X^{(k+\frac{1}{2})}) \rightarrow \mathbf{0}. \quad (170)$$

In addition, note that $\text{grad } F(X)$ is continuous by Assumption 2(b), which suggests

$$\text{grad } F(X^{(k)}) \rightarrow \text{grad } F(X^{(k+\frac{1}{2})}). \quad (171)$$

From Eqs. (170) and (171), it can be concluded that

$$\text{grad } F(X^{(k)}) \rightarrow \mathbf{0}.$$

The proof is completed.

APPENDIX G. PROOF OF PROPOSITION 7

Proof of (a). We will prove $F(X^{(k)}) = \sum_{\alpha \in \mathcal{A}} F^{\alpha(k)}$ by induction.

1) From Eq. (18), it can be shown that

$$\begin{aligned} &F(X^{(0)}) \\ &= \sum_{\alpha \in \mathcal{A}} \sum_{(i,j) \in \vec{\mathcal{E}}^{\alpha\alpha}} F_{ij}^{\alpha\alpha}(X^{(0)}) + \sum_{\substack{\alpha, \beta \in \mathcal{A}, \\ \alpha \neq \beta}} \sum_{(i,j) \in \vec{\mathcal{E}}^{\alpha\beta}} F_{ij}^{\alpha\beta}(X^{(0)}) \\ &= \sum_{\alpha \in \mathcal{A}} \left(\sum_{(i,j) \in \vec{\mathcal{E}}^{\alpha\alpha}} F_{ij}^{\alpha\alpha}(X^{(0)}) + \right. \\ &\quad \frac{1}{2} \sum_{\beta \in \mathcal{N}^\alpha} \sum_{(i,j) \in \vec{\mathcal{E}}^{\alpha\beta}} F_{ij}^{\alpha\beta}(X^{(0)}) + \\ &\quad \left. \frac{1}{2} \sum_{\beta \in \mathcal{N}_+^\alpha} \sum_{(i,j) \in \vec{\mathcal{E}}^{\beta\alpha}} F_{ij}^{\beta\alpha}(X^{(0)}) \right) \\ &= \sum_{\alpha \in \mathcal{A}} F^{\alpha(0)}, \end{aligned} \quad (172)$$

where the last equality results from Eq. (67).

2) Suppose $F(X^{(k)}) = \sum_{\alpha \in \mathcal{A}} F^{\alpha(k)}$ holds at k-th iteration. As a result of Eq. (69), we obtain

$$\begin{aligned} &\sum_{\alpha \in \mathcal{A}} G^{\alpha(k+1)} \\ &= \sum_{\alpha \in \mathcal{A}} G^{\alpha}(X^{\alpha(k+1)}|X^{(k)}) + \sum_{\alpha \in \mathcal{A}} F^{\alpha(k)} \\ &= \sum_{\alpha \in \mathcal{A}} G^{\alpha}(X^{\alpha(k+1)}|X^{(k)}) + F(X^{(k)}) \\ &= G(X^{(k+1)}|X^{(k)}), \end{aligned} \quad (173)$$

where the second and third equality are due to $F(X^{(k)}) = \sum_{\alpha \in \mathcal{A}} F^{\alpha(k)}$ and Eq. (36), respectively. From Eq. (66) and

$$\|X^{(k+1)} - X^{(k)}\|^2 = \sum_{\alpha \in \mathcal{A}} \|X^{\alpha(k+1)} - X^{\alpha(k)}\|^2,$$

it is straightforward to show

$$\begin{aligned} &\sum_{\alpha \in \mathcal{A}} \Delta G^{\alpha}(X^{\alpha(k+1)}|X^{(k)}) = \\ &\sum_{\substack{\alpha, \beta \in \mathcal{A}, \\ \alpha \neq \beta}} \sum_{(i,j) \in \vec{\mathcal{E}}^{\alpha\beta}} \left(F_{ij}^{\alpha\beta}(X) - E_{ij}^{\alpha\beta}(X|X^{(k)}) \right) - \\ &\quad \frac{\xi}{2} \|X^{(k+1)} - X^{(k)}\|^2. \end{aligned} \quad (174)$$

In addition, Eqs. (70) and (173) suggest

$$\begin{aligned} &\sum_{\alpha \in \mathcal{A}} F^{\alpha(k+1)} \\ &= \sum_{\alpha \in \mathcal{A}} G^{\alpha(k+1)} + \sum_{\alpha \in \mathcal{A}} \Delta G^{\alpha}(X^{\alpha(k+1)}|X^{(k)}) \\ &= G(X^{(k+1)}|X^{(k)}) + \sum_{\alpha \in \mathcal{A}} \Delta G^{\alpha}(X^{\alpha(k+1)}|X^{(k)}). \end{aligned} \quad (175)$$

Substituting Eqs. (35) and (174) into Eq. (175) yields.

$$\begin{aligned} \sum_{\alpha \in \mathcal{A}} F^{\alpha(k+1)} &= \sum_{\alpha \in \mathcal{A}} \sum_{(i,j) \in \vec{\mathcal{E}}^{\alpha\alpha}} F_{ij}^{\alpha\alpha}(X^{(k+1)}) + \\ &\quad \sum_{\substack{\alpha, \beta \in \mathcal{A}, \\ \alpha \neq \beta}} \sum_{(i,j) \in \vec{\mathcal{E}}^{\alpha\beta}} F_{ij}^{\alpha\beta}(X^{(k+1)}). \end{aligned}$$

We simplify the equation above with Eq. (18) and obtain

$$F(X^{(k+1)}) = \sum_{\alpha \in \mathcal{A}} F^{\alpha(k+1)}. \quad (176)$$

3) Therefore, it can be concluded that $F(X^{(k)}) = \sum_{\alpha \in \mathcal{A}} F^{\alpha(k)}$ holds for any $k \geq 0$.

Proof of (b). We will prove $\overline{F}^{(k)} = \sum_{\alpha \in \mathcal{A}} \overline{F}^{\alpha(k)}$ by induction.

1) Recall from Eqs. (65), (68) and (172) that $\overline{F}^{(0)} = F(X^{(0)})$, $\overline{F}^{\alpha(0)} = F^{\alpha(0)}$ and $F(X^{(0)}) = \sum_{\alpha \in \mathcal{A}} F^{\alpha(0)}$, which immediately yields

$$\overline{F}^{(0)} = F(X^{(0)}). \quad (177)$$

2) Suppose $\bar{F}^{(k)} = \sum_{\alpha \in \mathcal{A}} \bar{F}^{\alpha(k)}$ holds at k-th iteration. As a result of Eq. (65), we obtain

$$\bar{F}^{(k+1)} = (1 - \eta) \cdot \bar{F}^{(k)} + \eta \cdot F(X^{(k+1)}).$$

Note that Proposition 7(a) suggests $F(X^{(k+1)}) = \sum_{\alpha \in \mathcal{A}} F^{\alpha(k+1)}$. Apply $\bar{F}^{(k)} = \sum_{\alpha \in \mathcal{A}} \bar{F}^{\alpha(k)}$ and $F(X^{(k+1)}) = \sum_{\alpha \in \mathcal{A}} F^{\alpha(k+1)}$ on the right-hand side of the equation above results in

$$\begin{aligned} \bar{F}^{(k+1)} &= (1 - \eta) \cdot \sum_{\alpha \in \mathcal{A}} \bar{F}^{\alpha(k)} + \\ &\eta \cdot \sum_{\alpha \in \mathcal{A}} F^{\alpha(k+1)} = \sum_{\alpha \in \mathcal{A}} \bar{F}^{\alpha(k+1)}, \end{aligned} \quad (178)$$

where the last equality is due to Eq. (71).

3) Therefore, it can be concluded that $\bar{F}^{(k)} = \sum_{\alpha \in \mathcal{A}} \bar{F}^{\alpha(k)}$ holds for any $k \geq 0$. The proof is completed.

Proof of (c). Proposition 2 indicates $E_{ij}^{\alpha\beta}(X|X^{(k-1)}) \geq F_{ij}^{\alpha\beta}(X)$ and $E_{ij}^{\beta\alpha}(X|X^{(k-1)}) \geq F_{ij}^{\beta\alpha}(X)$, from which and Eq. (66) we obtain

$$\Delta G^{\alpha}(X^{\alpha}|X^{(k-1)}) \leq 0 \quad (179)$$

as long as $\xi \geq 0$. From Eqs. (70) and (179), it is immediate to conclude

$$F^{\alpha(k+1)} \leq G^{\alpha(k+1)} \quad (180)$$

for any $k \geq 0$. If $G^{\alpha(k+1)} \leq \bar{F}^{\alpha(k)}$, the equation above further suggests

$$F^{\alpha(k+1)} \leq G^{\alpha(k+1)} \leq \bar{F}^{\alpha(k)}. \quad (181)$$

From Eq. (71), we obtain

$$\bar{F}^{\alpha(k+1)} = (1 - \eta) \cdot \bar{F}^{\alpha(k)} + \eta \cdot F^{\alpha(k+1)}, \quad (182)$$

where note that $\eta \in (0, 1]$. Thus, we conclude that $\bar{F}^{\alpha(k+1)}$ is a convex combination of $\bar{F}^{\alpha(k)}$ and $F^{\alpha(k+1)}$, which and Eq. (181) lead to

$$F^{\alpha(k+1)} \leq \bar{F}^{\alpha(k+1)} \leq \bar{F}^{\alpha(k)}. \quad (183)$$

The proof is completed.

APPENDIX H. PROOF OF PROPOSITION 8

Proof of (a). We will prove $F^{\alpha(k)} \leq \bar{F}^{\alpha(k)}$ and $\bar{F}^{\alpha(k+1)} \leq \bar{F}^{\alpha(k)}$ by induction, from which it can be shown that $\bar{F}^{(k+1)} \leq \bar{F}^{(k)}$.

1) From lines 6, 7, 15, 16 of Algorithm 5, it can be shown that

$$F^{\alpha(-1)} = F^{\alpha(0)} = \bar{F}^{\alpha(-1)} = \bar{F}^{\alpha(0)}.$$

2) Suppose $k \geq 0$ and $F^{\alpha(k)} \leq \bar{F}^{\alpha(k)}$ holds at k-th iteration. In terms of $X^{\alpha(k+\frac{1}{2})}$, if the adaptive restart scheme for $X^{\alpha(k+\frac{1}{2})}$ is not triggered, it is immediate to show from line 7 of Algorithm 6 that

$$G^{\alpha(k+\frac{1}{2})} \leq \bar{F}^{\alpha(k)}. \quad (184)$$

On the other hand, if the adaptive restart scheme for $X^{\alpha(k+\frac{1}{2})}$ is triggered, line 8 of Algorithm 6 results in

$$\begin{aligned} G^{\alpha}(X^{\alpha(k+\frac{1}{2})}|X^{(k)}) &\leq H^{\alpha}(X^{\alpha(k+\frac{1}{2})}|X^{(k)}) \leq \\ &H^{\alpha}(X^{\alpha(k)}|X^{(k)}) = 0, \end{aligned} \quad (185)$$

where the first inequality and the last equality are due to Proposition 4(e) and Eq. (44), respectively. From Eqs. (69) and (185), we obtain

$$\begin{aligned} G^{\alpha(k+\frac{1}{2})} &= G^{\alpha}(X^{\alpha(k+\frac{1}{2})}|X^{(k)}) + F^{\alpha(k)} \leq \\ H^{\alpha}(X^{\alpha(k+\frac{1}{2})}|X^{(k)}) + F^{\alpha(k)} &\leq F^{\alpha(k)} \leq \bar{F}^{\alpha(k)}. \end{aligned} \quad (186)$$

Therefore, no matter whether the adaptive restart scheme is triggered or not, we conclude from Eqs. (184) and (186) that

$$G^{\alpha(k+\frac{1}{2})} \leq \bar{F}^{\alpha(k)} \quad (187)$$

always holds. Furthermore, if $X^{\alpha(k+1)}$ and $G^{\alpha(k+1)}$ result from line 17 of Algorithm 6, we obtain $X^{\alpha(k+1)} = X^{\alpha(k+\frac{1}{2})}$ and $G^{\alpha(k+1)} = G^{\alpha(k+\frac{1}{2})}$, which and Eq. (187) yield

$$G^{\alpha(k+1)} = G^{\alpha(k+\frac{1}{2})} \leq \bar{F}^{\alpha(k)}. \quad (188)$$

Otherwise, line 16 of Algorithm 6 and Eq. (187) suggest

$$G^{\alpha(k+1)} - \bar{F}^{\alpha(k)} \leq \phi \cdot (G^{\alpha(k+\frac{1}{2})} - \bar{F}^{\alpha(k)}) \leq 0. \quad (189)$$

Then, Eqs. (188) and (189) suggest

$$G^{\alpha(k+1)} \leq \bar{F}^{\alpha(k)} \quad (190)$$

always holds, from which and Proposition 7(c) we conclude

$$F^{\alpha(k+1)} \leq \bar{F}^{\alpha(k+1)} \leq \bar{F}^{\alpha(k)}. \quad (191)$$

3) Therefore, it can be concluded that $F^{\alpha(k)} \leq \bar{F}^{\alpha(k)}$ and $\bar{F}^{\alpha(k+1)} \leq \bar{F}^{\alpha(k)}$.

Summing both sides of $\bar{F}^{\alpha(k+1)} \leq \bar{F}^{\alpha(k)}$ over all the nodes α and implementing Propositions 7(a) and 7(b) yields

$$\bar{F}^{(k+1)} = \sum_{\alpha \in \mathcal{A}} \bar{F}^{\alpha(k+1)} \leq \sum_{\alpha \in \mathcal{A}} \bar{F}^{\alpha(k)} = \bar{F}^{(k)},$$

which suggests that $\bar{F}^{(k)}$ is nonincreasing. The proof is completed.

Proof of (b). Recalling that $F(X^{(k)}) \geq 0$ holds by definition for any $k \geq 0$ and $\bar{F}^{(k)}$ is the exponential moving average of $F(X^{(0)})$, $F(X^{(1)})$, \dots , $F(X^{(k)})$, we obtain $\bar{F}^{(k)} \geq 0$, i.e., $\bar{F}^{(k)}$ is bounded below. In addition, Proposition 8(a) indicates that $\bar{F}^{(k)}$ is nonincreasing, and thus, there exists F^{∞} such that $\bar{F}^{(k)} \rightarrow F^{\infty}$, from which and Eq. (65) it can be concluded that $F(X^{(k)}) \rightarrow F^{\infty}$ as well. The proof is completed.

Proof of (c). From Eq. (36), it can be shown that $G(X^{(k+1)}|X^{(k)})$ takes the form as

$$\begin{aligned} G(X^{(k+1)}|X^{(k)}) &= \sum_{\alpha \in \mathcal{A}} G^{\alpha}(X^{\alpha(k)}|X^{(k)}) + F(X^{(k)}) \\ &= \sum_{\alpha \in \mathcal{A}} G^{\alpha}(X^{\alpha(k)}|X^{(k)}) + \sum_{\alpha \in \mathcal{A}} F^{\alpha(k)}, \end{aligned}$$

where the last equality is due to Proposition 7(a). Applying Eq. (69) on the equation above results in

$$G(X^{(k+1)}|X^{(k)}) = \sum_{\alpha \in \mathcal{A}} G^{\alpha(k+1)}. \quad (192)$$

Recalling $G^{\alpha(k+1)} \leq \bar{F}^{\alpha(k)}$ from Eq. (190) and $\sum_{\alpha \in \mathcal{A}} \bar{F}^{\alpha(k)} = \bar{F}^{(k)}$ from Proposition 7(b), we obtain

$$G(X^{(k+1)}|X^{(k)}) = \sum_{\alpha \in \mathcal{A}} G^{\alpha(k+1)} \leq \sum_{\alpha \in \mathcal{A}} \bar{F}^{\alpha(k)} = \bar{F}^{(k)}. \quad (193)$$

From Eq. (193), it can be shown that

$$\bar{F}^{(k)} - F(X^{(k+1)}) \geq G(X^{(k+1)}|X^{(k)}) - F(X^{(k+1)}). \quad (194)$$

Substitute Eqs. (104) and (105) into the right-hand side of Eq. (194) and simplify the resulting equation:

$$\begin{aligned} \bar{F}^{(k)} - F(X^{(k+1)}) &\geq \frac{1}{2} \|X^{(k+1)} - X^{(k)}\|_{\Gamma^{(k)}}^2 - \\ &\quad \frac{1}{2} \|X^{(k+1)} - X^{(k)}\|_{M^{(k)}}^2. \end{aligned} \quad (195)$$

From Eqs. (141) and (195), we obtain

$$\begin{aligned} \bar{F}^{(k)} - \bar{F}^{(k+1)} &= \eta \cdot (\bar{F}^{(k)} - F^{(k+1)}) \geq \\ &\quad \frac{\eta}{2} \|X^{(k+1)} - X^{(k)}\|_{\Gamma^{(k)}}^2 - \frac{\eta}{2} \|X^{(k+1)} - X^{(k)}\|_{M^{(k)}}^2. \end{aligned}$$

From Eq. (93), note that $\Gamma^{(k)} - M^{(k)} \geq \xi \cdot \mathbf{I}$, and thus, there exists $\delta > 0$ such that the equation above is reduced to

$$\bar{F}^{(k)} - \bar{F}^{(k+1)} \geq \frac{\delta}{2} \|X^{(k+1)} - X^{(k)}\|^2 \quad (196)$$

as long as $\xi > 0$. Furthermore, Proposition 8(b) yields

$$\bar{F}^{(k)} - \bar{F}^{(k+1)} \rightarrow 0,$$

from which and Eq. (196), we obtain

$$\|X^{(k+1)} - X^{(k)}\| \rightarrow 0. \quad (197)$$

The proof is completed.

Proof of (d). In terms of $X^{\alpha(k+\frac{1}{2})}$, there are two possible cases:

1) If $X^{\alpha(k+\frac{1}{2})}$ is from line 3 of Algorithm 6, then line 7 of Algorithm 6 indicates

$$\bar{F}^{\alpha(k)} - G^{\alpha(k+\frac{1}{2})} \geq \psi \cdot \|X^{\alpha(k+\frac{1}{2})} - X^{\alpha(k)}\|^2. \quad (198)$$

2) If $X^{\alpha(k+\frac{1}{2})}$ is from line 8 of Algorithm 6, then note that Eq. (186) holds for any $k \geq 0$, which suggests

$$\begin{aligned} \bar{F}^{\alpha(k)} - G^{\alpha(k+\frac{1}{2})} &\geq H^{\alpha}(X^{\alpha(k+\frac{1}{2})}|X^{(k)}) - \\ &\quad G^{\alpha}(X^{\alpha(k+\frac{1}{2})}|X^{(k)}). \end{aligned}$$

Recalling the definitions of $G^{\alpha}(X^{\alpha(k+\frac{1}{2})}|X^{(k)})$ and $H^{\alpha}(X^{\alpha(k+\frac{1}{2})}|X^{(k)})$ in Eqs. (37) and (44), we rewrite the equation above as

$$\begin{aligned} \bar{F}^{\alpha(k)} - G^{\alpha(k+\frac{1}{2})} &\geq \frac{1}{2} \|X^{\alpha(k+\frac{1}{2})} - X^{\alpha(k)}\|_{\Pi^{\alpha(k)}}^2 - \\ &\quad \frac{1}{2} \|X^{\alpha(k+\frac{1}{2})} - X^{\alpha(k)}\|_{\Gamma^{\alpha(k)}}^2. \end{aligned} \quad (199)$$

Similar to $\Gamma^{(k)}$ and $\Pi^{(k)}$ in Eq. (111), we obtain

$$\Pi^{\alpha(k)} \geq \Gamma^{\alpha(k)} + (\zeta - \xi) \cdot \mathbf{I}. \quad (200)$$

Applying Eq. (200) on the right-hand side of Eq. (199) indicates

$$\bar{F}^{\alpha(k)} - G^{\alpha(k+\frac{1}{2})} \geq \frac{\zeta - \xi}{2} \|X^{\alpha(k+\frac{1}{2})} - X^{\alpha(k)}\|^2. \quad (201)$$

Then, as a result of Eqs. (198) and (201), there exists a constant scalar $\sigma' > 0$ such that

$$\bar{F}^{\alpha(k)} - G^{\alpha(k+\frac{1}{2})} \geq \frac{\sigma'}{2} \|X^{\alpha(k+\frac{1}{2})} - X^{\alpha(k)}\|^2 \quad (202)$$

if $\zeta > \xi > 0$. In addition, lines 16 to 18 of Algorithm 6 results in

$$\begin{aligned} \bar{F}^{\alpha(k)} - G^{\alpha(k+1)} &\geq \phi \cdot (\bar{F}^{\alpha(k)} - G^{\alpha(k+\frac{1}{2})}) \geq \\ &\quad \frac{\phi\sigma'}{2} \|X^{\alpha(k+\frac{1}{2})} - X^{\alpha(k)}\|^2, \end{aligned} \quad (203)$$

where the last inequality is from Eq. (202). Summing both sides of Eq. (203) over all the nodes $\alpha \in \mathcal{A}$ and simplifying the resulting equation with Proposition 7(b) and Eq. (192), we obtain

$$\bar{F}^{(k)} - G(X^{(k+1)}|X^{(k)}) \geq \frac{\phi\sigma'}{2} \|X^{(k+\frac{1}{2})} - X^{(k)}\|^2.$$

Recalling $G(X^{(k+1)}|X^{(k)}) \geq F(X^{(k+1)})$ from Proposition 3(b), the equation above indicates

$$\begin{aligned} \bar{F}^{(k)} - F(X^{(k+1)}) &\geq \bar{F}^{(k)} - G(X^{(k+1)}|X^{(k)}) \geq \\ &\quad \frac{\phi\sigma'}{2} \|X^{(k+\frac{1}{2})} - X^{(k)}\|^2. \end{aligned} \quad (204)$$

From Eqs. (141) and (204), it is immediate to show

$$\begin{aligned} \bar{F}^{(k)} - \bar{F}^{(k+1)} &\geq \eta \cdot (\bar{F}^{(k)} - F(X^{(k+1)})) \geq \\ &\quad \frac{\eta\phi\sigma'}{2} \|X^{(k+\frac{1}{2})} - X^{(k)}\|^2. \end{aligned}$$

Therefore, there exists a constant scalar $\delta' > 0$ such that

$$\bar{F}^{(k)} - \bar{F}^{(k+1)} \geq \frac{\delta'}{2} \|X^{(k+\frac{1}{2})} - X^{(k)}\|^2. \quad (205)$$

Since $\bar{F}^{(k)} \rightarrow F^{\infty}$, it can be concluded that

$$\|X^{(k+\frac{1}{2})} - X^{(k)}\| \rightarrow 0 \quad (206)$$

if $\zeta > \xi > 0$. The proof is completed.

Proof of (e) and (f). The proofs of Propositions 8(e) and 8(f) are almost the same as these of Propositions 6(e) and 6(f), which are thus omitted due to space limitation.

APPENDIX I. THE FORMULATION OF $\Gamma^{\alpha(k)}$ IN EQ. (37)

From Eqs. (35), (37), (88) and (89), it can be concluded that

$$\begin{aligned} & \frac{1}{2} \|X^\alpha - X^{\alpha(k)}\|_{\Gamma^{\alpha(k)}}^2 \\ &= \sum_{i=1}^{n_\alpha} \left[\frac{1}{2} \xi \|R_i^\alpha - R_i^{\alpha(k)}\|^2 + \frac{1}{2} \xi \|t_i^\alpha - t_i^{\alpha(k)}\|^2 \right] + \\ & \quad \sum_{(i,j) \in \vec{\mathcal{E}}^{\alpha\alpha}} \left[\frac{1}{2} \kappa_{ij}^{\alpha\alpha} \|(R_i^\alpha - R_i^{\alpha(k)})\tilde{R}_{ij}^{\alpha\alpha} - (R_j^\alpha - R_j^{\alpha(k)})\|^2 + \right. \\ & \quad \left. \frac{1}{2} \tau_{ij}^{\alpha\alpha} \|(R_i^\alpha - R_i^{\alpha(k)})\tilde{t}_{ij}^{\alpha\alpha} + t_i^\alpha - t_i^{\alpha(k)} - (t_j^\alpha - t_j^{\alpha(k)})\|^2 \right] + \\ & \quad \sum_{\beta \in \mathcal{N}_-^\alpha} \sum_{(i,j) \in \vec{\mathcal{E}}^{\alpha\beta}} \omega_{ij}^{\alpha\beta(k)} \left[\kappa_{ij}^{\alpha\beta} \|R_i^\alpha - R_i^{\alpha(k)}\|^2 + \right. \\ & \quad \left. \tau_{ij}^{\alpha\beta} \|(R_i^\alpha - R_i^{\alpha(k)})\tilde{t}_{ij}^{\alpha\beta} + t_i^\alpha - t_i^{\alpha(k)}\|^2 \right] + \\ & \quad \sum_{\beta \in \mathcal{N}_+^\alpha} \sum_{(j,i) \in \vec{\mathcal{E}}^{\beta\alpha}} \omega_{ji}^{\beta\alpha(k)} \left[\kappa_{ji}^{\beta\alpha} \|R_i^\alpha - R_i^{\alpha(k)}\|^2 + \right. \\ & \quad \left. \tau_{ji}^{\beta\alpha} \|t_i^\alpha - t_i^{\alpha(k)}\|^2 \right]. \end{aligned} \quad (207)$$

For notational clarity, we introduce

$$\begin{aligned} \vec{\mathcal{E}}_{i-}^{\alpha\beta} &\triangleq \{(i, j) | (i, j) \in \vec{\mathcal{E}}^{\alpha\beta}\}, \\ \vec{\mathcal{E}}_{i+}^{\alpha\beta} &\triangleq \{(i, j) | (j, i) \in \vec{\mathcal{E}}^{\beta\alpha}\}, \\ \mathcal{N}_{i-}^\alpha &\triangleq \{\beta \in \mathcal{A} | \exists (i, j) \in \vec{\mathcal{E}}^{\alpha\beta} \text{ and } \beta \neq \alpha\}, \\ \mathcal{N}_{i+}^\alpha &\triangleq \{\beta \in \mathcal{A} | \exists (j, i) \in \vec{\mathcal{E}}^{\beta\alpha} \text{ and } \beta \neq \alpha\}, \\ \mathcal{E}_i^{\alpha\beta} &\triangleq \vec{\mathcal{E}}_{i-}^{\alpha\beta} \cup \vec{\mathcal{E}}_{i+}^{\alpha\beta}, \\ \mathcal{N}_i^\alpha &\triangleq \mathcal{N}_{i-}^\alpha \cup \mathcal{N}_{i+}^\alpha. \end{aligned}$$

In addition, we define $\kappa_{ji}^{\beta\alpha} \triangleq \kappa_{ij}^{\alpha\beta}$, $\tau_{ji}^{\beta\alpha} \triangleq \tau_{ij}^{\alpha\beta}$, $\omega_{ij}^{\alpha\beta(k)} \triangleq \omega_{ji}^{\beta\alpha(k)}$, and

$$\kappa_{ij}^{\alpha\beta(k)} \triangleq \omega_{ij}^{\alpha\beta(k)} \cdot \kappa_{ij}^{\alpha\beta}, \quad (208)$$

$$\tau_{ij}^{\alpha\beta(k)} \triangleq \omega_{ij}^{\alpha\beta(k)} \cdot \tau_{ij}^{\alpha\beta} \quad (209)$$

for any $(i, j) \in \vec{\mathcal{E}}^{\alpha\beta}$.

Then, Eq. (207) indicates that $\Gamma^{\alpha(k)} \in \mathbb{R}^{(d+1)n_\alpha \times (d+1)n_\alpha}$ in Eq. (37) takes the form as

$$\Gamma^{\alpha(k)} = \begin{bmatrix} \Gamma^{\tau, \alpha(k)} & \Gamma^{\nu, \alpha(k)} \\ \Gamma^{\nu, \alpha(k)\top} & \Gamma^{\kappa, \alpha(k)} \end{bmatrix}, \quad (210)$$

in which $\Gamma^{\tau, \alpha(k)} \in \mathbb{R}^{n_\alpha \times n_\alpha}$, $\Gamma^{\nu, \alpha(k)} \in \mathbb{R}^{n_\alpha \times dn_\alpha}$ and $\Gamma^{\kappa, \alpha(k)} \in \mathbb{R}^{dn_\alpha \times dn_\alpha}$ are sparse matrices that are defined as

$$[\Gamma^{\tau, \alpha(k)}]_{ij} = \begin{cases} \xi + \sum_{e \in \mathcal{E}_i^{\alpha\alpha}} \tau_e^{\alpha\alpha} + \sum_{\beta \in \mathcal{N}_i^\alpha} \sum_{e \in \mathcal{E}_i^{\alpha\beta}} 2\tau_e^{\alpha\beta(k)}, & i = j, \\ -\tau_{ij}^{\alpha\alpha}, & (i, j) \in \vec{\mathcal{E}}^{\alpha\alpha}, \\ -\tau_{ji}^{\alpha\alpha}, & (j, i) \in \vec{\mathcal{E}}^{\alpha\alpha}, \\ 0, & \text{otherwise,} \end{cases}$$

$$[\Gamma^{\nu, \alpha(k)}]_{ij} = \begin{cases} \sum_{e \in \mathcal{E}_i^{\alpha\alpha}} \tau_e^{\alpha\alpha} \tilde{t}_e^{\alpha\alpha\top} + \sum_{\beta \in \mathcal{N}_i^\alpha} \sum_{e \in \mathcal{E}_i^{\alpha\beta}} 2\tau_e^{\alpha\beta(k)} \tilde{t}_e^{\alpha\beta\top}, & i = j, \\ -\tau_{ji}^{\alpha\alpha} \tilde{t}_{ji}^{\alpha\alpha\top}, & (j, i) \in \vec{\mathcal{E}}^{\alpha\alpha}, \\ 0, & \text{otherwise,} \end{cases}$$

$$[\Gamma^{\kappa, \alpha(k)}]_{ij} = \begin{cases} \xi \cdot \mathbf{I} + \sum_{e \in \mathcal{E}_i^{\alpha\alpha}} \kappa_e^{\alpha\alpha} \cdot \mathbf{I} + \sum_{e \in \mathcal{E}_i^{\alpha\alpha}} \tau_e^{\alpha\alpha} \cdot \tilde{t}_e^{\alpha\alpha} \tilde{t}_e^{\alpha\alpha\top} + \sum_{\beta \in \mathcal{N}_i^\alpha} \left(\sum_{e \in \mathcal{E}_i^{\alpha\beta}} 2\kappa_e^{\alpha\beta(k)} \cdot \mathbf{I} + \sum_{e \in \mathcal{E}_i^{\alpha\beta}} 2\tau_e^{\alpha\beta(k)} \cdot \tilde{t}_e^{\alpha\beta} \tilde{t}_e^{\alpha\beta\top} \right), & i = j, \\ -\kappa_{ij}^{\alpha\alpha} \cdot \tilde{R}_{ij}^{\alpha\alpha}, & (i, j) \in \vec{\mathcal{E}}^{\alpha\alpha}, \\ -\kappa_{ji}^{\alpha\alpha} \cdot \tilde{R}_{ij}^{\alpha\alpha\top}, & (j, i) \in \vec{\mathcal{E}}^{\alpha\alpha}, \\ 0, & \text{otherwise.} \end{cases}$$

APPENDIX J. THE FORMULATION OF $\Pi^{\alpha(k)}$ AND $\Pi_i^{\alpha(k)}$ IN EQS. (44) AND (45)

From Eqs. (41) and (88), it can be concluded that

$$\begin{aligned} & \frac{1}{2} \|X - X^{(k)}\|_{\Pi_i^{\alpha(k)}}^2 \\ &= \frac{1}{2} \zeta \|R_i^\alpha - R_i^{\alpha(k)}\|^2 + \frac{1}{2} \zeta \|t_i^\alpha - t_i^{\alpha(k)}\|^2 + \\ & \quad \sum_{(i,j) \in \vec{\mathcal{E}}_i^{\alpha\alpha}} \left[\kappa_{ij}^{\alpha\alpha} \|R_i^\alpha - R_i^{\alpha(k)}\|^2 + \right. \\ & \quad \left. \tau_{ij}^{\alpha\alpha} \|(R_i^\alpha - R_i^{\alpha(k)})\tilde{t}_{ij}^{\alpha\alpha} + t_i^\alpha - t_i^{\alpha(k)}\|^2 \right] + \\ & \quad \sum_{(i,j) \in \vec{\mathcal{E}}_{i+}^{\alpha\alpha}} \left[\kappa_{ji}^{\alpha\alpha} \|R_i^\alpha - R_i^{\alpha(k)}\|^2 + \tau_{ji}^{\alpha\alpha} \|t_i^\alpha - t_i^{\alpha(k)}\|^2 \right] + \\ & \quad \sum_{\beta \in \mathcal{N}_{i-}^\alpha} \sum_{(i,j) \in \vec{\mathcal{E}}_i^{\alpha\beta}} \omega_{ij}^{\alpha\beta(k)} \left[\kappa_{ij}^{\alpha\beta} \|R_i^\alpha - R_i^{\alpha(k)}\|^2 + \right. \\ & \quad \left. \tau_{ij}^{\alpha\beta} \|(R_i^\alpha - R_i^{\alpha(k)})\tilde{t}_{ij}^{\alpha\beta} + t_i^\alpha - t_i^{\alpha(k)}\|^2 \right] + \\ & \quad \sum_{\beta \in \mathcal{N}_{i+}^\alpha} \sum_{(j,i) \in \vec{\mathcal{E}}_{i+}^{\beta\alpha}} \omega_{ji}^{\beta\alpha(k)} \left[\kappa_{ji}^{\beta\alpha} \|R_i^\alpha - R_i^{\alpha(k)}\|^2 + \right. \\ & \quad \left. \tau_{ji}^{\beta\alpha} \|t_i^\alpha - t_i^{\alpha(k)}\|^2 \right]. \end{aligned} \quad (211)$$

From Eq. (211), it can be shown that $\Pi_i^{\alpha(k)} \in \mathbb{R}^{(d+1) \times (d+1)}$ in Eq. (45) can be written as

$$\Pi_i^{\alpha(k)} = \begin{bmatrix} \Pi_i^{\tau, \alpha(k)} & \Pi_i^{\nu, \alpha(k)} \\ \Pi_i^{\nu, \alpha(k)\top} & \Pi_i^{\kappa, \alpha(k)} \end{bmatrix}, \quad (212)$$

in which $\Pi_i^{\tau, \alpha(k)} \in \mathbb{R}$, $\Pi_i^{\nu, \alpha(k)} \in \mathbb{R}^{1 \times d}$ and $\Pi_i^{\kappa, \alpha(k)} \in \mathbb{R}^{d \times d}$ are defined as

$$\Pi_i^{\tau, \alpha(k)} = \zeta + \sum_{e \in \mathcal{E}_i^{\alpha\alpha}} 2\tau_e^{\alpha\alpha} + \sum_{\beta \in \mathcal{N}_i^\alpha} \sum_{e \in \mathcal{E}_i^{\alpha\beta}} 2\tau_e^{\alpha\beta(k)}, \quad (213)$$

$$\Pi_i^{\nu, \alpha(k)} = \sum_{e \in \mathcal{E}_i^{\alpha\alpha}} 2\tau_e^{\alpha\alpha} \tilde{t}_e^{\alpha\alpha\top} + \sum_{\beta \in \mathcal{N}_i^\alpha} \sum_{e \in \mathcal{E}_i^{\alpha\beta}} 2\tau_e^{\alpha\beta(k)} \tilde{t}_e^{\alpha\beta\top}, \quad (214)$$

$$\begin{aligned} \Pi_i^{\kappa, \alpha(k)} &= \zeta \cdot \mathbf{I} + \sum_{e \in \mathcal{E}_i^{\alpha\alpha}} 2\kappa_e^{\alpha\alpha} \cdot \mathbf{I} + \sum_{e \in \mathcal{E}_i^{\alpha\alpha}} 2\tau_e^{\alpha\alpha} \cdot \tilde{t}_e^{\alpha\alpha} \tilde{t}_e^{\alpha\alpha\top} + \\ &\sum_{\beta \in \mathcal{N}_i^{\alpha}} \left(\sum_{e \in \mathcal{E}_i^{\alpha\beta}} 2\kappa_e^{\alpha\beta(k)} \cdot \mathbf{I} + \sum_{e \in \mathcal{E}_i^{\alpha\beta}} 2\tau_e^{\alpha\beta(k)} \cdot \tilde{t}_e^{\alpha\beta} \tilde{t}_e^{\alpha\beta\top} \right), \end{aligned} \quad (215)$$

in which $\kappa_{ij}^{\alpha\beta(k)}$ and $\tau_{ij}^{\alpha\beta(k)}$ are given in Eqs. (208) and (209), respectively.

Similar to $\Gamma^{\alpha(k)} \in \mathbb{R}^{(d+1)n_\alpha \times (d+1)n_\alpha}$ in Eq. (210), $\Pi^{\alpha(k)} \in \mathbb{R}^{(d+1)n_\alpha \times (d+1)n_\alpha}$ in Eq. (44) also takes the form as

$$\Pi^{\alpha(k)} = \begin{bmatrix} \Pi^{\tau, \alpha(k)} & \Pi^{\nu, \alpha(k)} \\ \Pi^{\nu, \alpha(k)\top} & \Pi^{\kappa, \alpha(k)} \end{bmatrix}, \quad (216)$$

in which $\Pi^{\tau, \alpha(k)} \in \mathbb{R}^{n_\alpha \times n_\alpha}$, $\Pi^{\nu, \alpha(k)} \in \mathbb{R}^{n_\alpha \times dn_\alpha}$ and $\Pi^{\kappa, \alpha(k)} \in \mathbb{R}^{dn_\alpha \times dn_\alpha}$ are sparse matrices. Following Eqs. (43) to (45), it is straightforward to show that

$$\frac{1}{2} \|X^\alpha - X^{\alpha(k)}\|_{\Pi^{\alpha(k)}}^2 = \sum_{i=1}^{n_\alpha} \frac{1}{2} \|X_i^\alpha - X_i^{\alpha(k)}\|_{\Pi_i^{\alpha(k)}}^2.$$

From the equation above, $\Pi^{\tau, \alpha(k)} \in \mathbb{R}^{n_\alpha \times n_\alpha}$, $\Pi^{\nu, \alpha(k)} \in \mathbb{R}^{n_\alpha \times dn_\alpha}$ and $\Pi^{\kappa, \alpha(k)} \in \mathbb{R}^{dn_\alpha \times dn_\alpha}$ in Eq. (216) are defined as

$$\left[\Pi^{\tau, \alpha(k)} \right]_{ij} = \begin{cases} \Pi_i^{\tau, \alpha(k)}, & i = j, \\ 0, & \text{otherwise,} \end{cases}$$

$$\left[\Pi^{\nu, \alpha(k)} \right]_{ij} = \begin{cases} \Pi_i^{\nu, \alpha(k)}, & i = j, \\ 0, & \text{otherwise,} \end{cases}$$

$$\left[\Pi^{\kappa, \alpha(k)} \right]_{ij} = \begin{cases} \Pi_i^{\kappa, \alpha(k)}, & i = j, \\ 0, & \text{otherwise,} \end{cases}$$

in which $\Pi_i^{\tau, \alpha(k)} \in \mathbb{R}$, $\Pi_i^{\nu, \alpha(k)} \in \mathbb{R}^{1 \times d}$ and $\Pi_i^{\kappa, \alpha(k)} \in \mathbb{R}^{d \times d}$ are given in Eqs. (213) to (215).

APPENDIX K. THE CLOSED-FORM SOLUTION TO EQ. (56)

Substituting Eq. (212) into Eq. (56) and rewriting the resulting equation in terms of $X_i^\alpha = [t_i^\alpha \ R_i^\alpha] \in \mathbb{R}^{d \times (d+1)}$ leads to

$$\begin{aligned} (t_i^{\alpha(k+\frac{1}{2})}, R_i^{\alpha(k+\frac{1}{2})}) &= \\ \arg \min_{t_i^\alpha \in \mathbb{R}^d, R_i^\alpha \in SO(d)} &\frac{1}{2} \|t_i^\alpha - t_i^{\alpha(k)}\|_{\Pi_i^{\tau, \alpha(k)}}^2 + \\ &\Pi_i^{\nu, \alpha(k)} (R_i^\alpha - R_i^{\alpha(k)})^\top (t_i^\alpha - t_i^{\alpha(k)}) + \\ &\frac{1}{2} \|R_i^\alpha - R_i^{\alpha(k)}\|_{\Pi_i^{\kappa, \alpha(k)}}^2 + \\ &\langle \nabla_{t_i^\alpha} F(X^k), t_i^\alpha - t_i^{\alpha(k)} \rangle + \\ &\langle \nabla_{R_i^\alpha} F(X^k), R_i^\alpha - R_i^{\alpha(k)} \rangle. \end{aligned}$$

For notational simplicity, the equation above is simplified to

$$\begin{aligned} \min_{t_i^\alpha \in \mathbb{R}^d, R_i^\alpha \in SO(d)} &\frac{1}{2} \|t_i^\alpha\|_{\Pi_i^{\tau, \alpha(k)}}^2 + \Pi_i^{\nu, \alpha(k)} R_i^{\alpha\top} t_i^\alpha + \\ &\frac{1}{2} \|R_i^\alpha\|_{\Pi_i^{\kappa, \alpha(k)}}^2 + \langle \gamma_i^{\tau, \alpha(k)}, t_i^\alpha \rangle + \langle \gamma_i^{\kappa, \alpha(k)}, R_i^\alpha \rangle, \end{aligned} \quad (217)$$

in which

$$\gamma_i^{\tau, \alpha(k)} = \nabla_{t_i^\alpha} F(X^k) - t_i^{\alpha(k)} \Pi_i^{\tau, \alpha(k)} \in \mathbb{R}^d \quad (218)$$

and

$$\gamma_i^{\kappa, \alpha(k)} = \nabla_{R_i^\alpha} F(X^k) - R_i^{\alpha(k)} \Pi_i^{\kappa, \alpha(k)} \in \mathbb{R}^{d \times d}. \quad (219)$$

Recalling from Eq. (212) that $\Pi_i^{\tau, \alpha(k)} \in \mathbb{R}$ and $\Pi_i^{\tau, \alpha(k)} > 0$, we obtain that

$$t_i^\alpha = -R_i^\alpha \Pi_i^{\nu, \alpha(k)\top} \Pi_i^{\tau, \alpha(k)-1} - \gamma_i^{\tau, \alpha(k)} \Pi_i^{\tau, \alpha(k)-1} \quad (220)$$

minimizes Eq. (217) if $R_i^\alpha \in SO(d)$ is given. Then, substituting Eq. (220) into Eq. (217) yields

$$R_i^{\alpha(k+\frac{1}{2})} = \arg \min_{R_i^\alpha \in SO(d)} \frac{1}{2} \|R_i^\alpha\|_{\Xi_i^{\alpha(k)}}^2 - \langle v_i^{\alpha(k)}, R_i^\alpha \rangle, \quad (221)$$

in which

$$\Xi_i^{\alpha(k)} = \Pi_i^{\kappa, \alpha(k)} - \Pi_i^{\nu, \alpha(k)\top} \Pi_i^{\tau, \alpha(k)-1} \Pi_i^{\nu, \alpha(k)} \in \mathbb{R}^{d \times d} \quad (222)$$

and

$$v_i^{\alpha(k)} = \gamma_i^{\tau, \alpha(k)} \Pi_i^{\tau, \alpha(k)-1} \Pi_i^{\nu, \alpha(k)} - \gamma_i^{\kappa, \alpha(k)} \in \mathbb{R}^{d \times d}. \quad (223)$$

If we apply $R_i^{\alpha\top} R_i^\alpha = \mathbf{I}$ on Eq. (221), then Eq. (56) is equivalent to

$$R_i^{\alpha(k+\frac{1}{2})} = \arg \max_{R_i^\alpha \in SO(d)} \langle v_i^{\alpha(k)}, R_i^\alpha \rangle. \quad (224)$$

Thus, Eq. (56) is reduced to an optimization problem on $SO(d)$, which has a closed-form solution as follows.

Following [46], if $v_i^{\alpha(k)} \in \mathbb{R}^{d \times d}$ admits a singular value decomposition $v_i^{\alpha(k)} = U_i^{\alpha(k)} \Sigma_i^{\alpha(k)} V_i^{\alpha(k)\top}$ in which $U_i^{\alpha(k)}$ and $V_i^{\alpha(k)} \in O(d)$ are orthogonal (not necessarily special orthogonal) matrices, and $\Sigma_i^{\alpha(k)} = \text{diag}\{\sigma_1^{\alpha(k)}, \sigma_2^{\alpha(k)}, \dots, \sigma_d^{\alpha(k)}\} \in \mathbb{R}^{d \times d}$ is a diagonal matrix, and $\sigma_1^{\alpha(k)} \geq \sigma_2^{\alpha(k)} \geq \dots \geq \sigma_d^{\alpha(k)} \geq 0$ are singular values of $v_i^{\alpha(k)}$, then the optimal solution to Eq. (224) is

$$R_i^{\alpha(k+\frac{1}{2})} = \begin{cases} U_i^{\alpha(k)} \Lambda^+ V_i^{\alpha(k)\top}, & \det(U_i^{\alpha(k)} V_i^{\alpha(k)\top}) > 0, \\ U_i^{\alpha(k)} \Lambda^- V_i^{\alpha(k)\top}, & \text{otherwise,} \end{cases} \quad (225)$$

in which $\Lambda^+ = \text{diag}\{1, 1, \dots, 1\} \in \mathbb{R}^{d \times d}$ and $\Lambda^- = \text{diag}\{1, 1, \dots, -1\} \in \mathbb{R}^{d \times d}$. If $d = 2$, the equation above is equivalent to the polar decomposition of 2×2 matrices, and if $d = 3$, there are fast algorithms for singular value decomposition of 3×3 matrices [54]. As a result, Eq. (224) can be efficiently solved in the case of $SO(2)$ and $SO(3)$, both of which are commonly used in SLAM.

As long as $R_i^{\alpha(k+\frac{1}{2})} \in SO(d)$ is known, $t_i^{\alpha(k+\frac{1}{2})} \in \mathbb{R}^d$ can be exactly recovered using Eq. (220):

$$t_i^{\alpha(k+\frac{1}{2})} = -R_i^{\alpha(k+\frac{1}{2})} \Pi_i^{\nu, \alpha(k)\top} \Pi_i^{\tau, \alpha(k)-1} - \gamma_i^{\tau, \alpha(k)} \Pi_i^{\tau, \alpha(k)-1}. \quad (226)$$

Therefore, $X_i^{\alpha(k+\frac{1}{2})} = [t_i^{\alpha(k+\frac{1}{2})} \ R_i^{\alpha(k+\frac{1}{2})}] \in \mathbb{R}^{d \times (d+1)}$ is exactly solved, whose computation only involves matrix multiplication and singular value decomposition.